ABSTRACT

Title of dissertation: Insight into the Structure and Mechanism of Iodotyrosine Deiodinase, the First Mammalian Member of the NADH Oxidase / Flavin Reductase Superfamily

James Ambrose Watson, Jr.
Doctor of Philosophy, 2006

Dissertation directed by: Professor Steven E. Rokita
Department of Chemistry and Biochemistry

Iodotyrosine deiodinase (IYD) has remained poorly characterized for nearly 50 years in spite of its function as an iodine salvage pathway and its role in regulation of mammalian basal metabolism. IYD catalyzes the reductive deiodination of both mono- and diiodotyrosine, the iodinated side-products of thyroid hormone production. The Rokita lab previously purified IYD from porcine thyroids and identified a putative dehalogenase gene.

The work in this dissertation confirms the identity of the gene that encodes IYD through expression in HEK293 cells (K_M = 4.4 ± 1.7 μM and V_{max} = 12 ± 1 nmol hr^{-1} μg^{-1}) and, furthermore, identifies IYD as the first mammalian member of the NADH oxidase/flavin reductase superfamily, a protein fold previously found only in bacteria. In addition, a three-dimensional model of the NADH oxidase/flavin reductase domain of IYD was constructed

based on the x-ray crystal structure coordinates (Protein Data Bank code 1ICR) of the minor nitroreductase from *Escherichia coli*. The model also predicts structural features of IYD, including interactions between the flavin bound to IYD and one of three conserved cysteines.

To investigate the role of the NADH oxidase/flavin reductase domain plays in electron transfer, two truncation mutants were generated: IYD-NR (residues 81-285) and IYD-ΔTM (residues 34-285) encoding transmembrane-domain deleted IYD. The two mutants were expressed in HEK293 cells and their catalytic properties were measured. IYD-NR did not promote deiodination (V_{max} = 0.0 ± 0.4 nmol hr^{-1} μg^{-1}) of diiodotyrosine in a literature-derived iodide release assay. However, IYD-ΔTM was catalytically active toward DIT (K_M = 4.6 ± 1.3 μM and V_{max} = 7.0 ± 0.5 nmol hr^{-1} μg^{-1}) when the chemical reductant dithionite was used but did not promote NADPH-responsive deiodination. The subcellular location for both mutants was determined by ultracentrifugation. IYD-NR was observed in the insoluble fraction after centrifugation at 100,000 x g. However, IYD-ΔTM remained in the supernatant after centrifugation at 100,000 x g for 1 hour.

Insight into the Structure and Mechanism of Iodotyrosine Deiodinase, the First Mammalian Member of the NADH Oxidase / Flavin Reductase Superfamily

By

James Ambrose Watson, Jr.

Dissertation submitted to the Faculty of the Graduate School of the
University of Maryland, College Park in partial fulfillment
of the requirements for the degree of
Doctor of Philosophy
2006

Advisory Committee:

Professor Steven E. Rokita, Chair
Professor Philip R. DeShong
Professor Lyle D. Isaacs
Professor Douglas A. Julin
Professor Tom E. Porter

Acknowledgments

I begin by apologizing to those that I will undoubtedly forget to thank. There are many of you that have contributed to my success without ever knowing that you did. For this, I thank you.

In addition, I would like to thank Professor Rokita for his guidance during my time at University of Maryland. I appreciate the support and the many opportunities that you have given me. You have provided an example that has helped me grow both as a scientist, an educator, and a person. For this, I am truly grateful!

I would also like to thank my undergraduate advisor, Professor Kathleen Victoria Kilway. Thank you for your support and guidance. Thank you for believing in me and encouraging me to strive to be my best. More importantly, thank you for your friendship. I will always be in your debt.

Thank you to my committee, Professors DeShong, Isaacs, and Julin. You have been very helpful throughout my time at Maryland. I appreciate not only your scientific advice, but the many discussions during "happy hour." A special thanks to Professors DeShong and Isaacs for writing recommendation letters for my postdoctoral applications.

I am deeply indebted to Professor Iqbal Hamza and his laboratory for the use of their tissue culture facilities. A special thank you to Ms. Melissa Winn for taking the time to instruct me in tissue culture technique. Thank you to all the members of the Hamza lab for useful (and sometimes frivolous) discussions.

Thank you to all of the Department of Chemistry and Biochemistry staff that have made my time at Maryland successful…and interesting. Special thanks to Linda Zappasodi! I owe you! More thanks to Olivia Noble. You have always been there for me. Thanks to Taryn Faulkner for all your help. Thank you to the many others!

My residency on the second floor of Wing 5 has allowed me to interact with a whole host of characters, some sane…most not: thanks to members of the Kahn, Julin, Beckett, Cropp, Gerratana and Fenselau labs. I hope I have returned all the proverbial "cups of sugar" that I have borrowed over the years. Special thanks to Matt Servinsky for his assistance with Western blots. Thanks to the Kahn and Cropp labs for -80 °C freezer space.

Thanks to all the members of the Rokita lab past and present. Thanks to Mein Samala for assistance when I joined the Rokita Lab and to Takeo Ito for many useful discussions. Thank you to all the other postdocs that have come through the Rokita lab, I have learned something from each of you. Special thanks to all the graduate and undergraduate students that have been in the Rokita lab. I hope you have enjoyed your time as much as I have mine. Special thanks to David Lam, Ling Chen, and Jenn Gehret. I wish you continued success!!

Bill Walker, if you ever read this, look me up…I owe you a beer.

Amy Finch, you are a good friend and I wish you success in science and in life. Congrats again on your beautiful baby, Parker!

Neil Campbell, I have truly enjoyed the time that we have shared in the Rokita lab. You and Susannah will be welcome wherever I am.

Emily Weinert, boss shoes, sour burning ammonia, shaking fish, lacrosse camp, the old dudes, laser-powered barbecue, the bobblehead, and corn meal mush vs. polenta…the difference is salt. My life will never be the same. (I think this is good.) Thank you!!

Finally, my family: Thank you to my parents, Jim and Eleanor, whose young love made a little boy named Jimmy. A very special thank you to Tom. I could not have done this without your love, support, and friendship! I am orders of magnitude more grateful to you than you will ever know.

Table of Contents

List of Tables

Chapter 1

None

Chapter 2

None

Chapter 3

Chapter 4

Chapter 5

None

List of Equations

Chapter 1

None

Chapter 2

Chapter 3

None

Chapter 4

None

Chapter 5

None

List of Figures

Chapter 1

Chapter 2

Chapter 3

Chapter 4

List of Abbreviations

APS	ammonium persulfate
ATCC	American Type Culture Collection
ATP	adenosine triphosphate
BCA	bicinchoninic acid
CNS	central nervous system
Cys-SI	cysteine-sulfenyl iodide
DEAE	diethylaminoethyl
DMEM	Dulbecco's modified Eagle's medium
DIT	diiodotyrosine
$D^{125}IT$	diiodotyrosine labeled with ^{125}I iodine
DNA	deoxyribonucleic acid
dpm	disintegrations per minute
EDTA	ethylene diamine tetraacetic acid
FMN	flavin mononucleotide
$FMNH_2$	reduced flavin mononucleotide
FAD	flavin adenine dinucleotide
FRase I	flavin reductase from *Photobacterium fischeri*
FRP	flavin reductase P from *Vibrio harveyi*
GSH	glutathione (reduced form)
GSSG	glutathione (oxidized form)
GST	glutathione *S*-transferase
GS-TriCHQ	2,3,5-trichloro-6-*S*-glutathionylhydroquinone

HEK293	human embryonic kidney cell line
ID	iodothyronine deiodinase
I.M.A.G.E.	Integrated Molecular Analysis of Genomes and their Expression
IPTG	isopropyl-β-D-thiogalactoside
IYD	iodotyrosine deiodinase
IYD-ΔTM	transmembrane domain deleted iodotyrosine deiodinase
IYD-NR	nitroreductase domain of iodotyrosine deiodinase
kDa	kilodaltons
K_M	Michaelis-Menten constant
LB	Luria-Bertani broth
LB-Amp	Luria-Bertani broth supplemented with 100 μg/mL ampicillin
LB-Amp/Cm	Luria-Bertani broth supplemented with 100 mg/mL ampicillin and 25 mg/mL chloramphenicol
LB-Cm	Luria-Bertani broth supplemented with 25 μg/mL chloramphenicol
MALDI-TOF	matrix assisted laser desorption ionization-time of flight
MBP	maltose binding protein
MIT	monoiodotyrosine
MS	mass spectrometry
NAD^+	β-nicotinamide adenine dinucleotide (oxidized form)
NADH	β-nicotinamide adenine dinucleotide (reduced form)
$NADP^+$	β-nicotinamide adenine dinucleotide 2´-phosphate (oxidized form)
NADPH	β-nicotinamide adenine dinucleotide 2´-phosphate (reduced form)
NfnB-NfsB	minor nitroreductase from *Escherichia coli*

NfsA	major nitroreductase from *Escherichia coli*
NIS	sodium-iodide symporter
NOX	NADH oxidase from *Thermus thermophilus*
NOX/FRase	NADH oxidase / flavin reductase
Npx	NADH peroxidase
NR	nitroreductase
OD_{600}	optical density measured at 600 nm
PAGE	polyacrylamide gel electrophoresis
PCR	polymerase chain reaction
PDB	protein data bank
PSI-BLAST	position specific iterative-basic local alignment search tool
PTU	6-n-propyl-2-thiouracil
Redox	oxidation-reduction
RMSD	root mean square deviation
RPM	rotations per minute
SDS-PAGE	sodium dodecyl sulfate-polyacrylamide gel electrophoresis
S_NAr	nucleophilic aromatic substitution mechanism
SOC	super optimal catabolite-repression broth
TBST	tris-buffered sailine with tween-20
$S_{RN}1$	radical-mediated nucleophilic substitution mechanism
T_3	3-[4-(4-hydroxy-3-iodophenoxy)]-3,5-diiodophenylalanine
T_4	3-[4-(4-hydroxy-3,5-diiodophenoxy)]-3,5-diiodophenylalanine
TD	tetrachlorohydroquinone dehalogenase

TG	thyroglobulin
TPO	thyroid peroxidase
UCSF	University of California at San Francisco
V_{max}	maximum velocity
ZYP-0.8G	rich growth medium for preparation of frozen stocks for autoinduction
ZYP-5052	rich medium for autoinduction

Chapter 1

Background and Significance

1.1 Introduction to iodine metabolism in mammals

Even prior to the identification of the thyroid as the gland involved in goiter, (enlargement of the thyroid gland), goiter was observed more frequently in landlocked areas, which are typically iodine deficient.[2] Coindet formalized the connection between iodine and thyroid enlargement as early as 1820, when he identified potassium iodide for treatment of goitrous patients.[3] Few other advances were made in treatment of thyroid disorders until Kendall, inspired by Baumann's successful treatment of hypothyroid patients with thyroid extracts, isolated thyroxine from the thyroid gland in 1915.[4, 5] Although the thyroid has been extensively studied since Baumann's work, many of its processes remain poorly characterized at the molecular level.

This dissertation focuses on iodotyrosine deiodinase (IYD), a thyroidal reductive dehalogenase, which has received little attention despite its significant role as the only salvage pathway in iodine homeostasis (Figure 1-1). IYD catalyzes the reductive dehalogenation of mono- and diiodotyrosine (MIT and DIT, respectively), which are the byproducts of thyroid hormone production. IYD activity was first described over 50 years ago, but the enzyme failed to garner much attention until recently.[6-8]

Iodine is essential to metabolic regulation in mammals. For example, the heavily iodinated thyroid hormones (Figure 1-2), thyroxine or T_4 (3-[4-(4-hydroxy-3,5-

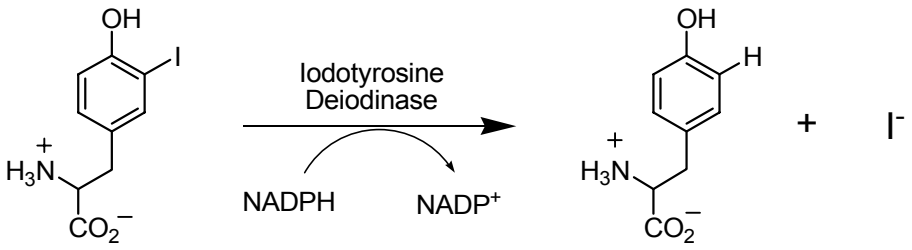

Figure 1-1. Iodotyrosine deiodinase catalyzes the dehalogenation of mono- and diiodotyrosine.

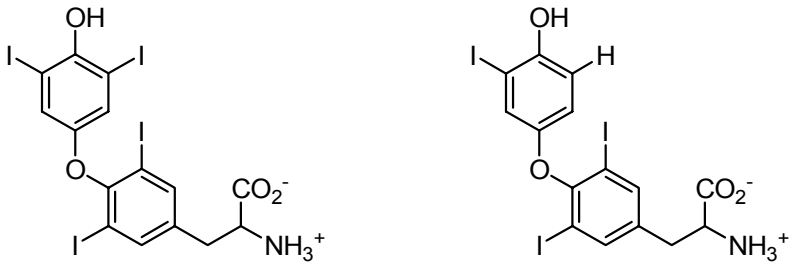

T_4 T_3

Figure 1-1. The thyroid hormones, T_4 and T_3.

diiodophenoxy)-3,5-diiodophenylalanine) and T_3 (3-[4-(4-hydroxy-3-iodophenoxy)-3,5-diiodophenylalanine), elicit a broad range of metabolic and developmental effects at both the organismal and molecular levels.[9, 10] The production of thyroid hormones is regulated by the hypothalamus and pituitary.[11] T_4 is often considered a prohormone to T_3, because T_3 is several-fold more active biologically, and approximately 80% of T_3 is derived from extrathyroidal deiodination of T_4.[11] In contrast, T_4 is produced exclusively by the thyroid, where it is stored in the follicular lumen until its release is stimulated by thyroid stimulating hormone.[11]

1.2 The chemistry and biology of iodothyronine deiodinase

Iodotyrosine deiodinase is not the only reductive dehalogenase associated with iodine homeostasis and metabolic regulation. T_4 is converted into T_3 and other deiodinated metabolites by three isoenzymes known as iodothyronine deiodinase (ID), (Figure 1-3).[12, 13] 5′-Deiodination (outer-ring deiodination) is performed by 5`-deiodinase type I (ID1) and 5′-deiodinase type II (ID2).[14] 5-Deiodination (inner-ring deiodination) is catalyzed by ID1 and a third type deiodinase (ID3).[14] The three enzymes are differentiated on the basis of substrate and cofactor preferences, kinetics, susceptibility to inhibitors, and tissue distribution.

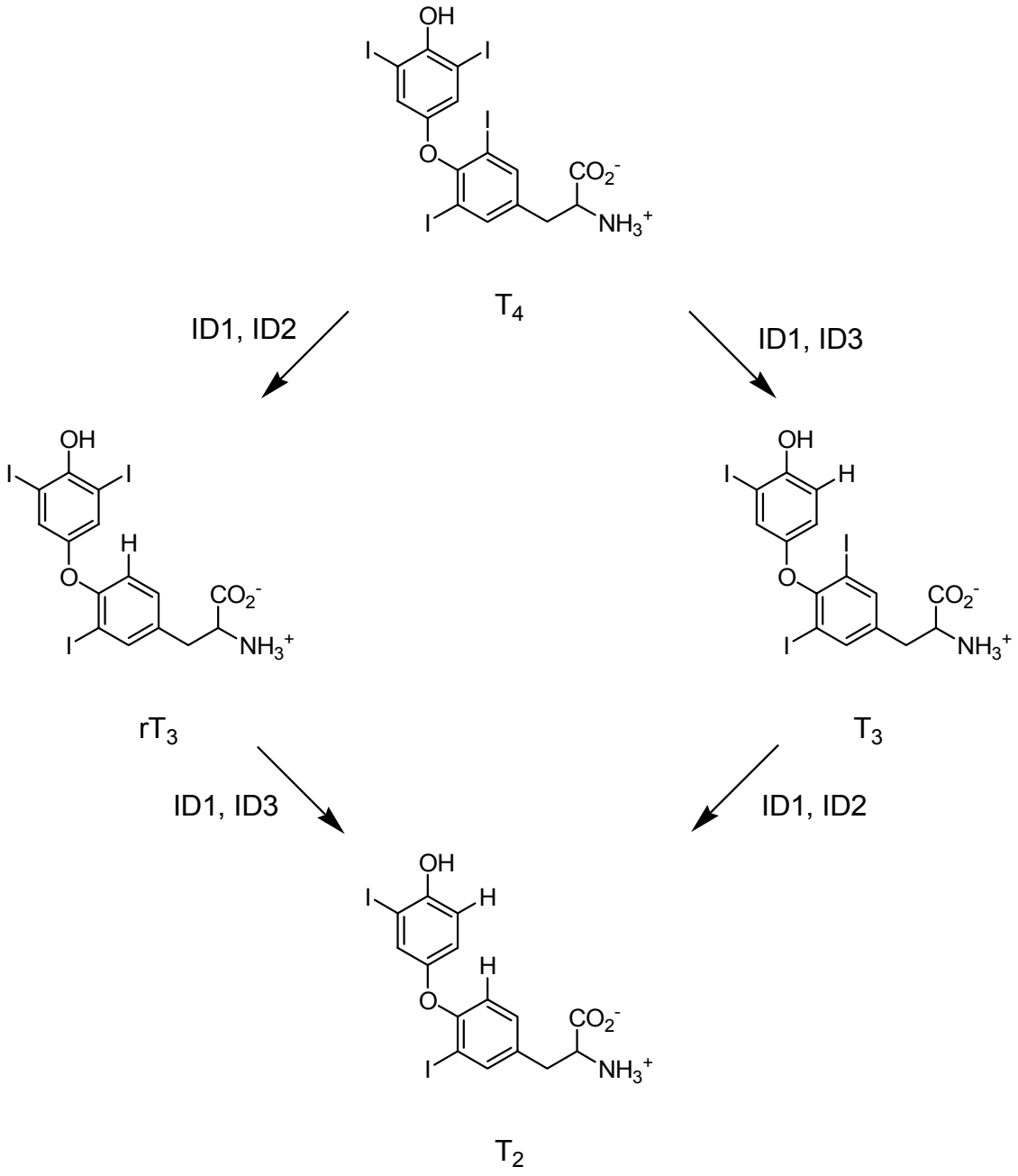

Figure 1-2. Three isoenzymes of iodothyronine deiodinase, a reductive dehalogenase, catalyze the interconversion of thyroid hormones. Only ID1 catalyzes both 5- and 5′-deiodination.

Type I iodothyronine deiodinase. Type I iodothyronine deiodinase (ID1) is the best characterized of the three selenocysteine-containing isoenzymes that catalyze thyroid hormone deiodination. Unlike ID2 and ID3, ID1 catalyzes both inner- and outer-ring deiodination.[14] ID1 accepts substrates in the order of rT3 >> T_4 > T_2 and does not accept

MIT or DIT.[14] While the identity of the physiological reductant is not known, ID1 utilizes dithiothreitol (DTT) (1-10 mM) as a reductant *in vitro* and exhibits ping-pong, bi bi kinetics with T_4 and reduced thiol as substrates indicative of a two-step mechanism.[15, 16] The enzyme is susceptible to inhibition by 6-n-propyl-2-thiouracil (PTU), iodoacetate salts, aurothioglucose, and iopanoate salts.[12] Hepatic ID1 has been suggested to be responsible for the deiodination of circulating T_4 for systemic use, but the enzyme is also expressed to some extent in thyroid, kidney, liver, and the central nervous system (CNS).[12]

Type II iodothyronine deiodinase. Type II iodothyronine deiodinase (ID2) also catalyzes outer-ring deiodination, but it is putatively responsible for production of T_3 for localized use in peripheral tissues, in contrast to ID1, which generates T_3 for systemic use.[14, 17] ID2 preferentially accepts T_4 over rT_3 as substrate.[12, 18] *In vitro,* ID2 also requires reduced thiols for catalysis, but at significantly higher levels (>10 mM DTT) than ID1.[14] Kinetic studies have shown that a sequential mechanism is operative in which both substrate and thiol-cofactor are present before product conversion.[19, 20] High concentrations of T_4 and of rT_3 inhibit ID2.[21] Resistance to inhibition by PTU is used to distinguish ID2 from ID1, although some studies have suggested that PTU concentrations greater than 100 μM inhibit ID2 under some circumstances.[22, 23] ID2 is highly expressed in pituitary, brain, brown adipose, and placental tissues.[24-27]

Type III iodothyronine deiodinase. Type III deiodinase (ID3) catalyzes inner-ring, or 5-deiodination, of T_4 and T_3 to yield, respectively, rT_3 or T_2, both of which exhibit greatly decreased biological activity relative to T_4 and T_3.[28] Neither rT_3 nor T_2 binds to nuclear T_3 hormone receptors under physiological conditions.[29, 30] Instead, the

two compounds have been suggested to play a regulatory role in T_3 production.[12, 31-33] T_4 and T_3 are substrates for the enzyme and their 4′-*O*-sulfation strongly stimulates the rate of their deiodination.[34] In contrast, 4′-*O*-sulfation of T_4 completely obviates deiodination by ID1.[34] As with ID1 and ID2, reduced thiols are cofactors *in vitro*, but the cofactor must be present much higher concentrations (>70 mM DTT), compared to ID1 and ID2 (1-10 mM and >10 mM, respectively).[12, 33] Kinetic studies have indicated a sequential mechanism similar to that of ID2.[35] The enzyme is inhibited by iopanoate and thiouracil derivatives.[14, 18] High concentrations of ID3 are found in all tissues except those expressing high concentrations of ID1 (*i.e.,* liver, kidney, and thyroid).[33]

Iodothyronine deiodinase mechanism. A molecular mechanism for the IDs has been proposed[19, 32] (Figure 1-4) and may provide a model for IYD due to their similar dehalogenation reactions. A conserved, redox-active selenocysteine residue is responsible for catalysis in ID, although an active-site sulfhydryl residue was previously suspected based on *N*-ethyl maleimide susceptibility.[36, 37] The presence of selenocysteine in the ID active site has now been observed in species as diverse as frogs, chickens, fish, and humans.[14] The mechanism is thought to proceed by aromatic-ring protonation or by tautomerization of the phenolic hydroxyl, followed by nucleophilic attack on iodine by the selenide.[32] The transient selenyl iodide intermediate is reduced *in vivo* by an unknown cofactor or by thiols *in vitro*.[32] Halophilic attack by thiolates[38, 39] and selenides[40] has been reported in non-enzymatic reactions, so it follows that iodothyronine deiodinases could behave in this manner.

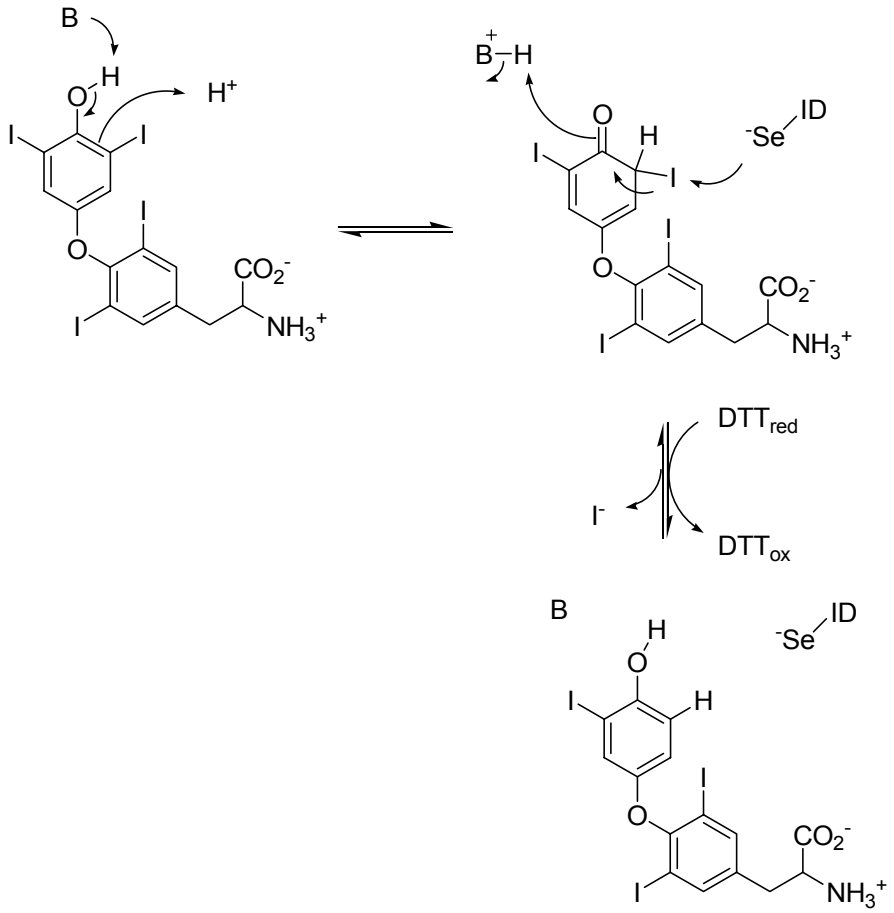

Figure 1-3. Mechanism of iodothyronine deiodinase. Tautomerization of the the phenol is followed by nucleophilic attack on iodine by the conserved selenocysteine residue.

1.3 Intrathyroidal iodine metabolism

In response to iodide's relative scarcity in many parts of the world, the thyroid has evolved a remarkably efficient system of iodide uptake and sequestration to ensure that sufficient I^- is available for thyroid hormone synthesis (Figure 1-5). Iodide is transported into the thyroid from the blood stream by the Na^+/I^- symporter (NIS), a transmembrane protein expressed in the basal cell membrane of the thyroid's follicular cells.[41] The NIS is capable of concentrating I^- by a factor of 20- to 50-fold over the plasma concentration in the normal thyroid. Iodide influx into the cell is an ATP-dependent process that is regulated by thyroid stimulating hormone.[41, 42] As the Na^+-K^+ ATPase lowers the

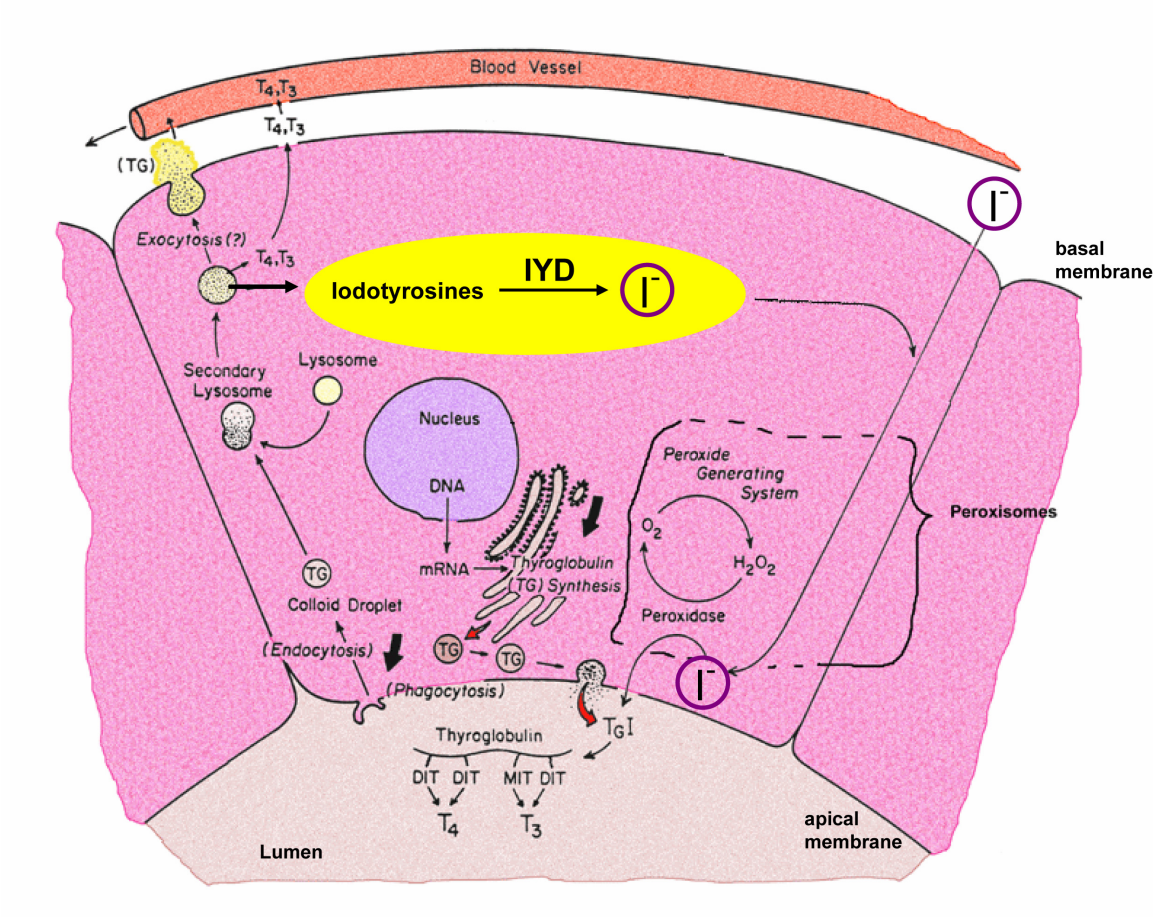

Figure 1-4. Intrathyroidal iodine metabolism. Iodide is transported into thyrocytes at the basal membrane and incorporated into tyrosine residues in thyroglobulin (TG). Iodide is salvaged from iodotyrosines via a single-enzyme pathway for reincorporation into thyroid hormones. Free iodide is circled in purple and the IYD salvage step is highlighted in yellow. Figure adapted.[1]

cytoplasmic concentration of Na^+, a driving force for concurrent transport of I^- is created.[41, 43] This driving force allows the efficient uptake of I^- despite its low plasma concentration (<1 μg/mL).[41, 43]

Iodide is incorporated into thyroglobulin (TG), the main protein component of the thyroidal colloid, near the apical cell membrane by thyroid peroxidase (TPO). Significant dispute exists over the mechanism of this enzyme.[13, 44-51] Three possible iodination mechanisms that have received the most attention include a free radical mechanism, iodonium ion (I^+) as the iodinating species, and hypoiodite (OI^-) as the active

species, although none of these has been demonstrated conclusively.[44, 48-51] Following iodination of the tyrosyl residues, two iodotyrosines, most commonly diiodotyrosines, are coupled by TPO, *via* an iodophenyl radical, to yield T_4 or T_3 and dehydroalanine.[44, 45, 52, 53] Mature TG is then secreted into the follicular lumen, where it is stored until needed.[46]

Before the coupled iodotyrosine residues can be released as thyroid hormones, mature TG must be internalized into the cell from the follicular lumen. The colloid is taken up by micropinocytosis into small vesicles that fuse with endosomes, where the TG is proteolyzed to release free thyroid hormones, T_4 and T_3, and any uncoupled MIT and DIT residues.[13, 46] The free thyroid hormones are very hydrophobic and must be transported to peripheral cells bound to serum transport proteins.[33]

Mono- and diiodotyrosines released during TG proteolysis cannot be directly reutilized for TG biosynthesis and are deiodinated by iodotyrosine deiododinase, the subject of the present study. The salvaged iodide and tyrosines are then available for TG synthesis and are thus recycled as a means of conserving the environmentally-scarce iodide.

1.4 Iodotyrosine deiodinase

Early clinical observations of iodotyrosine deiodination. Dehalogenation of iodotyrosines was first observed by analysis of dog liver slices.[8] Soon after, some cases of hypothyroidism in patients suffering from congenital goiter and/or cretinism were attributed to deficient IYD activity.[6, 7, 54] All of these patients excreted higher than normal levels of radioactive iodotyrosines following administration of $^{131}I^-$.[6, 7, 54]

Biochemical characterization of iodotyrosine deiodinase. The earliest enzymology studies of IYD were performed on thyroid sections and homogenates, but in

the 1970's, the enzyme from bovine thyroid was purified and partially characterized.[55] The approximately 42 kDa homodimeric enzyme reportedly bound a single flavin mononucleotide (FMN) per homodimer ($K_a = 1.47 \times 10^8\ M^{-1}$), which suggests that the prosthetic group is bound to only one peptide chain or is somehow cooperatively shared between the two subunits.[55]

NADPH had been previously identified as the native electron donor for the microsomal enzyme;[56] however, NADPH-responsive activity was lost upon steapsin or cholate solubilization of the microsomal enzyme during isolation.[55, 57] The very low oxidation-reduction (redox) potential (-412 mV) of the fully reduced enzyme, in combination with the loss of NADPH responsiveness upon solubilization, is suggestive of an as-yet-unidentified cofactor or reductase that mediates electron transfer between the NADPH ($E°' = -317$ mV)[58] and the IYD flavin.[55] As a result of the lost activity, addition of strong chemical reducing agents, such as dithionite (-660 mV) or methyl viologen (-446 mV), is necessary when performing assays *in vitro*.[55, 57, 59]

Coupled assays in which NADPH-responsive activity is restored after solubilization have been achieved using systems such as NADPH/methyl-viologen//NADP/cytochrome C reductase and NADPH/ferrodoxin//ferrodoxin/NADP reductase.[60] In the search for an electron mediator, IYD was treated with a variety of metal chelating agents. Dithizone, a potent chelator of Co^{+2}, Cu^{+2}, and Hg^{+2}, had no effect on the enzymatic activity.[60] The iron-chelating reagents o-phenanthroline and 2,2´-dipyridyl were found to reduce activity in the microsomal enzyme by 50% and 48%, respectively, while ethylenediaminetetraacetic acid (EDTA) had no effect.[60] However, EDTA is known to have difficulty probing highly hydrophobic pockets in some enzymes.

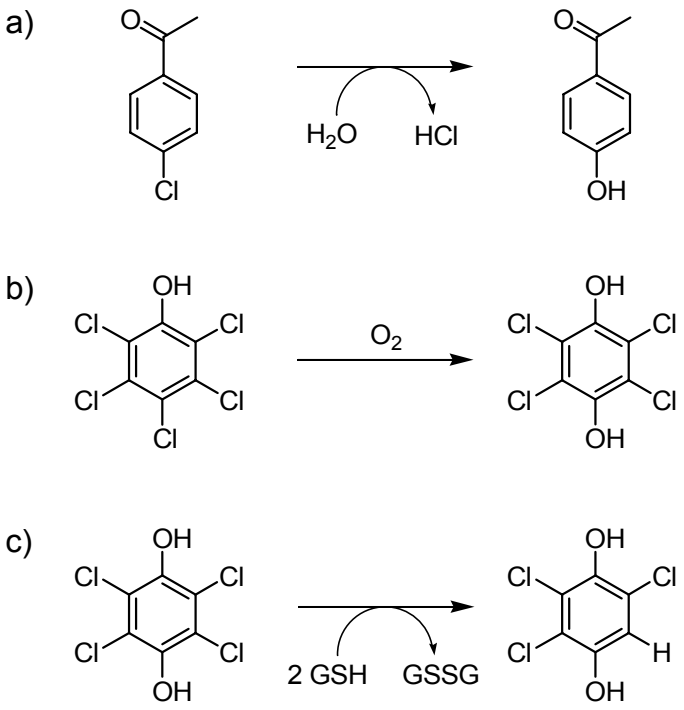

Figure 1-5. Bacterial dehalogenases have been categorized by mechanism into three groups: a) hydrolytic, b) oxygen dependent, and c) reductive.

Despite the inconsistent results with the iron chelators, iron remains the most likely mediator in the electron transfer from NADPH to IYD.[60] The metal chelators inhibited only NADPH-responsive activity suggesting that the reductase is affected, not IYD.[60, 61]

1.5 The catalytic mechanism of iodotyrosine deiodinase

Dehalogenases have been mechanistically categorized as hydrolytic, oxygen-dependent, or reductive dehalogenases (Figure 1-6).[62, 63] Hydrolytic enzymes utilize water as a source of hydroxyl groups to replace the halogen, elemental oxygen atoms are used in replacement by oxygen dependent enzymes, and reductive dehalogenation involves replacement of the halogen by hydrogen following some electron transfer events.

Though there is no precedent for flavin-mediated reduction of aryl halides, other dehalogenases can provide a framework within which to understand IYD catalysis.

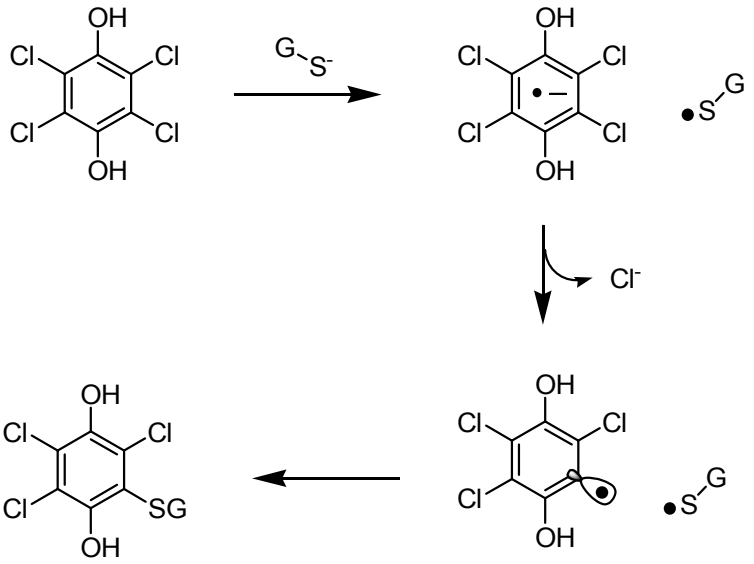

Figure 1-6. $S_{RN}1$-like mechanism proposed for the initial steps catalyzed by tetrachlorohydroquinone dehalogenase.

Within the realm of reductive dehalogenation, two pathways are commonly found: 1) replacement of the halogen by hydrogen, or hydrogenolysis, and 2) elimination of two halogens from neighboring carbons, or vicinal reduction, to yield an alkene.[62, 64] An electron donor is required in all cases of reductive dehalogenation, and, in all known examples, the halogen is released as the halide anion.[62, 63, 65] Substrates include aliphatic, olefinic, and aromatic halohydrocarbons.[62, 63, 65]

Possible anion radical ($S_{RN}1$) mechanism for IYD catalysis. Flavins mediate both one- and two-electron processes, so both single-electron transfer (2 x $1e^-$) and two-electron transfer (1 x $2e^-$) pathways should be considered. Delivery of an electron to substrate would yield a radical anion intermediate, which then could lose its halogen substituent in a unimolecular fashion. An $S_{RN}1$ mechanism (Figure 1-7) was proposed for the initial steps catalyzed by tetrachlorohydroquinone dehalogenase (TD) from *Sphingobium chlorophenolicum*. Recently however, 2,3,5-trichloro-6-S-glutathionylhydroquinone (GS-TriCHQ) (the final product depicted in figure 1-7) was

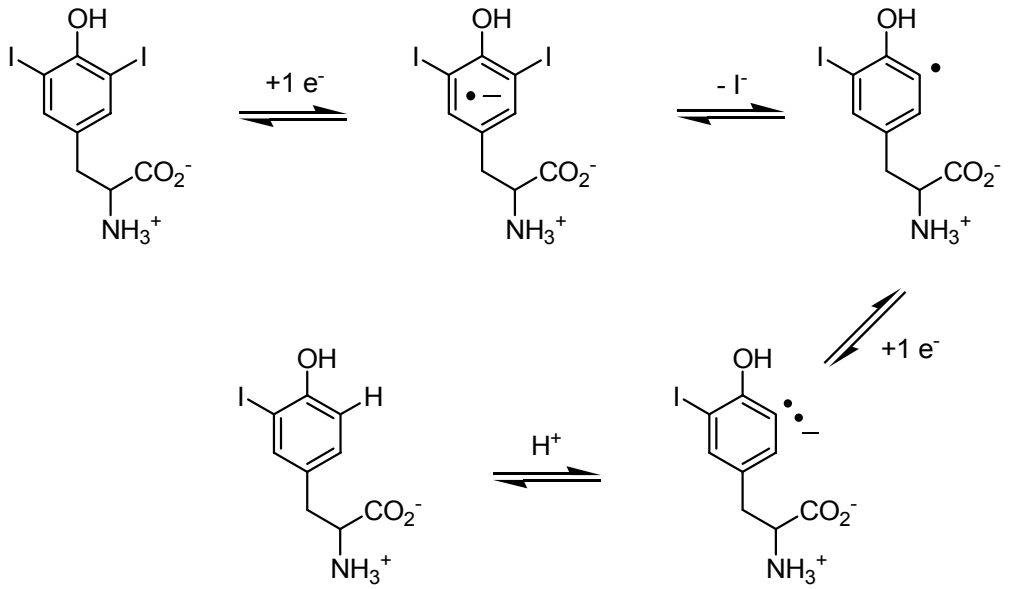

Figure 1-7. Possible one-electron mechanism for dehalogenation by IYD via an $S_{RN}1$-pathway.

found to be kinetically incompetent in the dehalogenation reaction, which eliminated nucleophilic aromatic substitution as a mechanistic pathway. An alternative mechanism will be described later in this section.

Despite the exclusion of the $S_{RN}1$ mechanism in TD, a radical anion pathway should still be considered for IYD (Figure 1-8), as *o*-iodophenols have been found to readily undergo the $S_{RN}1$ reaction and have even been suggested to experience steric acceleration.[66, 67] However, deprotonation of the phenol increases the electron density on the aromatic ring and has been found to inhibit the $S_{RN}1$ reaction pathway.[68] The relatively low pKa for MIT (8.53)[69] and DIT (6.5)[70] suggests that it is possible that the phenolate is the species present in the active site of IYD, decreasing the likelihood of the $S_{RN}1$ pathway. Furthermore, decreased dehalogenation rates have been noted for iodotyrosine substrates with electron withdrawing groups.[61] The $S_{RN}1$ reaction is accelerated by electron withdrawing groups, although addition of a nitro substituent to the aromatic ring completely eliminates the $S_{RN}1$ pathway.[71, 72]

Figure 1-8. S_NAr reaction catalyzed by glutathione *S*-transferase.

Possible S_NAr mechanism for IYD catalysis. Evidence for two-electron reductions mediated by flavin-containing enzymes is readily available in the literature and basic enzymology textbooks. For example, glutathione *S*-transferases (GSTs) catalyze the S_NAr addition of the tripeptide glutathione (GSH) to a wide variety of electrophiles, which can result in adventitious dehalogenation of halogenated substrates (Figure 1-9).[73-78] The widely used spectrophotometric assay for GST activity monitors the addition of GSH to 1-chloro-2,4-dinitrobenzene, a well characterized S_NAr reaction.[79]

An S_NAr-like reaction by IYD (Figure 1-10) could involve formation of a

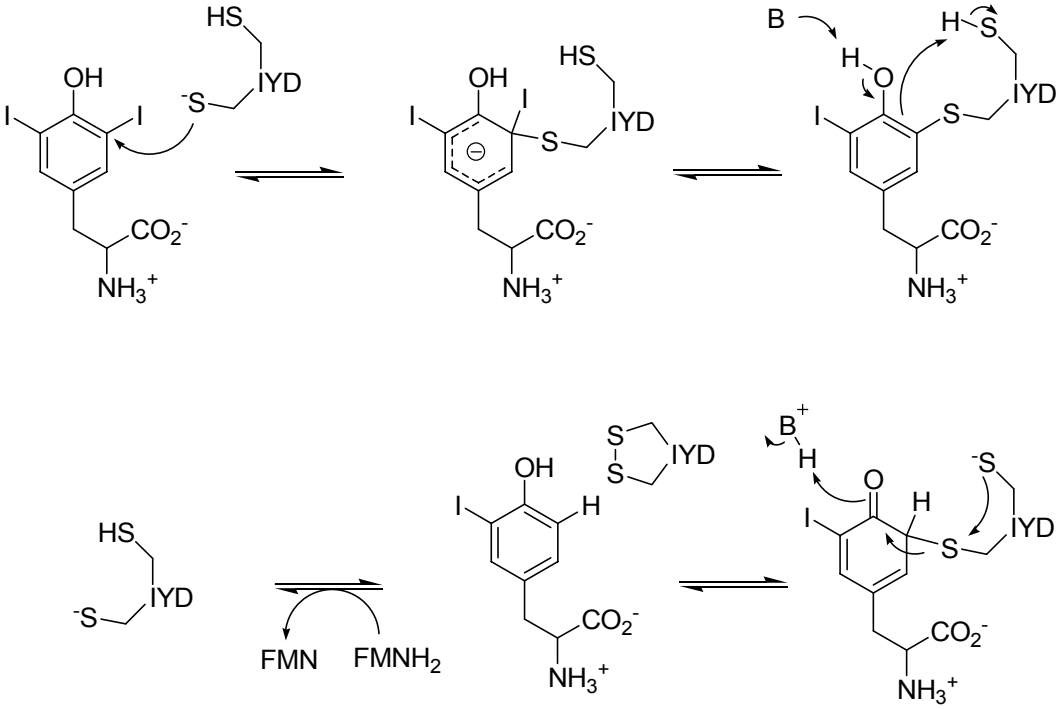

Figure 1-9. Suggested two-electron mechanism for IYD catalysis via an S_NAr-like pathway.

Meisenheimer complex through nucleophilic attack by a cysteine-thiolate residue to form an enzyme-substrate thioether, similar to GSTs. The enzyme-substrate adduct could then be reduced by another nearby cysteine thiolate in a process similar to that of the flavoprotein disulfide oxidoreductases (*e.g.,* lipoamide dehydrogenase, glutathione reductase, and trypanothione reductase).[80-82] Yeast glutathione reductase[82] provides a representative example of electron flow for possible reduction of the disulfide bond formed during an IYD S_NAr reaction.

Proposed mechanism for IYD catalysis. The molecular basis of IYD catalysis most likely consists of strategies similar to those used by ID and TD. The mechanism of ID was discussed in section 1.2. An $S_{RN}1$-like mechanism was proposed for TD earlier in this chapter; however a proposed glutathionyl intermediate was found to be kinetically incompetent. An alternative mechanism (Figure 1-11) has been suggested to proceed via a non-aromatic tautomer, similar to tyrosine phenol lyase[83] and ID (Figure 1-4). The

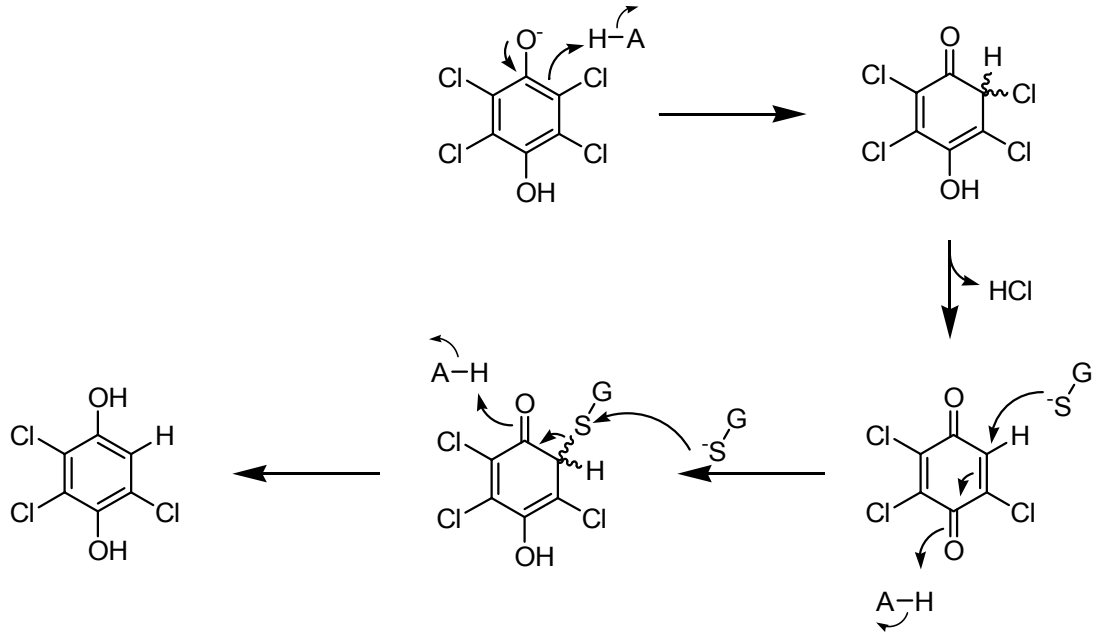

Figure 1-10. Mechanism proposed for tetrachlorohydroquinone dehalogenase.

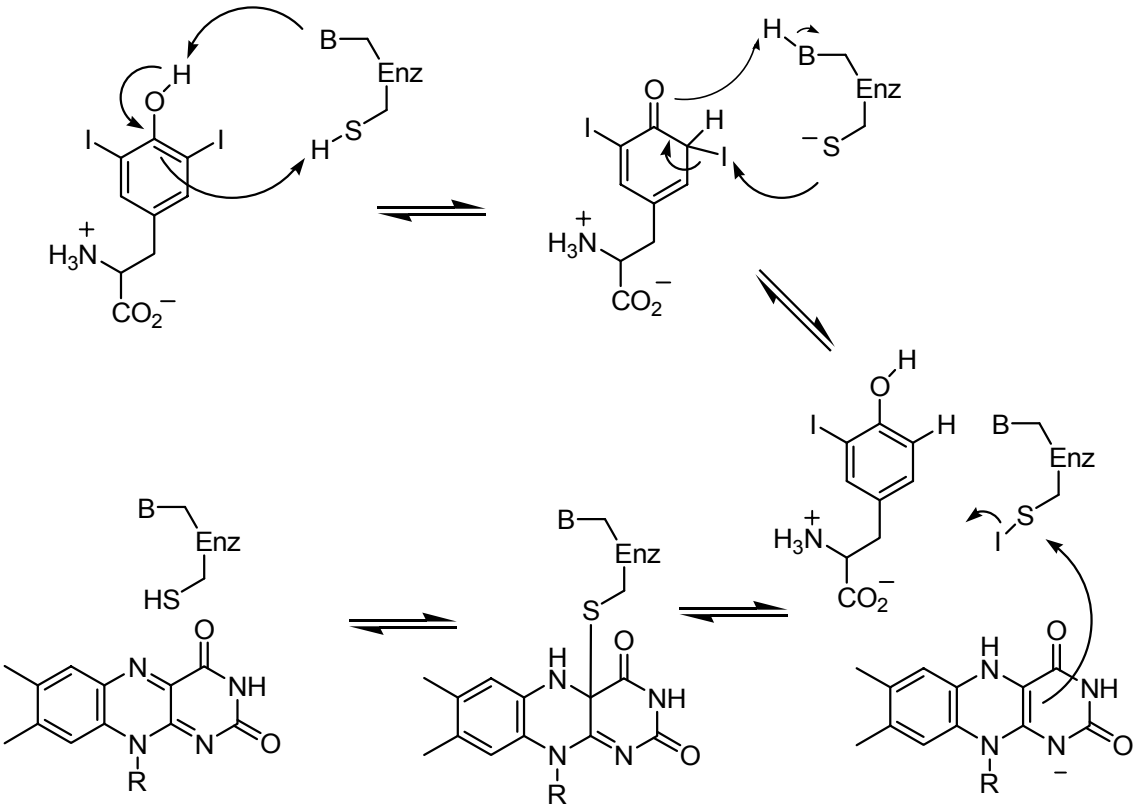

Figure 1-11. Proposed mechanism of catalysis for IYD. Tautomerization of the phenol yields a highly electrophilic intermediate for nucleophilic attack on iodide. The cysteine-sulfenyl iodide is reduced by electron transfer from the bound flavin.

"ketonized" substrate undergoes chloride elimination to generate trichlorobenzoquinone, which is attacked in Michael-type fashion by glutathione.

If IYD promoted such a tautomerization (Figure 1-12), the electrophilic character of the substrate would significantly increase. Rearomatization could then provide the driving force for nucleophilic attack by a cysteine-thiolate residue. A similar tautomerization has been proposed for the mechanism of chemical deiodination of *o*-iodo-hydroxylated arenes, including phenols, quinolols, and naphthols, by tertiary amines.[84] Furthermore, the chemical reduction of aryl iodides by thiols has been found to proceed via nucleophilic attack at iodide, not carbon.[38, 39]

The Rokita lab has previously reported that pyridonyl alanines are competitive inhibitors of IYD.[61, 85] The high affinity of D,L-3-(*N*-methyl-2-pyridon-5-yl)alanine (K_I = 24 nM) results from the keto-group of the pyridone mimicking the proposed tautomeric intermediate.[61, 85] The unsubstituted D,L-3-(*N*, 3-dimethyl-2-pyridon-5-yl)alanine exhibits a greatly decreased binding affinity (K_I = 11,000 nM) because it undergoes tautomerization in aqueous environments.[61, 85]

Nucleophilic attack at iodide by an active site cysteine from IYD would result in formation of a cysteine-sulfenyl iodide (Cys-SI). The sulfur in the Cys-SI would be in the same oxidation state as found in enzymes bearing cysteine-sulfenic acids, such as NADH peroxidase (Npx) and the peroxiredoxins.[86-89] Unlike other flavoprotein reductases, Npx contains only a single redox-active cysteine residue that is converted to a cysteine-sulfenic acid intermediate by nucleophilic attack on the terminal oxygen of the C_{4a} peroxide derivative of the bound flavin.[89] IYD may catalyze a simlar electron transfer from the bound flavin to the cysteine-sulfenyl iodide to regenerate active enzyme.

1.6 Specific Aims.

The long term goal of this project has been, and remains, to understand the basis for iodotyrosine deiodinase catalysis at the molecular level. Toward that end, my research addressed the following:

1) IYD has been recalcitrant to characterization at the molecular level because it is associated with microsomal membranes.[55] After persistent effort, however, the putative IYD was purified and submitted for protein sequence determination.[61, 90] This

dissertation confirms the identity of the cDNA that encodes IYD and examines aspects of its evolutionary origins through bioinformatics analysis.

2) Development of a structural model for iodothyronine deiodinase has provided the opportunity to examine previously its structure and mechanism.[91] Determination of IYD's protein sequence permitted development of a three-dimensional model that provides insight into the mechanism. Furthermore, the structural model was useful in development of a heterologous expression system for a soluble mutant of IYD, which eliminates the need for tedious extraction from thyroid microsomes.

3) Increased availability of IYD offers the opportunity to probe its catalytic mechanism using techniques that have been developed since the 1970's when the enzyme was first characterized. The redox potential of IYD is at the extreme low end of the spectrum of values observed for flavoproteins.[92] As such, the role that structure plays in the electron transfer mechanism will be probed to gain a more thorough understanding of IYD catalysis.

Chapter 2

Iodotyrosine Deiodinase Is the First Mammalian Member of the NADH Oxidase / Flavin Reductase Superfamily

2.1 Introduction

Iodotyrosine deiodinase (IYD) was purified from a steapsin-treated thyroid particulate fraction to near homogeneity in 1979, using ammonium sulfate precipitation followed by chromatography on DEAE-cellulose, hydroxylapatite, and gel filtration.[55] Attempts by the Rokita lab to repeat this purification failed.[61] However, an alternative purification strategy was developed using limited trypsinolysis, followed by anion exchange (Q fast flow), dye (Cibacron blue 3GA), and hydrophobic (phenyl-Sepharose) chromatography, successively (Figure 2-1).[61, 90] The final protein isolate exhibited a 500-fold increase in specific activity, relative to the starting Triton X-100 solubilized microsomal preparation.[61, 90]

The major protein isolated by the procedure was excised from a denaturing polyacrylamide gel equivalent to that illustrated in Figure 2-1 and submitted for limited

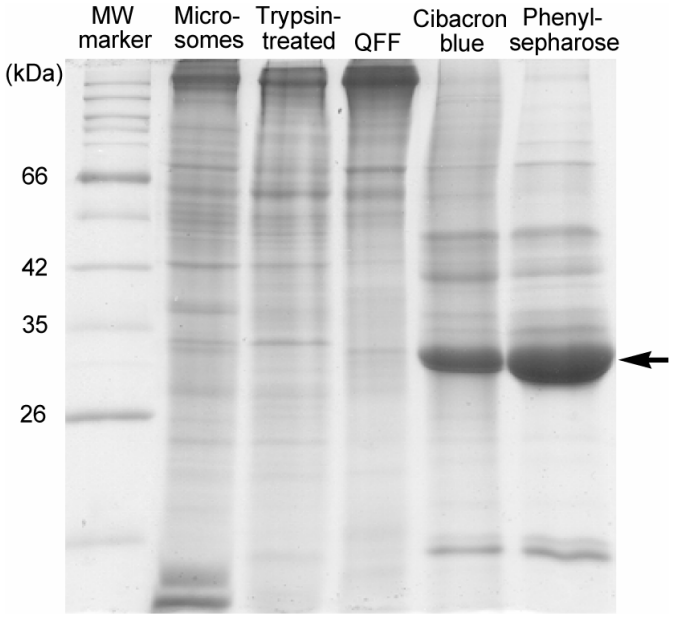

Figure 2-1. Purification of IYD, monitored by denaturing polyacrylamide gel electrophoresis. The arrow indicates the band submitted for sequencing of the putative IYD.

proteolysis and sequencing.[61, 90] The resulting peptides did not coincide with any known proteins, as determined by their molecular ions (MALDI-TOF MS).[61, 90, 93] Peptide fragments were also separated by reverse-phase chromatography, and four were selected for Edman degradation, yielding sequences of ARPWVDEDLKDSTDV, RSQEFYELLNK, LLMLLPVGYPSK, and VPMEVIDNVIK.[61, 90] All of these sequences were present in a single protein annotated as a flavoprotein from genomic sequencing of various mammals.[61, 90, 93]

Furthermore, the protein fraction with deiodinase activity from the Cibacron blue 3GA column was analyzed using a two-dimensional electrophoretic strategy (Figure 2-2).[61, 90] IYD activity was observable in a single band of the first dimension native gel.[61,

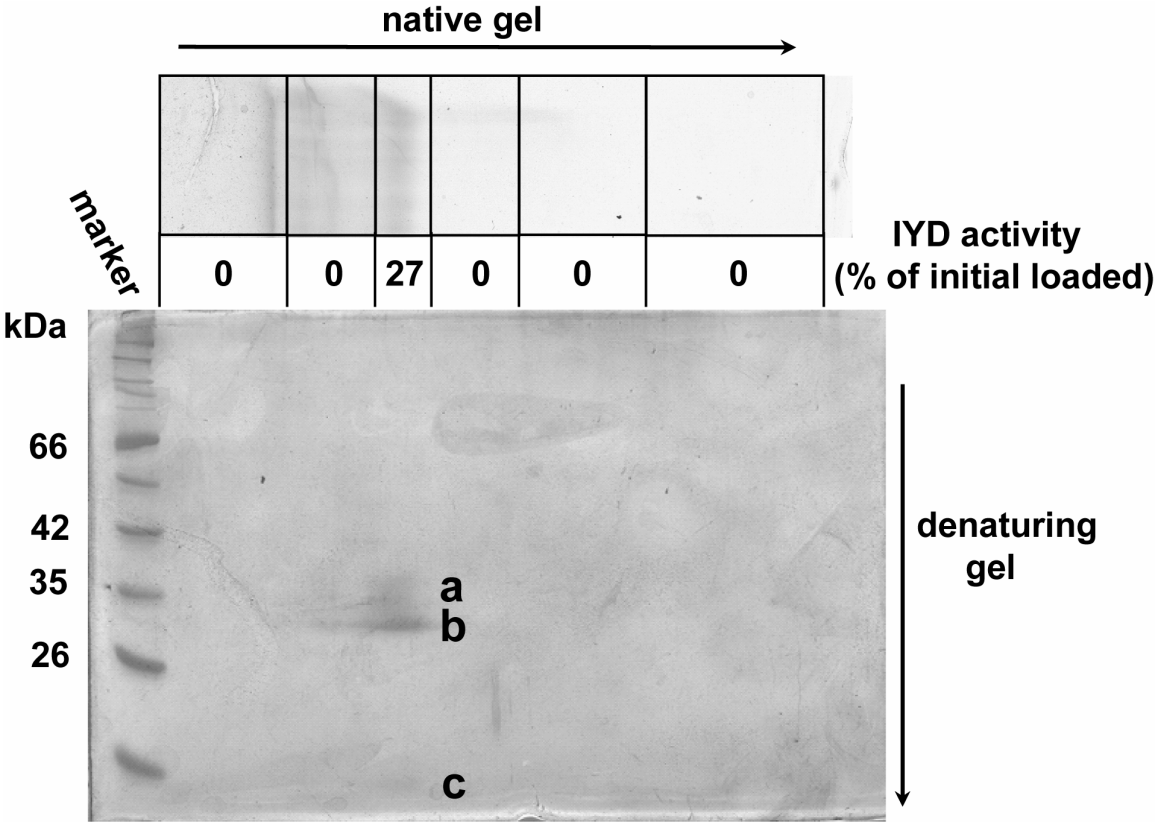

Figure 2-2. Two-dimensional electrophoretic analysis of soluble IYD fragment. IYD activity was detected in a single region of the native gel. Three bands (a, b, and c) from the second dimension denaturing gel were submitted for amino acid sequencing.

[90] The second-dimension denaturing gel provided three bands corresponding to the putative IYD.[61, 90] Mass spectrometric sequencing of band a identified four sequences (MVVESAYEVIK, FIIPQIVK, IVVVTAGVR, NSADTLWGIQK) that were present in porcine lactate dehydrogenase (LDH).[61, 90] Differential inhibition of LDH and IYD activities using oxamate, a competitive inhibitor of LDH, confirmed the inability of LDH to promote deiodination.[61, 90] Mass spectrometry and Edman degradation of bands b and c yielded additional sequences from the putative IYD: EATVPD(I/L)PR and KPLDQIMVT.[61, 90]

Our laboratory has proposed a mechanism for IYD,[85, 90] but the poor quality and availability of the enzyme from porcine microsomes has prevented further study. Chromatographic purification and sequencing of porcine IYD has identified the gene that putatively encodes IYD.[61] To confirm the identity of the gene encoding IYD, active enzyme has been expressed in human embryonic kidney (HEK293) cells. In addition, the amino acid sequence data has been used to analyze the relationship between IYD and ID. Furthermore, the similarity of bacterial proteins belonging to the NADH oxidase/flavin reductase (NOX/FRase) superfamily identifies IYD as the first mammalian member of this structural class.

2.2 Experimental Procedures

Materials. Porcine thyroids were obtained from Hatfield Quality Meats (Hatfield, PA). Oligodeoxynucleotide primers were synthesized by Integrated DNA Technologies, Inc. (Coralville, IA). All restriction enzymes, Vent polymerase, and DNA T4 ligase were obtained from New England Biolabs (Ipswich, MA), unless specified otherwise. All other reagents were molecular biology grade or highest grade available

and used without further purification. [^{125}I]-Diiodotyrosine (D^{125}IT) was prepared from DIT, as described in the literature,[59] using carrier-free Na^{125}I purchased from Perkin Elmer (Wellesley, MA).

General methods. Microsomal IYD was isolated from porcine thyroids, as described in the literature, and solubilized using 1.5% Triton X-100 in lieu of steapsin.[59, 61] IYD activity was assessed by monitoring $^{125}I^-$ release in a discontinuous assay[59] using the following modified equation to calculate the rate.

Activity Assay. Typically, protein preparations (100 μL) were added to 300 μL of Solution 2 (1.66 mM methimazole, 0.1 mM flavin adenine dinucleotide (FAD), 666 mM potassium chloride, 333 mM potassium phosphate (pH 7.4), and 166 mM 2-mercaptoethanol), 100 μL 100 mM DIT, 300 μL ddH_2O, and 100 μL D^{125}IT (~50 mCi/mmol). The reaction was initiated by addition of 100 μL 10 % sodium dithionite (w/v) in 5 % sodium bicarbonate (w/v). The samples were incubated for 30 minutes at 25 °C and quenched by addition of 100 μL 0.1 % DIT (w/v) in 0.1 N NaOH.

Total radioactivity for each reaction was determined from a 250 μL aliquot (S) to which 4.75 mL 10% acetic acid was added. The remaining assay mixture (850 μL) was applied to a cation exchange column (3.5 mL Bio-Rad AG 50W-X8 resin) and the effluent collected (A). The column was washed with 4.15 mL 10% acetic acid with the eluent collected in vial A. A second wash (5 mL) was collected in another vial (B). Each sample was diluted with 15 mL Scintisafe Plus 50% scintillation fluid and the radioactivity of the samples was measured on a Perkin-Elmer 1600TR scintillation counter.

$$F_1 = \frac{\frac{dpm\ A + dpm\ B}{0.85}}{\frac{dpm\ S}{0.25}} \qquad \text{equation 1}$$

The fraction F_1 is the percent of iodide released during the assay and is calculated according to equation 1, where dpm S, dpm A, and dpm B are the ^{125}I contents of the three samples. F_1 is corrected by subtracting the background value, F_0, (calculated according to equation 1), the percent of iodide in an assay mixture lacking enzyme. The

$$(F_1 - F_0)\ X\ \frac{60\ min\ hr^{-1}}{30\ min}\ X\ 10\ nmol\ X\ 2 \qquad \text{equation 2}$$

rate (equation 2) is calculated by multiplying the corrected F_1 value by a factor to convert the incubation time (30 minutes) into hours and by the initial amount of substrate present in the assay (e.g. 10 nmol). The result is multiplied by 2, because there are two possible deiodination sites, but statistically only one is labeled with ^{125}I. An additional factor of 1.3 (1100µL / 850 µL) used in the literature[59] was omitted when calculating the rate, as it is redundant because equation 1 calculates the fraction of iodide released during the assay.

Protein concentration was measured using the BCA assay, according to the manufacturer's (Pierce) instructions. Discontinuous Laemmli gels[94] were used to monitor protein using a Bio-Rad Mini Protean 3 gel electrophoresis system (8 cm (L) x 0.75 mm (W) x 8.5 cm (H)). The resulting distribution of proteins was detected by staining with Coomassie Brilliant Blue. The concentrations of unpurified IYD species were estimated by multiplying the total protein concentration by the fraction of IYD, determined using densitometry of bands on the denaturing PAGE gels (Appendix A).

Catalytic constants for IYD were determined by plotting the initial rate of iodide release versus DIT concentration, and the resulting data were fit to the Michaelis-Menten equation with Origin 7.0 (Microcal) (Appendix B).

Bioinformatic analysis of the gene encoding IYD. Sequence homology searches (BLAST) of the Genbank database[95] were performed using the porcine sequence data obtained by Jessica Friedman.[61] Multiple sequence alignments of the retrieved mammalian IYD sequences, iodothyronine deiodinases, and NADH oxidase/flavin reductase (NOX/FRase) superfamily members were obtained by analysis with ClustalW 1.83.[96] A phylogenetic tree was constructed using the mammalian IYD sequences and bacterial sequences for NOX/FRase proteins with previously determined x-ray crystal structutres that were retrieved in the BLAST search. The mouse cDNA sequence was analyzed for the presence of selenocysteine insertion elements by SECISearch 2.19,[97] available at http://genome.unl.edu/SECISearch.html. The secondary structure predictions of mouse IYD were carried out using 3D-PSSM Web Server[98] version 2.6.0 (http://www.sbg.bio.ic.ac.uk/~3dpssm/index2.html). Alignments were rendered using ESPript 2.2, available at http://espript.ibcp.fr/ESPript/ESPript/index.php.

Subcloning of *Mus musculus* IYD. The IYD cDNA (I.M.A.G.E. clone 5064638 from ATCC) was amplified by PCR using oligodeoxynucleotide primers 5′-AAGCTTAAGCTTCGATCCGCCACCATGTTTCTCCTCACCCCA-3′ and 5′-GCCGCGGCGGCCGCCTATACTGTCACCATGAT-3′ to generate blunt-ended DNA with BamH I and Not I restriction sites at its termini. The PCR product and (+)-pcDNA3.1/Zeo (Invitrogen) were digested with BamH I and Not I, and the vector was dephosphorylated with antarctic alkaline phosphatase (Invitrogen). The insert and vector

were then ligated using T4 DNA ligase and transformed into One Shot TOP10 cells (Invitrogen), following the manufacturer's instructions. Plasmid DNA was isolated from ampicillin-resistant colonies, using QIAprep spin miniprep kit (Qiagen), and characterized by digestion with EcoRI, PstI or StyI. Plasmids exhibiting the expected digestion pattern after gel electrophoresis (1% agarose, 125 V, 30 minutes) were sent for DNA sequencing (Gene Gateway).

Expression of *Mus musculus* IYD in HEK293. Human embryonic kidney (HEK) 293 cells were maintained in Dulbecco's modified Eagle's medium (DMEM, Invitrogen) supplemented with 10% fetal calf serum (Atlanta Biologicals) and 1% penicillin-streptomycin-glutamine (Invitrogen). The plasmid containing the IYD cDNA (12 μg) was mixed with 30 μL of Lipofectamine 2000 in Opti-MEM (Invitrogen) and then added to cells (~90% confluent) in 10 cm dishes. After 6 hours, the media was exchanged to DMEM. After 48 hours of incubation, the cells were washed with Dulbecco's phosphate buffered saline (Invitrogen) and harvested into the same solution. After centrifugation (300 x g) for 5 minutes at 4 °C, the cell pellet was resuspended in 1 mL 50 mM sodium phosphate (pH 7.2) supplemented with 0.25 M sucrose and 0.1 mM DTT. The cells were lysed by three cycles of freezing (liquid N_2) and thawing (37 ^{o}C), followed by three passages through a 20 gauge needle. The lysate was used in IYD assays without further purification.

2.3 Results and Discussion

Bioinformatic analysis of IYD. The amino acid sequence of the putative IYD is highly conserved throughout mammals, ranging from mouse to pig to human (Fig. 2-3). Amino acid identity within this group is greater than 80% and similarity is greater than

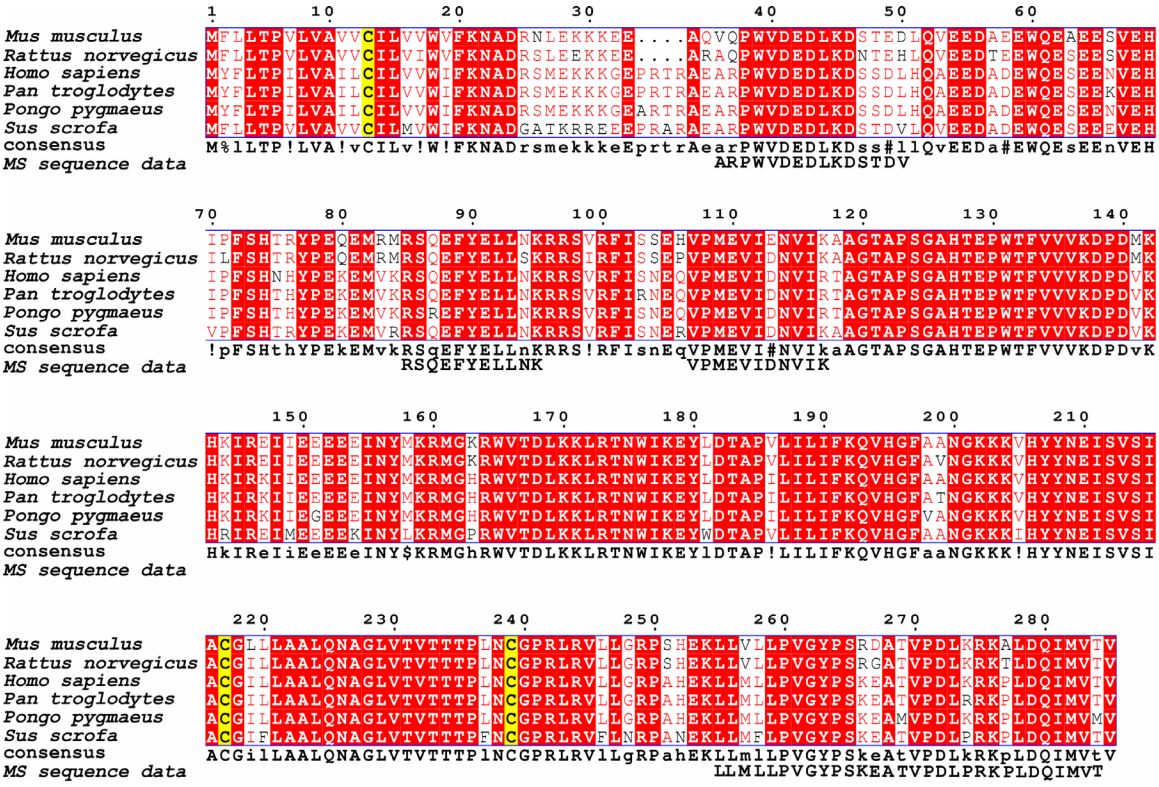

Figure 2-3. Amino acid sequence comparison of IYD. Sequence homology (BLAST) searches of the Genbank database were performed using the porcine sequence data obtained from isolated peptides. A multiple sequence alignment of mammalian IYD sequences was obtained using Clustal W 1.83. Sequence gaps are indicated by (.), the consensus sequence is shown below the alignment, and the porcine sequence data is below the alignment. Conserved Cys13, Cys217, and Cys 239 are highlighted in yellow. Genbank accession numbers: *Mus musculus* (NP081667), *Rattus norvegicus* (NP001020171), *Homo sapiens* (NP981932), *Pan troglodytes* (XP527537), *Pongo pygmaeus* (CAH89696), and *Sus scrofa* (NP999581).

90%. All of the mammalian genes retrieved encode three cysteines, and at least one of these residues is expected to play a central role in catalysis. The amino acid sequences from the peptide fragments submitted for MS and Edman sequencing correspond to residues from Ala36 to Val285 of the mouse protein. Cys13 is not present in the soluble IYD obtained by trypsinolysis, suggesting that it is not involved in catalysis.

Alignment of IYD and the three ID isozymes from *Mus musculus* reveals that the two enzymes share little sequence homology, despite the similarity of the reactions catalyzed by each (Figure 2-4). Within the IDs, the conserved selenocysteine residue is

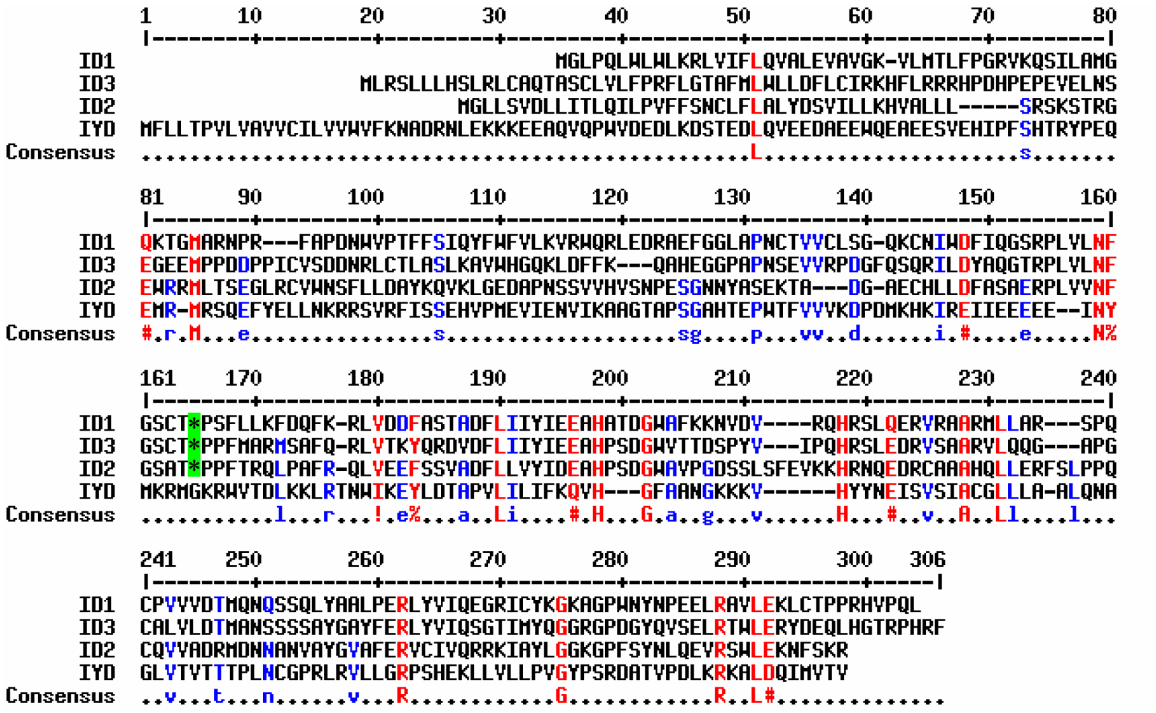

Figure 2-4. Alignment of IYD and ID sequences from Mus musculus. The conserved selenocysteine (*) residues in ID are highlighted in green. Red and blue indicate consensus between the sequences at 90% and 70%, respectively. The consensus sequence is shown below the alignment. Genbank accession numbers: ID1(Q61153), ID2 (Q9Z1Y9), ID3 (Q91ZI8), and IYD (BC023358).

apparent, but the conserved cysteine residues from IYD are far removed. Moreover, analysis of the cDNA for IYD using SECISearch does not predict the presence of a selenocysteine residue, as would be expected if IYD were more closely related to IDs.

IYD is a member of the NADH oxidase/flavin reductase superfamily. The IYD protein sequence can be divided into three domains (Figure 2-5). The largest domain (3) extends from residue 82 to the *C*-terminus (residue 285) and exhibits

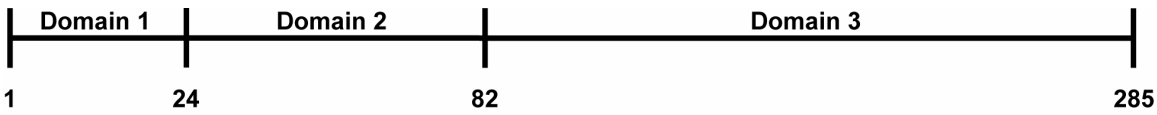

Figure 2-5. Predicted domain structure of IYD. The hydrophobic domain 1 is predicted to anchor the protein to the membrane. Domain 2 has some α-helical character between residues 49 and 67. Domain 3 exhibits homology to the NADH oxidase/flavin reductase superfamily of proteins commonly found in bacteria. Domain boundaries are numbered by the amino acid residue.

homology to the NOX/FRase superfamily of proteins that is commonly found in bacteria. The intermediate domain (2) is not related to known folding patterns or sequences, but is predicted to contain an α-helical region between residues 49 and 67 when analyzed using 3-D PSSM (Web Server version 2.6.0, http://www.sbg.bio.ic.ac.uk/~3dpssm/index2.html).

The *N*-terminal domain (1) is very lipophilic and is predicted to act as the transmembrane anchor by the transmembrane helix prediction program TMHMM,[99] further supporting the idea that Cys13 does not participate in catalysis. Although SignalP[100] identified Ala23-Asp24 as a possible site for signal peptide cleavage, the probability predicted for hydrolysis at this site is low (22%). In contrast to our prediction, residues 213-229 of human IYD (residues 209-225 in mouse IYD) had previously been proposed as a membrane anchor based on an expectation that the *N*-terminal signal sequence would be hydrolyzed.[101] However, this putative transmembrane anchor is central to the predicted NOX/FRase domain, and no known examples of the superfamily are associated with membranes. Because the NOX/FRase proteins are soluble, globular proteins, removal of the *N*-terminal lipophilic anchor will likely cause little disruption of IYD's structure or function. Furthermore, loss of this domain would generate the appropriate molecular weight observed for the soluble IYD fragment obtained by proteolysis and chromatography.[61]

IYD exhibited a surprising level of similarity to bacterial proteins within the NOX/FRase superfamily (Figure 2-6). Representatives of this superfamily are widely distributed in bacteria, but IYD is the only example identified in mammals. Comparison of IYD to NOX/FRase superfamily members with known crystal structures, using

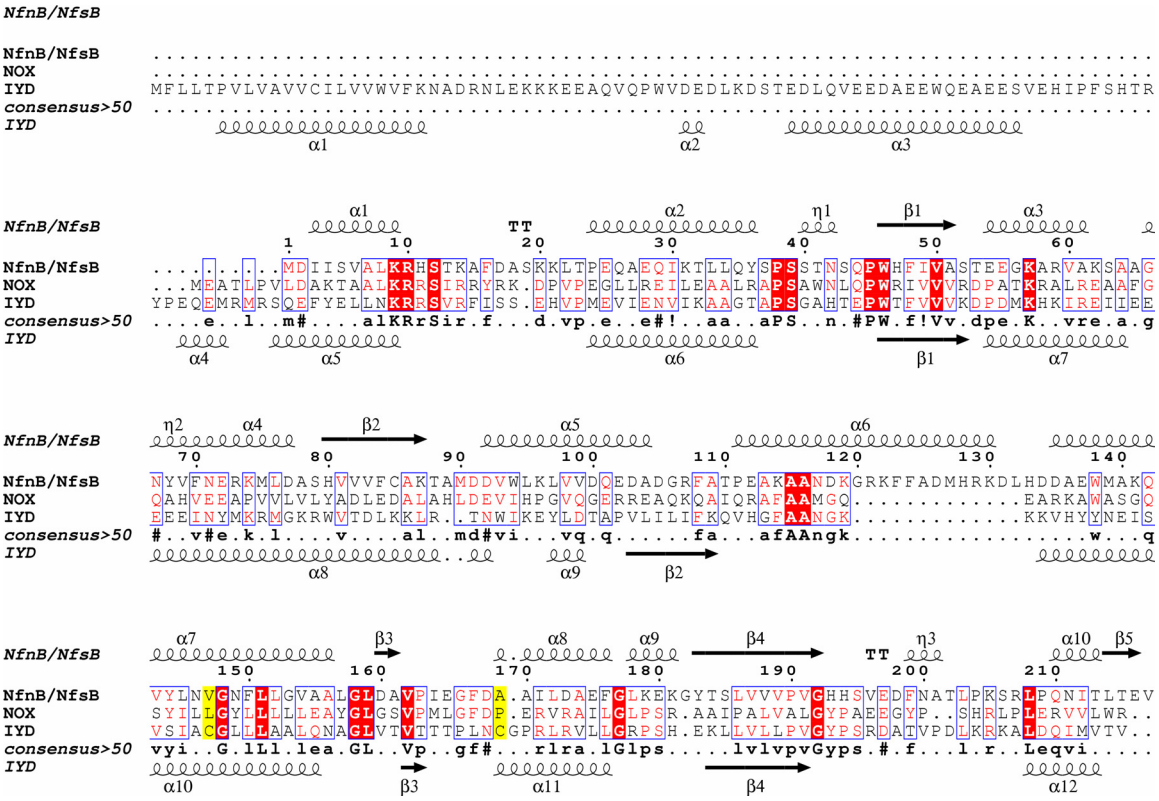

Figure 2-6. Alignment of E. coli minor nitroreductase (NfnB-NfsB) , T. thermophilus NADH oxidase (NOX), and M. musculus IYD. Strucutural elements for NfnB-NfsB are derived from its crystal structure (PDB code: 1ICR). IYD secondary structure was predicted using 3D-PSSM Web Server, version 2.6.0. Cysteine residues (217 and 239) conserved in IYD are highlighted in yellow.

ClustalW, suggested greatest sequence identity (24%) is shared between IYD and NADH oxidase (NOX)[102] from *Thermus thermophilus*. More surprisingly, IYD shares 50% identity with a putative oxidoreductase from *Flavobacteriales bacterium* HTCC2170 (accession number ZP_01107680) between residues 69-283, including conservation of Cys217.

A phylogenetic analysis was performed using the retrieved mammalian sequences corresponding to domain 3 and the sequences from NOX/FRase proteins for which an x-ray crystallographic structure was available (Figure 2-7). The analysis provided the expected relationship between the various mammals. Furthermore, the results show that

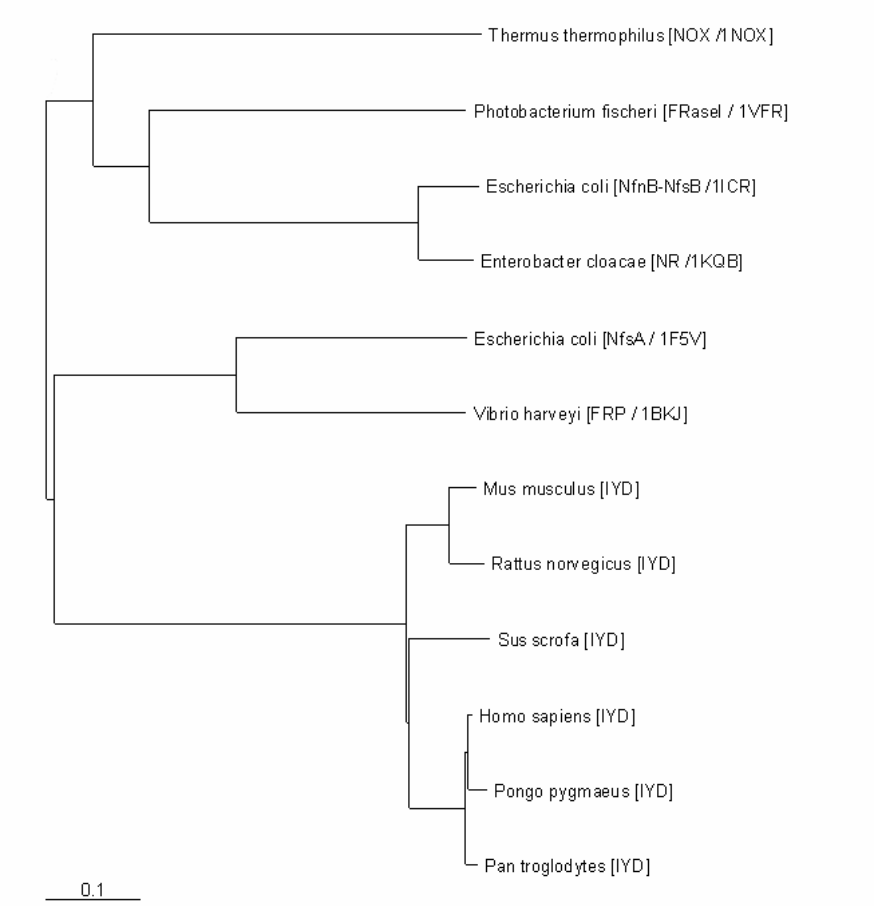

Figure 2-7. Phylogenetic relationship of mammalian IYD and bacterial NADH oxidase/flavin reductase superfamily members. Analysis was performed using mammalian IYD sequences corresponding to domain 3. Brackets indicate the common protein abbreviation/PDB identifier. Horizontal branch lengths are drawn to scale with the scale bar indicating the number of amino acid substitutions per site. NOX, NADH oxidase; FRase I, NAD(P)H-utilizing flavin reductase; NR, nitroreductase; FRP, flavin reductase P.

greatest similarity is shared between IYD and the subset of proteins in the superfamily exemplified by flavin reductase P from *Vibrio harveyi*.

The bacterial proteins are not expected to have dehalogenase activity, because the proteins generally lack the conserved cysteine residues at positions 217 and 239 of the mammalian proteins. Instead, bacterial homologues within this superfamily are associated with a variety of different activities, including conversion of FMN to 5,6-dimethylbenzimidazole during B_{12} (cobalamin) biosynthesis (BluB),[103] reduction of

Table 2-1. DNA sequence and amino acid translation of pcDNA3.1(+)/IYD.

TGG	CTA	GCG	TTT	AAA	CTT	AAG	CTT	GGT	ACC	*GAG*	*CTC*	GGA	TCC	GCC	ACC
ATG	TTT	CTC	CTC	ACC	CCA	GTC	TTG	GTA	GCA	GTT	GTC	TGT	ATC	TTG	GTT
M	F	L	L	T	P	V	L	V	A	V	V	C	I	L	V
GTA	TGG	GTC	TTT	AAA	AAT	GCC	GAC	AGG	AAC	CTA	GAG	AAA	AAG	AAG	GAG
V	W	V	F	K	N	A	D	R	N	L	E	K	K	K	E
GAG	GCT	CAA	GTT	CAG	CCC	TGG	GTG	GAT	GAA	GAC	TTG	AAA	GAC	AGC	ACA
E	A	Q	V	Q	P	W	V	D	E	D	L	K	D	S	T
GAA	GAC	CTT	CAA	GTG	GAA	GAA	GAT	GCT	GAG	GAG	TGG	CAA	GAG	GCA	GAG
E	D	L	Q	V	E	E	D	A	E	E	W	Q	E	A	E
GAG	AGT	GTG	GAG	CAC	ATC	CCG	TTC	TCT	CAC	ACC	CGA	TAC	CCA	GAA	CAG
E	S	V	E	H	I	P	F	S	H	T	R	Y	P	E	Q
GAA	ATG	AGG	ATG	AGG	TCC	CAG	GAA	TTC	TAT	GAG	CTC	CTC	AAT	AAG	AGA
E	M	R	M	R	S	Q	E	F	Y	E	L	L	N	K	R
CGC	TCC	GTC	AGG	TTT	ATC	AGC	AGC	GAG	CAC	GTC	CCA	ATG	GAA	GTC	ATT
R	S	V	R	F	I	S	S	E	H	V	P	M	E	V	I
GAA	AAT	GTC	ATC	AAA	GCA	GCA	GGA	ACA	GCT	CCA	AGT	GGG	GCC	CAT	ACA
E	N	V	I	K	A	A	G	T	A	P	S	G	A	H	T
GAG	CCC	TGG	ACC	TTT	GTG	GTG	GTG	AAG	GAC	CCA	GAC	ATG	AAG	CAT	AAG
E	P	W	T	F	V	V	V	K	D	P	D	M	K	H	K
ATC	AGA	GAG	ATT	ATC	GAA	GAG	GAG	GAA	GAA	ATA	AAT	TAC	ATG	AAA	AGG
I	R	E	I	I	E	E	E	E	E	I	N	Y	M	K	R
ATG	GGA	AAG	CGA	TGG	GTC	ACA	GAC	CTG	AAG	AAA	CTG	AGA	ACC	AAC	TGG
M	G	K	R	W	V	T	D	L	K	K	L	R	T	N	W
ATT	AAG	GAG	TAC	TTG	GAC	ACC	GCC	CCA	GTT	CTG	ATC	CTC	ATT	TTC	AAA
I	K	E	Y	L	D	T	A	P	V	L	I	L	I	F	K
CAA	GTC	CAT	GGT	TTT	GCT	GCG	AAT	GGA	AAG	AAG	AAG	GTC	CAC	TAC	TAC
Q	V	H	G	F	A	A	N	G	K	K	K	V	H	Y	Y
AAC	GAG	ATC	AGT	GTG	TCC	ATC	GCC	TGT	GGC	CTC	CTG	CTG	GCT	GCA	CTG
N	E	I	S	V	S	I	A	C	G	L	L	L	A	A	L
CAG	AAT	GCA	GGG	CTA	GTG	ACG	GTC	ACT	ACC	ACT	CCC	CTC	AAC	TGT	GGT
Q	N	A	G	L	V	T	V	T	T	T	P	L	N	C	G
CCT	CGT	CTG	AGG	GTG	CTC	CTG	GGC	CGC	CCC	TCA	CAT	GAG	AAG	CTG	TTG
P	R	L	R	V	L	L	G	R	P	S	H	E	K	L	L
GTG	CTA	CTT	CCT	GTG	GGG	TAC	CCC	AGC	AGA	GAT	GCC	ACA	GTG	CCT	GAC
V	L	L	P	V	G	Y	P	S	R	D	A	T	V	P	D
CTC	AAG	CGG	AAA	GCT	CTG	GAC	CAG	ATC	ATG	GTG	ACA	GTA	TAG	CTC	GAG
L	K	R	K	A	L	D	Q	I	M	V	T	V	*		
TCT	*AGA*	GGG	CCC	GTT	TTA	AAC	CCG	CTG	ATC	AGC	CTC	GAC	TGT	GCC	TTC

nitroaromatics (NR, NfsA, and NfnB-NfsB),[104-106] and generation of reduced flavin for use by luciferase and other enzymes (FRaseI, FRP).[107-109] The physiological role of other homologues such as NOX has not been determined.[102]

Expression of IYD in HEK293 cells. When peptide sequences of IYD from pig were first determined, the cDNA sequence of the mouse gene was the most complete. Consequently, the mouse cDNA was subcloned into pcDNA3.1(+) (Table 2-1) and

expressed in human embryonic kidney (HEK293) cells to verify that the cDNA for IYD had been properly assigned. Cells transfected with pcDNA3.1(+)/IYD (280 mg) expressed a protein with the appropriate molecular weight (33 kDa).

The lysate of these cells exhibited deiodinase activity in contrast to a control lysate derived from HEK293 cells that were not transfected with the IYD gene. A K_M value of 4.4 ± 1.7 μM was measured for DIT (Appendix B), using dithionite as the reductant. This value is consistent with those ranging from 2.0 - 9.3 μM previously reported for IYD isolated from calf, sheep, pig, rat, and human. V_{max} (12 ± 1 nmol/hr per ug of IYD) and k_{cat} (6.4 ± 0.7 min^{-1}) were also estimated based on the molecular weight of IYD, the total amount of protein (100 μg) and the fractional concentration of IYD (1%), as determined by gel electrophoresis and densitometry (Appendix A).

Additionally, the expressed protein promoted deiodination of DIT in the presence of the native electron donor, NADPH (50 μM), although the K_M for DIT (2.02 ± 1.9 μM) was slightly lower than the K_M determined in the presence of dithionite. The V_{max} value (1.1 ± 0.4 nmol/hr per μg of IYD) was substantially lower than the V_{max} measured in the presence of dithionite and likely reflected a limited concentration in HEK293 cells of the reductase that is thought to be necessary for shuttling reducing equivalents between NADPH and IYD.

The complete absence of this reductase has recently been used to explain the lack of NADPH-dependent deiodination by human IYD expressed in CHO cells.[101] The human gene exhibits 84% identity to the mouse gene and was identified by serial analysis of genes preferentially expressed in the thyroid.[101] Subsequent expression of the human

gene in HEK293 cells confirmed the assignment, supporting our identification by isolation and characterization of the soluble domain of the porcine protein.

Evolutionary strategies for reductive dehalogenation. Nature has developed at least three different, but chemically related, mechanisms for reductive cleavage of aryl halide bonds. Iodotyrosine deiodinase, ID, and TD utilize a common strategy for dehalogenation that requires nucleophilic, redox-active amino acid residues for catalysis. Exogenous thiols are sufficient to drive catalysis in TD and ID. However, IYD is not sensitive to thiol cofactors, but instead requires the increased reducing power of NADPH and flavin mononucleotide.

Despite the strong similarity between their proposed mechanisms, TD, ID, and IYD have very different structural origins. Iodotyrosine deiodinase belongs to the NADH oxidase/flavin reductase superfamily, while iodothyronine deiodinase and tetrachlorohydroquinone dehalogenase derive from the thioredoxin and glutathione *S*-transferase superfamilies, respectively.[91, 110] It is even more remarkable that the mammalian thyroid has used two different structural motifs to catalyze such similar reactions as deiodination of thyroid hormones and iodotyrosines.

Chapter 3

Three-Dimensional Model and Prokaryotic Expression of the Iodotyrosine Deiodinase Nitroreductase Domain

3.1 Introduction

All flavin-binding proteins have been classified into three families, based on their folding pattern: 1) the reductases (e.g., ferredoxin reductase), 2) the FAD/NAD-linked reductases (e.g., glutathione reductase) and 3) the NAD(P)H/flavin reductases (e.g., NADH oxidase and flavin reductase).[111] In spite of the low sequence homology (10-39% similarity) between NADH oxidase (NOX) from *Thermus thermophilus*,[102] flavin reductase (FRP) from *Vibrio harveyi*,[107, 108] flavin reductase (FRase I) from *Vibrio (*sometimes *Photobacterium) fischeri,*[112] nitroreductase (NR) from *Enterobacter cloacae,*[113] and the major (NfsA)[114] and minor (NfnB-NfsB)[115] nitroreductases from *Escherichia coli,* x-ray crystallographic studies have revealed that these proteins share a similar core fold, commonly referred to as a nitroreductase (NR) domain. Iodotyrosine deiodinase is the only flavoprotein known to catalyze reductive dehalogenation of aryl halide substrates and has recently been identified as the only mammalian member of the NADH oxidase/flavin reductase superfamily.

Within this family, NOX (22.8 kDa per monomer), FRase I (24.8 kDa), NfnB-NfsB (23.9 kDa), and NR (24.0 kDa) are more similar to each other than to FRP (26.3 kDa), which may constitute a separate family that includes NfsA (26.8 kDa).[107, 113] All NOX/FRase proteins with known crystal structures are homodimers of interlocking subunits with active sites located at their dimer interfaces.[102, 107, 108, 112-115] The flavin cofactors are also buried at the dimer interface and make contacts with both monomers.[102, 107, 108, 112-115] Although a definitive nicotinamide binding site has not been identified, all NOX/FRase proteins oxidize reduced nicotinamides with concomitant

reduction of the bound flavin. NOX and its related enzymes show no preference for NADPH over NADH, while FRP and NfsA utilize NADPH preferentially.

The NOX-like enzymes can also be distinguished from the FRP-like enzymes on a structural basis (Figure 3-1).[107] First, a short loop in the FRP and NfsA structures is replaced by a longer loop-helix-loop motif in the other enzymes.[107] Second, the FRP enzymes contain an unusual 3_{10} helix in contact with the flavin, while the NOX proteins do not.[107] Third, three helices (I, J, and K) and a disordered loop (residues 201-209) found in the FRP enzymes are absent in the NOX enzymes.[107]

Given the sequence and secondary structure similarities between IYD and the NOX/FRase superfamily, it is possible to develop a three-dimensional model of the nitroreductase domain based on the crystal structure coordinates of the bacterial enzymes. In addition, the similarities found between the proteins suggest that the NR domain from IYD may be responsible for enzymatic activity and that expression of IYD might be possible in a prokaryotic host.

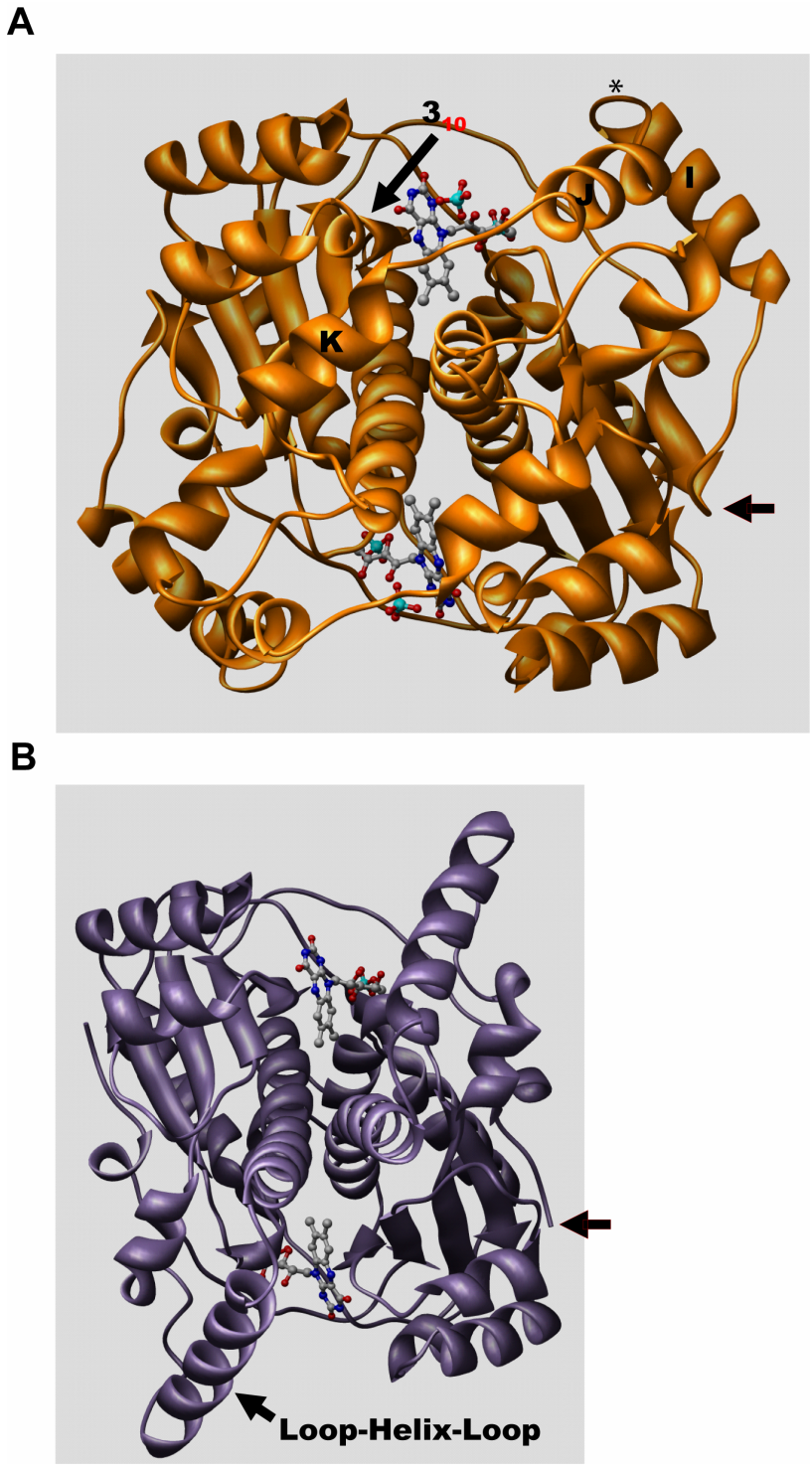

Figure 3-1. Structural features are used to distinguish members of the NADH oxidase/flavin reductase superfamily. A) Flavin reductase P (FRP, PDB code 1BKJ) from *Vibrio harveyi*. B) NADH oxidase (NOX, PDB code 1NOX) from *Thermus thermophilus*. The unlabeled arrows indicate the differences in the *C*-terminus of the FRP-like and NOX-like proteins.

3.2 Experimental Procedures

Three-dimensional homology model of iodotyrosine deiodinase. The three-dimensional model of mouse IYD was calculated using the crystal structure coordinate set of the minor oxygen-insensitive nitroreductase of *Escherichia coli* (PDB id: 1ICR). All steps of homology model building were performed by the program MODWEB,[116, 117] available at http://alto.compbio.ucsf.edu/modweb-cgi/submit/form.cgi. The IYD sequence was submitted to the fully-automated server using default values. The output contained the three-dimensional model, including all nonhydrogen main-chain and side-chain atoms. The model was used without further refinement. The predicted homology model of IYD was evaluated by the Structure Analysis and Verification Server at http://nihserver.mbi.ucla.edu/SAVS/.[118-122]

Construction of plasmids for IYD expression. DNA fragments containing the IYD gene (I.M.A.G.E. clone 5064638 from ATCC) were amplified by PCR, using the appropriate primers from Table 3-1. The PCR products were digested with the appropriate restriction endonuclease (Table 3-1) and subsequently purified by gel electrophoresis (1% agarose, 125V, 35 minutes). The parent plasmid for each construct was digested using the appropriate restriction enzymes and heat inactivated (60 °C, 20

Table 3-1. Oligonucleotide primers used generate IYD expression plasmids.

Plasmid	Oligonucleotide Primer	Restriction Endonuclease
pET102 (Trx)	5′-CACCGATACCCAGAACAGGATGAGG-3′	TOPO cloned
	5′-TCACGATGCGGCCGCAGGCACTGT-3′	TOPO cloned
pMal-c2 & pMal-p2 (MBP)	5′-GAATTC*GGATCC*ATGAGGATGAGGTCCCAGGAA-3′	BamH I
	5′- GAATTC*AAGCTT*CTATACTGTCACCATGAT-3′	Hind III
pET43.1 (NusA)	5′-GACGACGACAAGATGAGGATGAGGTCCCAGGAA-3′	Ek/LIC cloned
	5′-GAGGAGAAGCCCGGTCTATACTGTCACCATGAT-3′	Ek/LIC cloned

minutes). The reaction mixture was supplemented with antarctic phosphatase buffer according to the manufacturer's directions, and treated with Antarctic phosphatase (5U, 20 minutes). The reaction was again heat inactivated (60 °C, 20 minutes) and used without further purification.

The IYD-containing insert (30 nmol) and the parent plasmid (10 nmol) were ligated using T4 DNA ligase (20 U, 16 °C, 10 hours) and subsequently transformed into XL-I blue or Top10 F` *E. coli* (electroporation 1700 V, 1 mm gap cuvette). The transformed bacteria were rescued in 1 mL SOC medium at 37 °C, with gentle shaking for 1 hour prior to selection on LB agar plates supplemented with 100 μg/mL ampicillin. Plasmid DNA from antibiotic resistant colonies was digested with EcoR I, Pst I, or Sty I. Plasmids from colonies exhibiting the expected fragmentation were submitted for DNA sequencing (Gene Gateway, Hayward, CA).

Transformation of BL21(DE3) and Rosetta2(DE3) *E. coli* for protein expression. *E. coli* were transformed using an Eppendorf electroporator 2510, according to the manufacturer's directions. Briefly, an aliquot of electrochemically competent *E. coli* (100 μL) was thawed on ice and transformed with 50 ng plasmid DNA (1700 V, 1 mm gap cuvette). The transformed bacteria were rescued with 1 mL SOC medium and incubated at 37 °C for 1 hour before plating on LB-amp plates (plates used for Rosetta2(DE3) were additionally supplemented with 20 μg/mL chloramphenicol).

Isopropyl-β-D-thiogalactoside-induced expression of fusion proteins. A single colony of *E. coli* containing the expression plasmid was used to inoculate 5 mL Luria-Bertani broth supplemented with ampicillin (LB-Amp) or supplemented with ampicillin and chloramphenicol (LB-Amp/Cm) for growth overnight at 37 °C with gentle shaking

(200 RPM). The overnight growth was diluted 1:100 into the same media in a baffled flask (5 times volume of culture) and allowed to grow with shaking (200 RPM) to the desired OD_{600} (OD_{600} = 0.4-1.0), before addition of IPTG (0.01 – 5 mM) to the desired final concentration. The culture was incubated at the desired temperature (16, 23, 30, or 37 °C) with vigorous shaking (250 RPM). Aliquots (1 mL) were removed from the culture at regular intervals to assess protein expression. The aliquots were centrifuged (16,000 x g) in a tabletop microcentrifuge for two minutes, the supernatant was decanted, and the bacterial pellet was frozen in liquid nitrogen for storage at -80 °C. At the end of the time course, the bacterial pellets were thawed on ice and lysed by either three freeze-thaw cycles or by BugBuster (Novagen).

Autoinduction of protein expression. A single colony of *E. coli* containing the expression plasmid was used to inoculate ZYP-0.8G medium.[123] The culture was grown overnight (37 °C, 250 RPM) and used (0.2 mL) to inoculate 200 mL ZYP-5052 medium in a 1 L baffled flask. The culture was grown 24 hours at 30 °C while monitoring the OD_{600} to ensure that stationary phase was achieved. The culture was harvested by centrifugation at 6,000 x g for 15 minutes and frozen in liquid nitrogen before storage at -80 °C. The bacterial pellet was thawed and lysed, as described above.

Protein extraction from porcine microsomes using BugBuster. Porcine microsomes (1 g) were suspended in 5 mL BugBuster protein extraction solution (Novagen). The suspension was gently shaken (100 RPM) in a 15 mL Falcon tube overnight at 4 °C. The solution was centrifuged (100,000 x g) for 1 hour and the supernatant decanted for use in enzymatic assays.

3.3 Results and Discussion

Three-dimensional model of predicted IYD nitroreductase domain (IYD-NR). A three-dimensional model of the nitroreductase domain of IYD (Figure 3-2) was

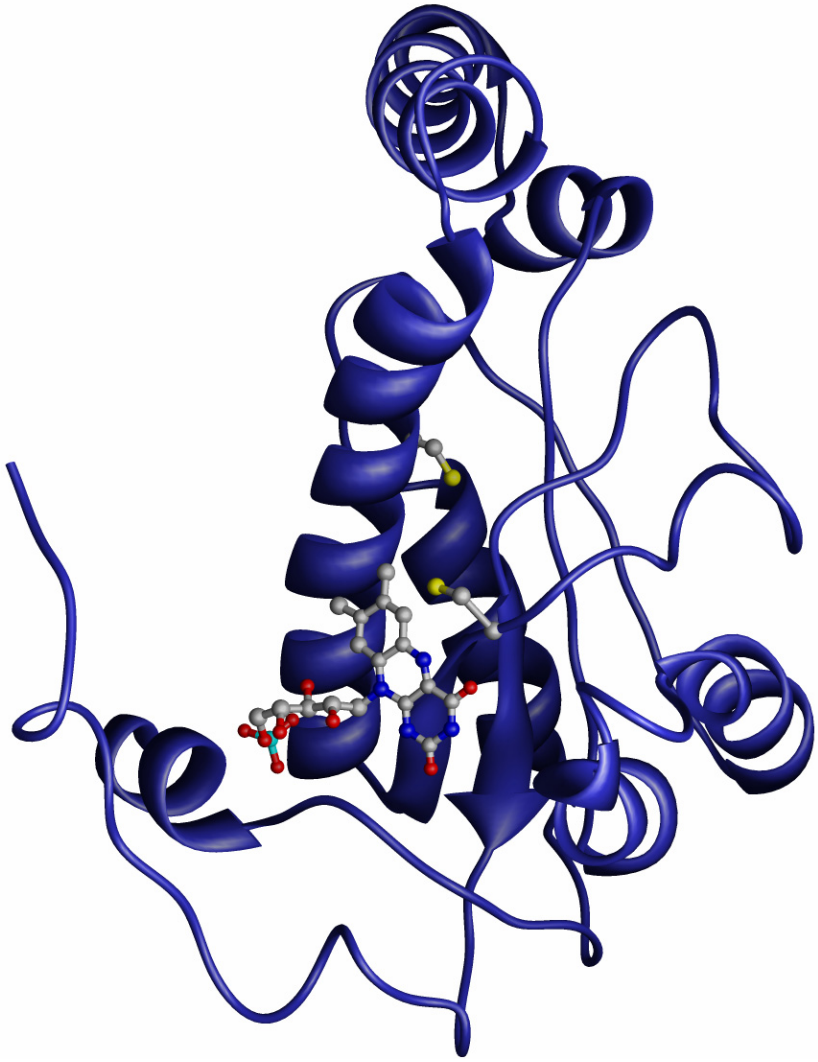

Figure 3-2. Three dimensional model of the NADH oxidase/flavin reductase domain from iodotyrosine deiodinase constructed using the crystal structure coordinates (PDB 1ICR) of the minor nitroreductase from E. coli. Residues 88-285 were modeled by threading the IYD sequence through the crystal structure coordinates of NfnB-NfsB and its bound flavin. The flavin and two conserved cysteine residues are shown in ball and stick representation. This image was produced using the UCSF Chimera package from the Resource for Biocoomputing, Visualization, and Informatics at the University of California, San Francisco (supported by National Institutes of Health Grant P41 RR-01081).

developed using the fully automated MODWEB server and the crystal structure coordinates of NfnB-NfsB (PDB 1ICR). The model template is chosen automatically by MODWEB based on a series of alignments of primary and predicted secondary structure of the target on local and global scale.[124] The suitability of the model was evaluated using the Structure Analysis and Verification Server.[118-122] The RMSD (root mean square deviation) of Cα for the all residues in the model relative to the crystal structure coordinates is 4.128 Å. The RMSD is indicative of how well the target and template structures agree. A large RMSD (>3.5 Å) might cast doubt on the accuracy of the model. However, inspection of the model superimposed on the template using Chimera[125] (Figure 3-3) reveals much of this deviation occurs in a helix-loop-helix region between residues 173 and 207 and the *C*-terminal region 273-285. The RMSD of Cα calculated for the remaining residues is 0.459 Å, indicating a high probability that the target sequence and template share the same protein fold. Furthermore, the conserved cysteine residues, the dimer interface, and, presumably, the active site are found within the region of higher accuracy.

The IYD-NR model includes neither a Rossman fold nor an NADPH binding domain. The Rossman fold is also absent in the NOX/FRase superfamily, yet the bacterial proteins still utilize NADH and/or NADPH as a source of hydride for reduction of FMN or FAD. [102, 107, 108, 112-115] In the lone crystal structure in which an electron donor is present, the nucleotide adopts an unusual folded conformation in which the nicotinamide and adenine rings are stacked in the active site.[107] Nicotinic acid has also been found to reside in a similar orientation.[115]

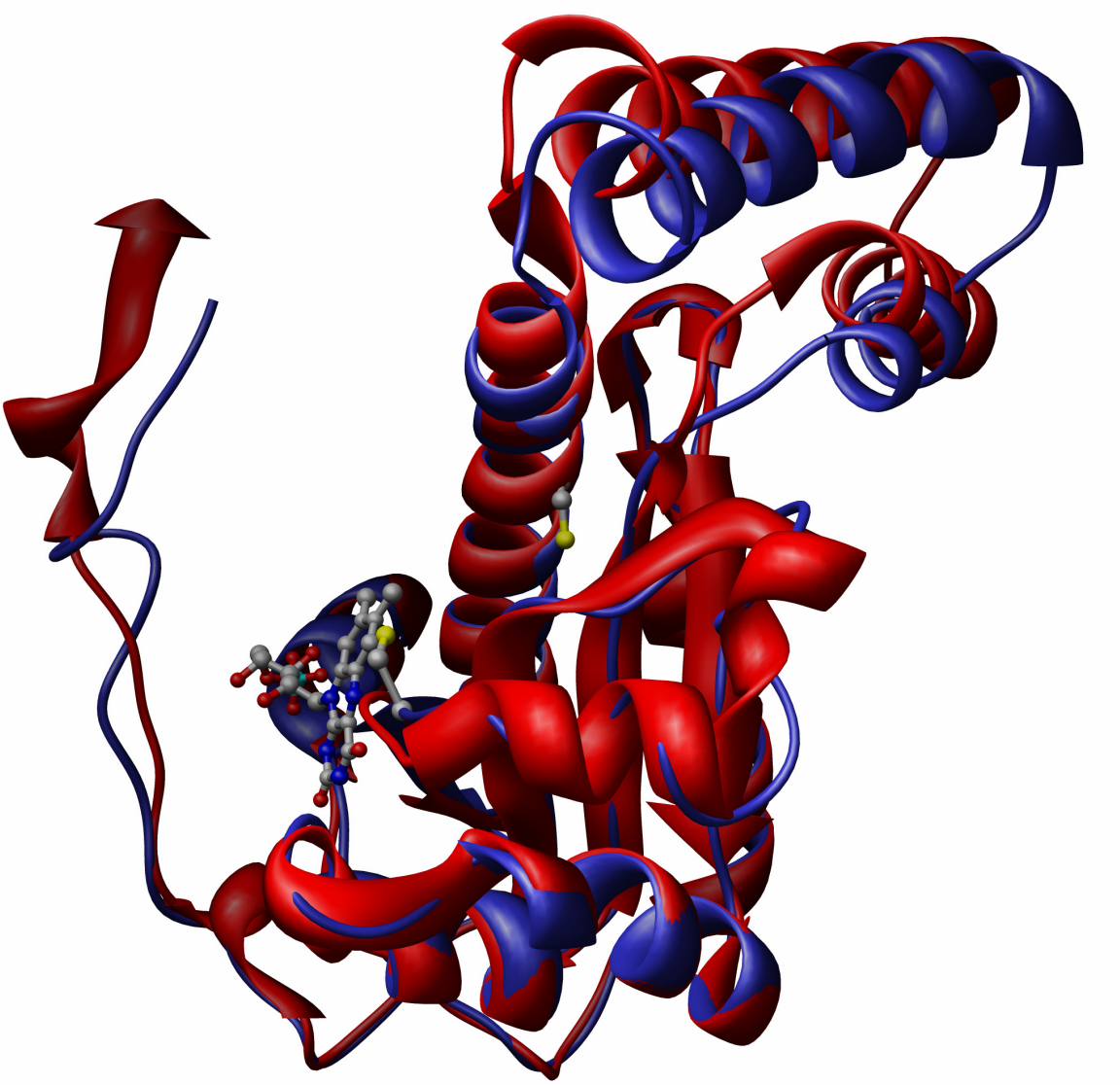

Figure 3-3. Three-dimensional model of IYD-NR (blue) superimposed on the crystal structure of NfnB-NfsB (red). The region experiencing the greatest deviation from the crystal structure of NfnB-NfsB is the helix-loop-helix shown in the upper right corner of the figure.

Although nicotinamide binding of the NOX/FRase superfamily is not well characterized structurally, the mechanism of flavin reduction by FRP and FRase I, as well as the subsequent transfer of the reduced flavin to luciferase, has been thoroughly studied.[108, 109, 126, 127] In contrast to the bacterial enzymes, IYD does not appear to accept electrons directly from reduced nicotinamides,[60, 101] and its flavin exhibits an unusually

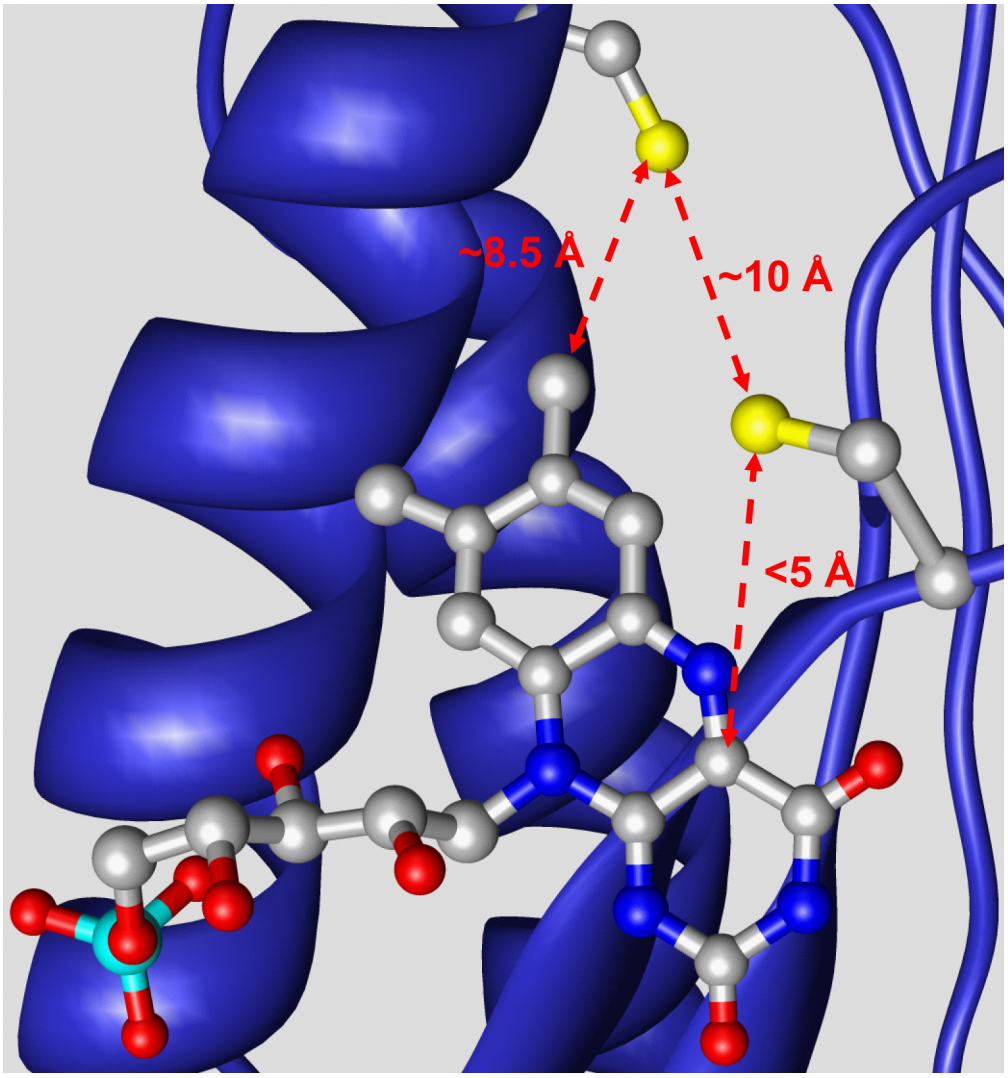

Figure 3-4. Cysteine residues 217 and 239 are in close proximity to the flavin in the homology model. In particular, Cys217 is less than 5 A from C4a of the FMN, a common site of flavin reactivity.

low potential (- 412 mV),[57] relative to the flavin bound to NR (-190 mV)[106] and FRP (-255 mV)[126].

The three-dimensional model predicts that Cys217, Cys239, and the isoalloxazine ring of the FMN bound to IYD are all in close proximity (Figure 3-4). In particular, the sulfur atom of Cys239 is less than 5 Å from the C4a of the FMN isoalloxazine ring, one of the key sites for interaction with a thiol in other flavoproteins containing redox-active

cysteine residues.[92, 128, 129] The sulfur atom of Cys217 also is predicted to be within 10 Å of Cys239 and within 8.5 Å of the 7-methyl group of the flavin.

The absence of IYD's conserved cysteines in the bacterial proteins suggests a gain of function in the NADH oxidase/flavin reductase superfamily to support reductive deiodination of MIT and DIT. The flavin-cysteine interactions identified in the model were implicit in the mechanism previously suggested for IYD and had been suggested experimentally,[57, 60] but these interactions will need confirmation by crystallographic and other experimental studies.

If the cysteine-flavin interactions are confirmed, then IYD will be the first representative of a new class of proteins containing flavin and a redox-active cysteine residue. Most of the previously described dithiol-containing flavoproteins contain two redox-active cysteine residues in their active site and belong to the pyridine nucleotide-disulfide oxidoreductase superfamily.[92] Flavoproteins such as NADH peroxidase also belong to this class, despite the presence of a single active site cysteine.[130] The second class of enzymes includes sulfhydryl oxidase[131] from chicken egg white, Erv2p[132] from yeast, and quiescin Q6[133] from human fibroblasts.

Prokaryotic expression of the nitroreductase domain from IYD. Preliminary expression experiments were performed using the JF1-pGEX plasmid, which encodes glutathione *S*-transferase (GST) fused to the *N*-terminus of IYD-NR.[61] Expression under the conditions surveyed resulted in a protein of ~28 kDa, with a small amount of the expected size protein (52 kDa) in inclusion bodies.[61] The ~28 kDa protein was suggested to be the GST fusion tag alone, a result of proteolysis of a poorly folded target protein.[61]

An alternative fusion partner, thioredoxin, has been reported to promote the proper folding of proteins when used as a fusion partner for heterologous expression in *E. coli*.[134] The pET102/IYD-NR plasmid encoding thioredoxin (14 kDa) fused to the *N*-terminus of IYD-NR was expressed in BL21(DE3) *E. coli,* using the manufacturer's suggested conditions of 37 °C and 1 mM IPTG for induction, and the cell lysate was analyzed by polyacrylamide gel electrophoresis (PAGE). Despite repeated attempts to express the thioredoxin fusion, no bands of induced protein were visible by PAGE analysis (Figure 3-5).

Interestingly, the growth rate of *E. coli* cultures expressing pET102/IYD-NR was noticeably decreased relative to cultures transformed with the pET102/LacZ positive control vector. The slow growth in combination with the absence of protein production suggested that even the minimal levels of expression found in the uninduced *E. coli* might be toxic enough to prevent expression in the BL21(DE3) host. Several alternative *E. coli* strains have specifically been developed to express toxic proteins. These strains often take advantage of some of the unique aspects of the pET expression system.

E. coli strain BL21(DE3)pLysS constitutively expresses T7 lysozyme, a natural inhibitor of the T7 RNA polymerase that results in more tightly regulated expression of potentially toxic genes. pET102/IYD-NR was transformed into BL21(DE3)pLysS and expression was attempted using low concentrations (50 μM) of IPTG. However, no induced protein was observed on PAGE analysis, suggesting that some problem other than IYD-NR toxicity existed.

In addition to protein toxicity, premature termination during translation could result in both the truncation of the GST construct and the absence of detectable

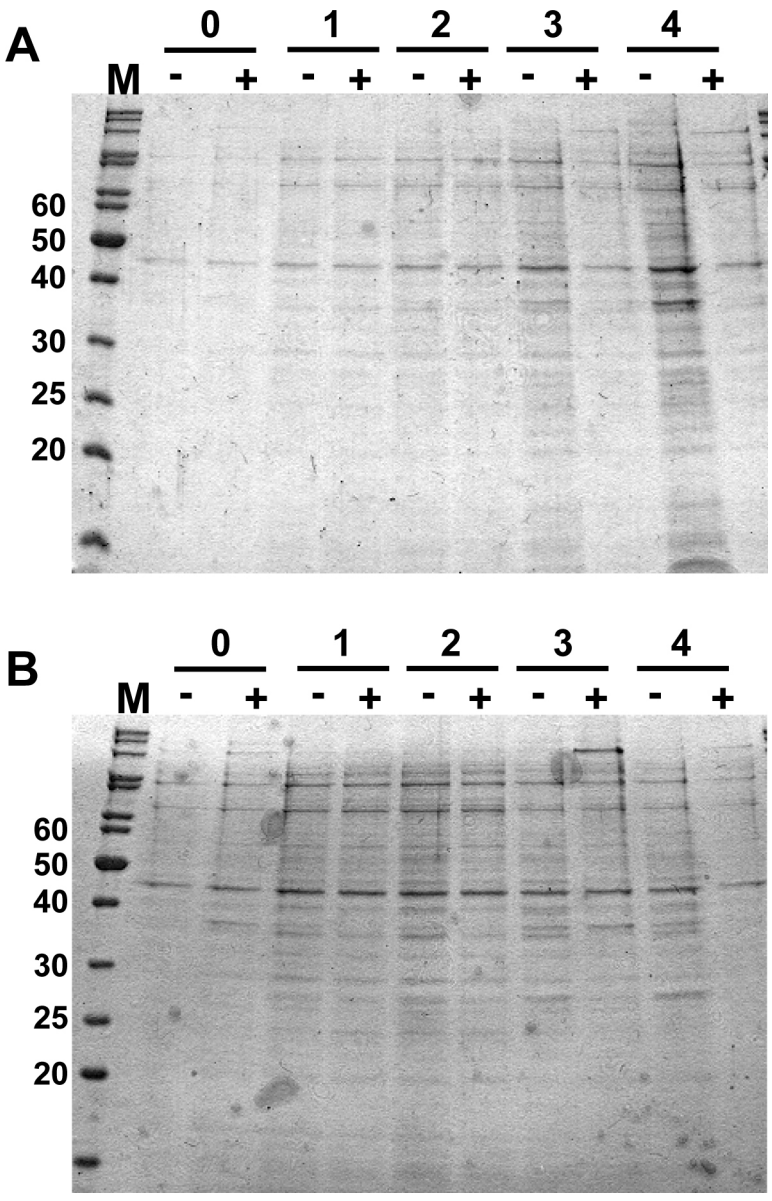

Figure 3-5. Expression of thioredoxin/IYD-NR (~38 kDa) in *E. coli* (BL21(DE3)), monitored by denaturing polyacrylamide gel electrophoresis. A) Supernatant after centrifugation of cell lysate at 16,000 x g for 10 minutes. B) Insoluble pellet after centrifugation revealed IYD-NR was contained in inclusion bodies. Proteins were resolved on a 5% stacking / 12% resolving gel and visualized by staining with Coomassie Brilliant Blue. No inducible protein is seen. "+" and "-" indicate induced with IPTG or uninduced, respectively. Numbers indicate time in hours after induction.

thioredoxin fusion protein. Premature termination of proteins has been ascribed to the differing codon usage frequencies between the host and gene source organisms. Analysis

of the nucleotide sequence[135] indicated the presence of ten arginine (AGG, AGA, CGA), two leucine (CTA), one isoleucine (ATA), and four proline (CCC) residues in the mouse gene encoded by codons that are infrequently used in *E. coli* (Table 3-2). More importantly, two of the arginine codons occurred in the first three residues of the IYD-NR sequence and may be responsible for early termination of translation with the GST/IYD-NR and Trx/IYD-NR fusion proteins.

Table 3-2. Nucleotide sequence and amino acid translation of IYD-NR indicating codons used infrequently by E. coli. Codons are color coded by residue: red, arginine; orange, proline; blue, isoleucine; and green, leucine

ATG	AGG	ATG	AGG	TCC	CAG	GAA	TTC	TAT	GAG	CTC
M	R	M	R	S	Q	E	F	Y	E	L
CTC	AAT	AAG	AGA	CGC	TCC	GTC	AGG	TTT	ATC	AGC
L	N	K	R	R	S	V	R	F	I	S
AGC	GAG	CAC	GTC	CCA	ATG	GAA	GTC	ATT	GAA	AAT
S	E	H	V	P	M	E	V	I	E	N
GTC	ATC	AAA	GCA	GCA	GGA	ACA	GCT	CCA	AGT	GGG
V	I	K	A	A	G	T	A	P	S	G
GCC	CAT	ACA	GAG	CCC	TGG	ACC	TTT	GTG	GTG	GTG
A	H	T	E	P	W	T	F	V	V	V
AAG	GAC	CCA	GAC	ATG	AAG	CAT	AAG	ATC	AGA	GAG
K	D	P	D	M	K	H	K	I	R	E
ATT	ATC	GAA	GAG	GAG	GAA	GAA	ATA	AAT	TAC	ATG
I	I	E	E	E	E	E	I	N	Y	M
AAA	AGG	ATG	GGA	AAG	CGA	TGG	GTC	ACA	GAC	CTG
K	R	M	G	K	R	W	V	T	D	L
AAG	AAA	CTG	AGA	ACC	AAC	TGG	ATT	AAG	GAG	TAC
K	K	L	R	T	N	W	I	K	E	Y
TTG	GAC	ACC	GCC	CCA	GTT	CTG	ATC	CTC	ATT	TTC
L	D	T	A	P	V	L	I	L	I	F
AAA	CAA	GTC	CAT	GGT	TTT	GCT	GCG	AAT	GGA	AAG
K	Q	V	H	G	F	A	A	N	G	K
AAG	AAG	GTC	CAC	TAC	TAC	AAC	GAG	ATC	AGT	GTG
K	K	V	H	Y	Y	N	E	I	S	V
TCC	ATC	GCC	TGT	GGC	CTC	CTG	CTG	GCT	GCA	CTG
S	I	A	C	G	L	L	L	A	A	L
CAG	AAT	GCA	GGG	CTA	GTG	ACG	GTC	ACT	ACC	ACT
Q	N	A	G	L	V	T	V	T	T	T
CCC	CTC	AAC	TGT	GGT	CCT	CGT	CTG	AGG	GTG	CTC
P	L	N	C	G	P	R	L	R	V	L
CTG	GGC	CGC	CCC	TCA	CAT	GAG	AAG	CTG	TTG	GTG
L	G	R	P	S	H	E	K	L	L	V
CTA	CTT	CCT	GTG	GGG	TAC	CCC	AGC	AGA	GAT	GCC
L	L	P	V	G	Y	P	S	R	D	A
ACA	GTG	CCT	GAC	CTC	AAG	CGG	AAA	GCT	CTG	GAC
T	V	P	D	L	K	R	K	A	L	D
CAG	ATC	ATG	GTG	ACA	GTA	TAG				
Q	I	M	V	T	V	*				

To circumvent premature termination, several tRNA-supplemented *E. coli* strains have been commercially developed and have been successfully used to express mammalian proteins that contain codons used infrequently by *E. coli*. The *E. coli* strain Rosetta2(DE3) (Novagen) expresses tRNAs to supplement all of the rare codons found in the mouse IYD-NR sequence. Rosetta2(DE3) cells were transformed with pET102/IYD-NR and expression was induced using IPTG. As expected, PAGE analysis of the cell lysate showed an induced protein of the expected size (Figure 3-6). However, the protein was found exclusively in inclusion bodies.

Inclusion body formation is a poorly understood phenomenon that frequently prevents successful overexpression of soluble proteins in bacteria. The most commonly cited reason for inclusion body formation is improper folding of the protein that results in aggregation and precipitation. While the reasons for inclusion body formation are not fully understood, a number of variables have been found to promote expression of soluble protein.

Two solutions that are commonly suggested to improve expression of soluble protein are 1) to vary the cell density at which protein expression is induced and 2) to vary the concentration of IPTG used to induce expression. These variables were systematically surveyed (OD_{600} = 0.2-1 and [IPTG] = 0.01-5 mM) with the expectation that alteration of some variable would result in soluble expression of the IYD-NR fusion. However, none of the conditions surveyed resulted in expression of soluble IYD-NR or of detectable activity when assayed with ^{125}I labeled DIT.

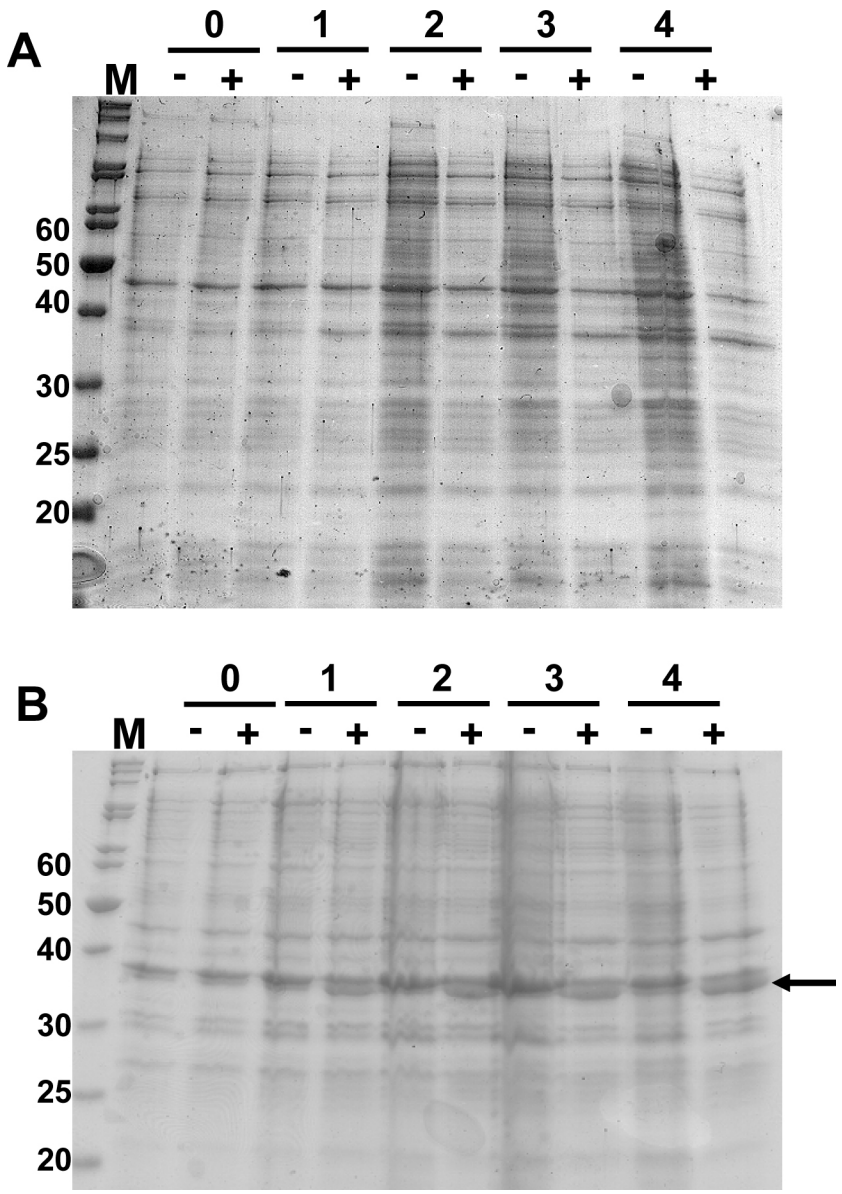

Figure 3-6. IYD-NR (~38 kDa) expressed in Rosetta2(DE3) *E. coli*. A) Supernatant after centrifugation of cell lysate at 16,000 x g for 10 minutes. B) Insoluble pellet after centrifugation revealed presence of IYD-NR in inclusion bodies. M = molecular weight standard. "-" / "+" indicate absence or addition of 50 μM IPTG. Arrow indicates induced protein. Numbers indicate time in hours.

Alternatively, lower temperatures have been found to promote expression of soluble protein including human interferon α-2 and bacterial luciferase.[136-138] The decrease in temperature has been suggested to slow the rate of protein production,

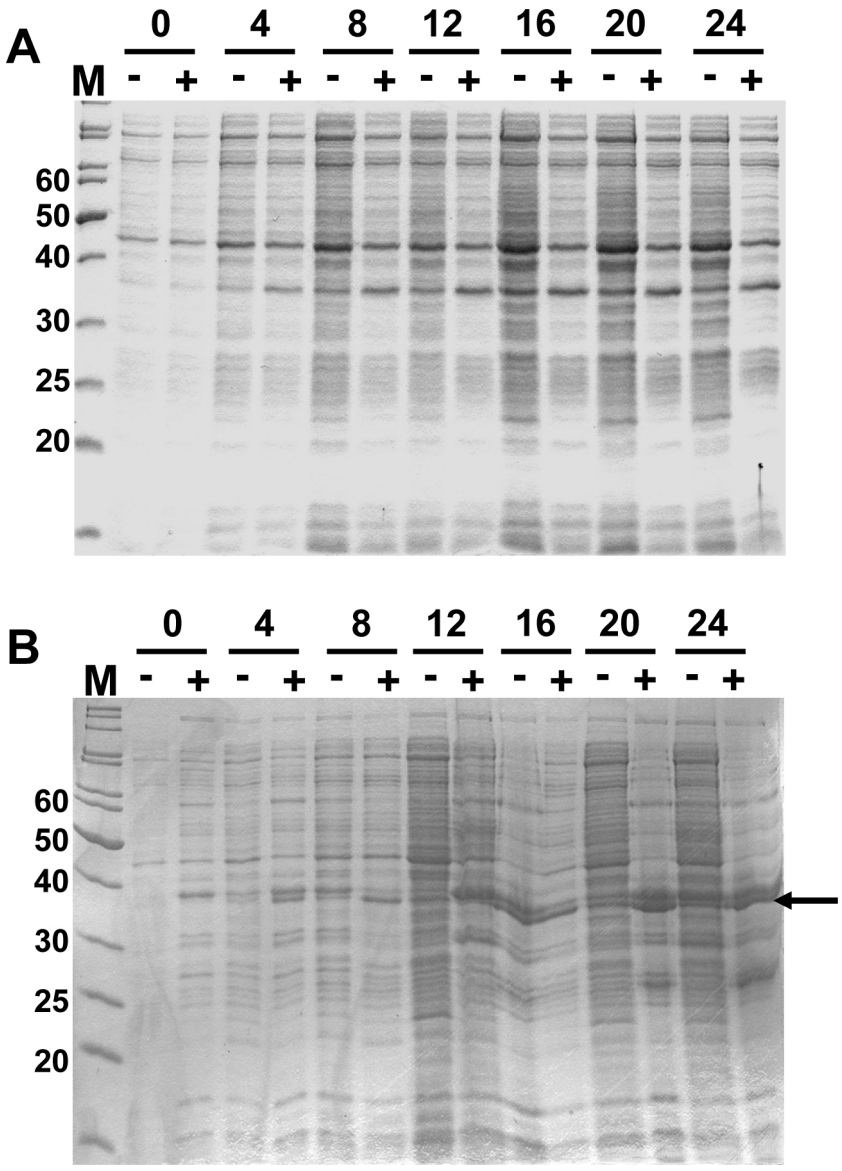

Figure 3-7. Expression of IYD-NR at 16 °C in Rosetta2(DE3) *E. coli*. A) Supernatant after centrifugation at 16.000 x g for 10 minutes. B) Insoluble pellet after centrifugation. Culture was grown to OD_{600} = 0.6, induced with 50 μM IPTG, and aliquots were removed at 4 hour intervals for PAGE analysis. "+" and "-" indicate induced with IPTG or uninduced, respectively. Numbers indicate time after induction in hours.

thereby allowing time for proper folding of the nascent protein.[138] Rosetta2(DE3) cells transformed with pET102/IYD-NR were grown at room temperature to an OD_{600} appropriate for expression, shifted to 16 °C for 1 hour to allow temperature equilibration and induced with IPTG. As in the earlier experiments, PAGE analysis (Figure 3-7)

showed that the IYD-NR fusion was expressed exclusively in inclusion bodies. In addition, no IYD activity was detectable using the iodide release assay.

Another strategy that has proven successful when attempting to express proteins that are recalcitrant to fold is based on the ability of lactose to stimulate protein production in the pET system.[139] The bacterial culture is grown in an "autoinduction" medium that is supplemented with glucose and lactose. As the bacteria consume the glucose supply in the medium, they are forced to utilize the lactose, which results in expression of genes under control of the *lac* promoter. T7 RNA polymerase is an integral component of the pET system that is under control of a modified promoter, *lacUV5,* resulting in expression only after consumption of the glucose in the medium. Expression of the Trx/IYD-NR fusion under autoinduction conditions did not increase production of soluble protein, nor was activity detectable using the iodide release assay.

In addition to Trx and GST, many fusion protein systems have been developed for promoting expression of soluble protein. Maltose binding protein (MBP) is a convenient fusion partner, as it can be used as a purification tag. In addition, two variants of the plasmid result in either cytosolic (pMal-c2) or periplasmic (pMal-p2) expression of the target protein, due to absence or presence of the MalE signal sequence. The NusA protein was identified by an analysis of the *E. coli* genome and is putatively the most soluble protein expressed by that organism. Like MBP, GST serves as a convenient purification tag, but, more importantly, has enzymatic activity that can be used to assess the protein for proper folding.

IYD-NR was subcloned into commercially available vectors for fusion to MBP (pMal-c2/IYD-NR and pMal-p2/IYD-NR), NusA (pET43.1/IYD-NR), and GST

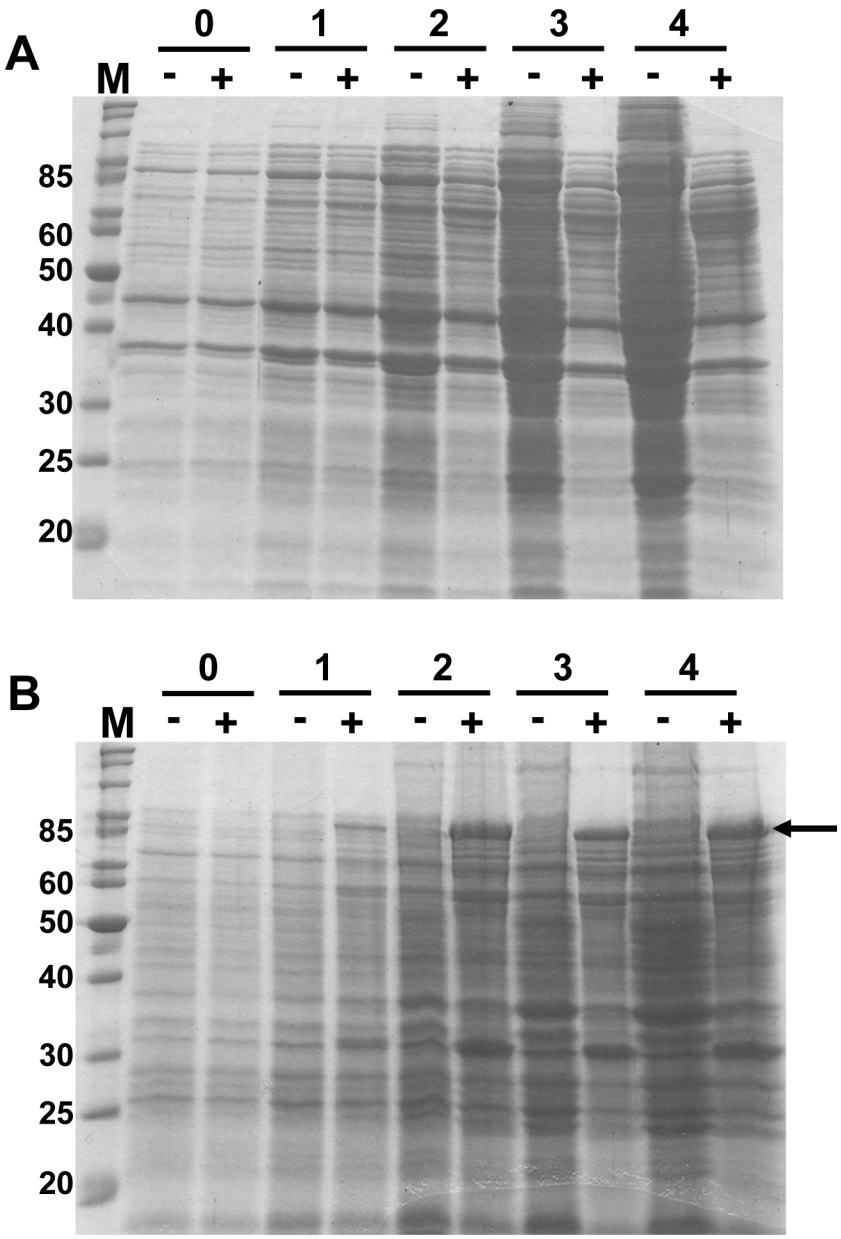

Figure 3-8. Expression of NusA/IYD-NR (84.1 kDa) in Rosetta2(DE3) *E. coli* at 23 °C with 50 μM IPTG. A) Supernatant after centrifugation at 16.000 x g for 10 minutes. B) Insoluble pellet after centrifugation. Culture was induced at OD600 = 0.6 and aliquots removed at 1 hour intervals for PAGE analyusis. Arrow indicates NusA/IYD-NR.

(pGEX/IYD-NR by Ling Chen) were constructed. As with the thioredoxin fusion protein, many conditions were surveyed for the ability to produce soluble protein. Unfortunately, soluble IYD-NR fusion protein was undetectable by either PAGE analysis or radioactive iodide release assay. See Figure 3-8 for a representative expression of

NusA/IYD-NR fusion protein. More information must be obtained regarding the minimal amount of the IYD-NR structure necessary for enzyme activity.

Chapter 4

Electron Transfer in Iodotyrosine Deiodinase

4.1 Introduction

The mammalian thyroid has evolved two distinct but chemically similar mechanisms for reductive deiodination. For both iodothyronine deiodinase (ID)[19, 140] and iodotyrosine deiodinase (IYD),[61, 85] catalysis is thought to proceed via tautomerization of the phenol to generate a highly electrophilic intermediate (Figure 4-1). During catalysis, the first of two proposed electron transfers (from enzyme to substrate) reduces the substrate molecule with concomitant oxidation of an active-site residue. A second electron transfer (from electron donor to enzyme) regenerates reduced, active enzyme. To date, little progress has been made toward understanding electron transfer from NADPH to the C-I bond in IYD. The gene encoding ID was first identified over a decade ago[37] and the mechanism proposed for ID may provide a useful comparison for IYD.

The electron transfer step from enzyme to substrate in ID is thought to be driven by the nucleophilicity and redox capacity of the conserved selenocysteine residue found in all three isozymes.[36, 37, 141] Site-directed mutagenesis was used to illustrate the catalytic advantage of selenium over sulfur in the deiodination reaction.[141] Specifically, the SeCys126Cys mutant of ID1 resulted in a 300-fold decrease in apparent k_{cat} compared to T_4 deiodination by the wild-type enzyme while K_M increased only three-fold.[141] A number of other enzymes use the unique properties of selenocysteine to catalyze redox reactions including formate dehydrogenase, thioredoxin reductase, glutathione peroxidase and methionine R-sulfoxide reductase.[97, 142]

Furthermore, a conserved cysteine residue in ID1 (Cys124) and ID3 (Cys142) is one residue away from the selenocysteine and putatively forms a mixed seleno-sulfide adduct that influences the efficiency with which DTT regenerates the active enzyme.[143]

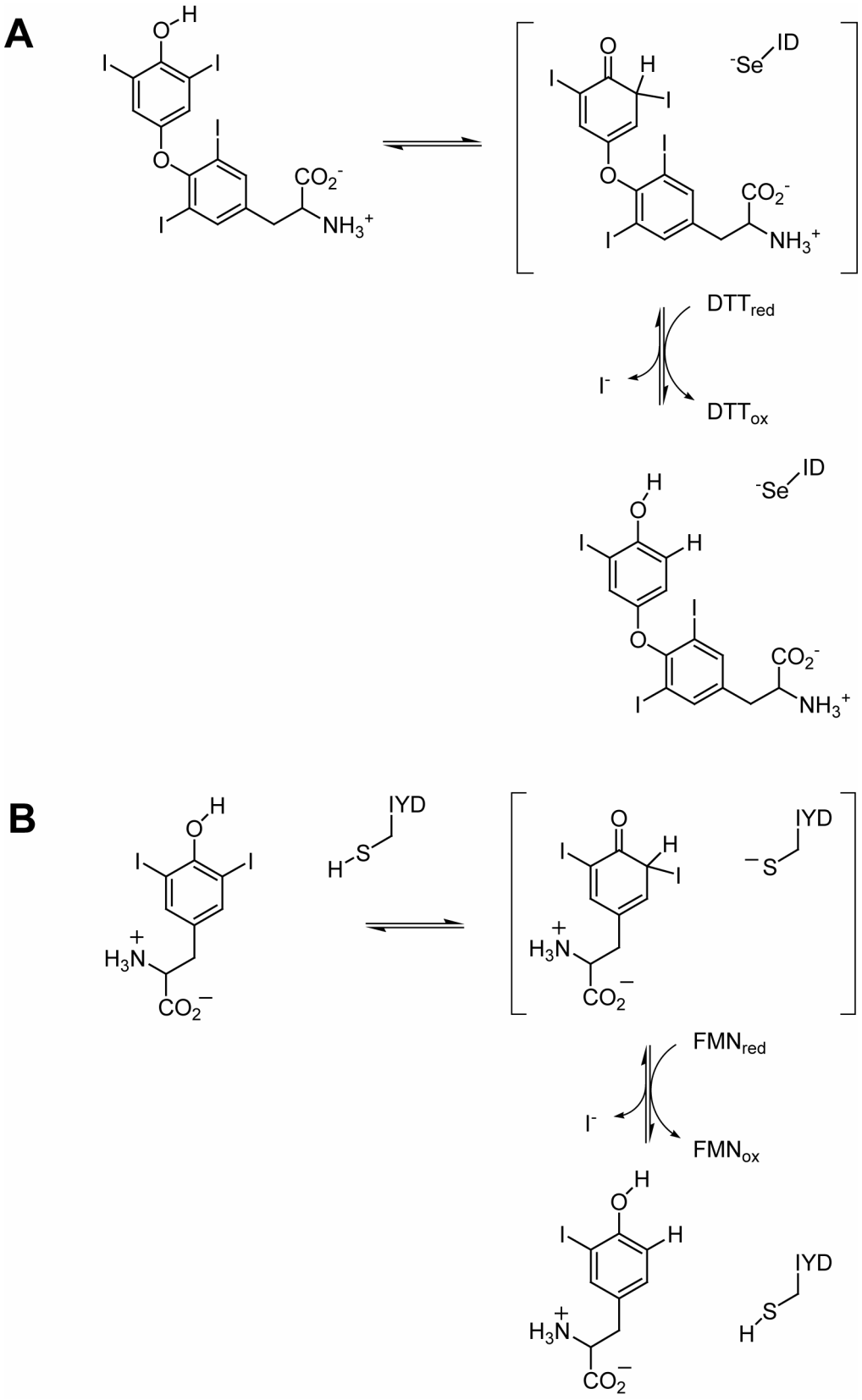

Figure 4-1. Comparison of catalytic mechanisms proposed for A) iodotyrosine deiodinase and B) iodothyronine deiodinase.

However, the cysteine-selenocysteine interaction is not required for catalysis as demonstrated by the Cys124Ala mutant of ID1 having unchanged activity *in vivo* relative to wild type, as well as by ID2, which has a conserved alanine residue instead of the cysteine.[144] An even more remarkable example of the deiodinating power of selenocysteine comes from a catalytic antibody that was capable of T_4 deiodination after chemical introduction of selenocysteine residues.[145]

IYD, however, does not contain a selenocysteine residue,[90, 97, 101] but likely relies on the nucleophilicity and redox activity of a cysteine residue for catalysis.[57, 85] Cysteine-promoted, non-enzymatic deiodination of iodotyrosines has even been observed under reasonably biological conditions (pH 7.23, 37 °C).[146, 147] In addition, incubation with a cysteine-specific inhibitor, *N*-ethyl maleimide (NEM), completely inhibited IYD in the presence of NADPH and prevented reconstitution of active enzyme by addition of FMN to the apoenzyme.[60]

The recently identified IYD gene encodes three cysteine residues (Figure 2-3); however, Cys13 is within a predicted transmembrane anchor and is not expected to participate in IYD catalysis. Cys217 is part of an SxxC motif and possibly participates in catalysis. The SxxC motif is a variant of the classical CxxC motif found in many redox-active dithiol containing proteins including a mammalian protein disulfide isomerase homolog[148] as well as yeast peroxiredoxin and glutathione *S*-transferase.[149] Furthermore, the homology model developed in chapter 3 predicts a Cys239-flavin C4a interaction that is commonly found in cysteine-containing flavoproteins.

Electron transfer from electron donor to enzyme is the least well characterized half-reaction in ID. The identity of the biological electron donor is still not known.

However, activity can be stimulated *in vitro* using thiols (e. g., dithiothreitol, gluthathione, and dihydrolipoamide),[15, 150-152] and by NADPH in a thioredoxin-thioredoxin reductase coupled assay.[153]

Likewise, little is known about electron transfer from NADPH to IYD. As mentioned in chapter 1, a reductase has long been suspected of mediating IYD's reduction *in vivo*.[55, 60, 154] The reductase was first suggested after finding that the NADPH-responsive activity was solubilized by sodium cholate, but not by steapsin (a crude pancreatic extract of lipases).[55, 154] Furthermore, column chromatography of the sodium cholate preparation resulted in loss of the NADPH-responsive activity implying that IYD was purified away from the reductase.[55, 154]

The reductase was subsequently suggested to be a non-heme iron protein based on the inhibition of NADPH-supported deiodination upon treatment with the iron chelators, o-phenanthroline and 2,2′-bipyridyl. [60, 154] Interestingly, EDTA did not inactivate NADPH-driven catalysis.[60] The authors asserted that EDTA does not inhibit IYD because it is unable to "penetrate hydrophobic regions," as was seen with soybean lipoxygenase.[155] More recently, the inability of IYD expressed in Chinese hamster ovary (CHO) cells to support NADPH-driven deiodination was attributed to the absence of the reductase in that cell line.[101]

No members of the NADH oxidase / flavin reductase (NOX/FRase) superfamily catalyze dehalogenation, however they may provide insight into the electron transfer mechanism, particularly with respect to electron transfer from donor to enzyme. Flavin reductase P (FRP)[107, 108, 126, 127, 156, 157] from *Vibrio harveyi* and the NADH/NADPH-utilizing general flavin reductase (FRaseI)[109, 158, 159] from *Vibrio fischeri* transfer reduced

flavin to luciferase as a component of the bacterial luciferase-flavin reductase system that results in bioluminescence of the producing organisms.[160] Furthermore, both enzymes have had thorough mechanistic examinations. [107-109, 126, 127, 156-159] Electron transfer from the putative reductase to IYD can be thought of as the reverse reaction of the transfer of flavin from FRP/FRaseI to luciferase.

Both FRP and FRaseI undergo a monomer-dimer equilibrium that allows heterodimer formation with luciferase. In the presence of luciferase, the flavin bound to FRP or FRaseI is utilized as a substrate for reduction by electron transfer from the nicotinamide donor and is delivered directly to luciferase. In the absence of luciferase, the bound flavin functions as a cofactor and shuttles between its oxidized and reduced states, but remains bound to the enzyme. The mechanism of electron transfer proceeds by NAD(P)H binding, reduction of the bound flavin, $NAD(P)^+$ release. This half reaction is followed by binding of the substrate flavin, electron transfer from the cofactor-flavin to the substrate-flavin, and release of the reduced substrate-flavin product.

Some of the features of electron transfer in the NOX/FRase superfamily may be useful in describing IYD's mechanism with minor modifications. In addition to the cofactor-flavin bound to IYD, the proposal requires a substrate-flavin that is shuttled to IYD from the reductase after reduction by NADPH. Furthermore, the IYD-bound cofactor-flavin would have to be reduced by the substrate-flavin, without direct transfer of electrons from substrate-flavin to cysteine-sulfenyl iodide.

This chapter aims to provide insight into the electron transfer mechanism used by IYD. A series of truncation mutants will be constructed to examine the role of the domains predicted in IYD. More specifically, the nitroreductase domain will be

examined as an independent domain for catalytic activity. Furthermore, the truncation mutants may provide insight into the structural requirements for production of a soluble IYD.

4.2 Experimental Procedures

General procedures. Total protein concentrations were measured using the BCA assay, according to the manufacturer's directions. V_{max} and k_{cat} were estimated based on the molecular mass of IYD, the total protein concentration, and the fractional concentration of the IYD construct, determined by densitometry of Coomassie stained PAGE gels.

Subcloning of *Mus musculus* IYD truncation mutants. In order to construct plasmids for expression of the IYD nitroreductase domain (IYD-NR) and the transmembrane-domain deletion mutant (IYD-ΔTM), appropriate fragments of the IYD gene (I.M.A.G.E. clone 5064638 from ATCC) were amplified by PCR. IYD-NR was amplified using oligonucleotide primers (0.5 μM) 5′-AAGCTTAAGCTT*GGATCC*GCCACCATGAGGATGAGGTCCCAGGAA-3′ and 5′-ATT*CTCGAG*CTAATGGTGATGGTGATGGTGTACTGTCACCATGAT-3′ (BamH I and Xho I restriction sites in italics and start/stop codons underlined). IYD-ΔTM was amplified using oligonucleotide primers (0.5 μM) 5′-AAGCTTAAGCTT*GGATCC*GCCACCATGGCTCAAGTTCAGCCC-3′ and 5′-ATT*CTCGAG*CTAATGGTGATGGTGATGGTGTACTGTCACCATGAT-3′ (italics and underlines as before). The PCR products were digested with BamH I (20 U) and Xho I (20 U). The vector, (+)-pcDNA3.1/Zeo (Invitrogen), was also digested with BamH I (20 U) and Xho I (20 U) and dephosphorylated using Antarctic alkaline phosphatase (2

U, Invitrogen). The insert (6 ng) and vector (14 ng) were then ligated using T4 DNA ligase (400 U) and transformed into One Shot TOP10 cells (Invitrogen) following the manufacturer's instructions. Plasmid DNA was isolated from ampicillin-resistant colonies using QIAprep spin miniprep kit (Qiagen) and characterized by digestion with EcoR I, Pst I or Sty I. Plasmids were analyzed by gel electrophoresis (1% agarose, 125 V, 30 minutes) and those exhibiting appropriately-sized DNA fragments were sent for DNA sequencing (Gene Gateway).

Subcloning of *Mus musculus* IYD hexahistadine tagged mutants. The *C*-terminal hexahistadine tag was introduced to IYD-NR and IYD-ΔTM by PCR as described above using the oligonucleotide primer 5′-ATT*CTCGAG*CTA**ATGGTGATGGTGATGGTG**TACTGTCACCATGAT-3′ to anneal at the 3′ end of the sequence (Xho I restriction site in italics, stop codon underlined, and His_6 tag in bold).

Expression of *Mus musculus* IYD truncation mutants in HEK293 cells. Human embryonic kidney (HEK) 293 cells were maintained in Dulbecco's modified Eagle's medium (DMEM, Invitrogen) supplemented with 10% fetal calf serum (Atlanta Biologicals) and 1% penicillin-streptomycin-glutamine (Invitrogen). Plasmids containing the individual constructs of IYD (12 μg) were incubated for 20 minutes with 30 μL of Lipofectamine 2000 in Opti-MEM (Invitrogen) and then added to cells (~90% confluent) in 10 cm dishes. After 6 hours, the liquid medium was exchanged to DMEM. Forty-eight hours after transfection, the cells were washed twice with 10 mL Dulbecco's phosphate buffered saline (DPBS, Invitrogen) and suspended in the same solution. The cells were centrifuged (300 x g) for 5 minutes at 4 °C and the cell pellet was resuspended

in 1 mL 50 mM sodium phosphate (pH 7.2) supplemented with 0.25 M sucrose and 0.1 mM DTT. The cells were lysed by three cycles of freezing (liquid N_2) and thawing (37 °C) followed by three passages through a 20 gauge needle. Catalytic constants for IYD were determined by plotting the initial rate of iodide release versus DIT concentration, and the resulting data were fit to the Michaelis-Menten equation with Origin 7.0 (Microcal). All reported values are from a minimum of three independent determinations.

Subcellular fractionation of IYD truncation mutants by preparative ultracentrifugation. The lysates (4 mL) from HEK293 cells (50 mg) transfected with plasmids encoding IYD-NR and IYD-ΔTM were centrifuged (500 x g, 15 min) to remove unlysed cells. The supernatant was transferred to polycarbonate tubes and further centrifuged for 30 minutes at 30K x g (4 °C) to pellet small cellular debris. The supernatant was further centrifuged for 1.5 hour at 100K x g (4 °C). The supernatant was decanted and the pellet resuspended in an equal amount of cell lysis buffer. Aliquots containing 20 μg protein in SDS-PAGE loading buffer were denatured at 90 °C for 15 minutes and loaded into a polyacrylamide gel (12% separating/5% stacking). The proteins were electrophoresed for 35 minutes at 200 V using a Mini Protean 3 electrophoresis system and either stained using Coomassie Brilliant Blue or used for Western blot analysis.

Western blot analysis. Proteins were transferred from an SDS-PAGE gel prepared as above to Invitrolon membrane (Invitrogen) at 30 V, 90 mA overnight (12 hour minimum) in a transblot apparatus (Bio-Rad) according to the manufacturer's directions (25 mM Tris (pH 8.3), 192 mM glycine and 0.1% SDS at 4 °C). Nonspecific

binding was blocked by incubation in 5% non-fat dry milk in TBST solution (10 mM Tris/HCl (pH 8.0), 150 mM NaCl, and 0.05% Tween-20) for 10 hours at 4 °C. The blot was incubated with Anti-His_6 monoclonal antibody (Novagen) overnight at 4 °C in 5% milk/TBST. The blot was washed (15 min x 3) in TBST prior to incubation with alkaline phosphatase-conjugated goat anti-mouse IgG (Pierce) for 1 hour in TBST at room temperature. The blot was washed (15 min x 3) in TBST. The blot was visualized using CDP-Star chemiluminescence substrate (Sigma Aldrich) and Storm phosphorimager (GE Healthsciences).

4.3 Results and Discussion

Wild type iodotyrosine deiodinase. The Rokita lab recently reported the identification of the gene encoding IYD by purification and sequencing of a soluble domain from IYD obtained by proteolytic release from porcine thyroidal microsomes.[90] Furthermore, Gnidehou et al identified the human gene by a serial analysis of gene expression in the thyroid.[101] As described in chapter 2, the gene encoding IYD from *Mus musculus* was expressed in HEK293 cells and found to be catalytically active toward DIT when stimulated by dithionite ($K_{M(DIT)}$ = 4.4 ± 1.7 μM, V_{max} = 12 ± 1).[90]

The enzyme was also responsive to NADPH, although a time dependent decrease in NADPH-responsive activity was noted. Thus, V_{max} measured immediately after cell lysis is 3.3 ± 0.6 nmol hr^{-1} μg^{-1} with NADPH and K_M for DIT is 5.3 ± 3.2 μM. The determination reported in chapter 2 (V_{max} = 1.1 ± 0.4 nmol/hr-1 per μg of IYD) was performed on enzyme that had been stored overnight, on ice, in a 4 °C refrigerator. The NADPH-derived K_M for DIT values agreed within error. Furthermore, dithionite-stimulated catalysis was unchanged for greater than 72 hrs so the three-fold decrease in

NADPH-dependent V_{max} after storage likely reflects the instability of the putative reductase.

Expression and deiodinase activity of the nitroreductase domain from IYD. Although prokaryotic expression of the nitroreductase domain had failed, the question about the ability of NR to support catalysis remained. To try to answer that question, the gene fragment corresponding to residues 82-285 of IYD (IYD-NR) was subcloned into (+)-pcDNA3.1/Zeo using PCR methods. An inducible band of protein was not visible by PAGE analysis (Coomassie stained) of the cell lysate from HEK293 cells expressing the plasmid encoding IYD-NR (Figure 4-2 A).

Moreover, deiodinase activity was undetectable in the iodide release assay despite addition of up to 200 μg total protein. Subcellular fractionation could be used to determine if IYD-NR was present in the cytosol or was insoluble, but would require a more sensitive technique for visualization. To increase the sensitivity with which IYD-NR could be detected, a hexahistadine sequence was appended to the *C*-terminus of the protein for use in Western blot analysis.

The lysate of HEK293 cells expressing IYD-NR/His_6 was analyzed by polyacrylamide electrophoresis after ultracentrifugation. Western blot analysis of the PAGE separated proteins (Figure 4-2 B) showed that (IYD-NR)/His_6 was present in the insoluble fraction of the lysate, explaining the absence of deiodinating activity. Although (IYD-NR)/His_6, and presumably IYD-NR also, was insoluble, perhaps a soluble domain of IYD could be expressed if a larger fragment of the protein was expressed.

Expression and deiodinase activity of transmembrane domain deleted IYD. The gene fragment encoding residues 34-285 of IYD were subcloned into (+)-

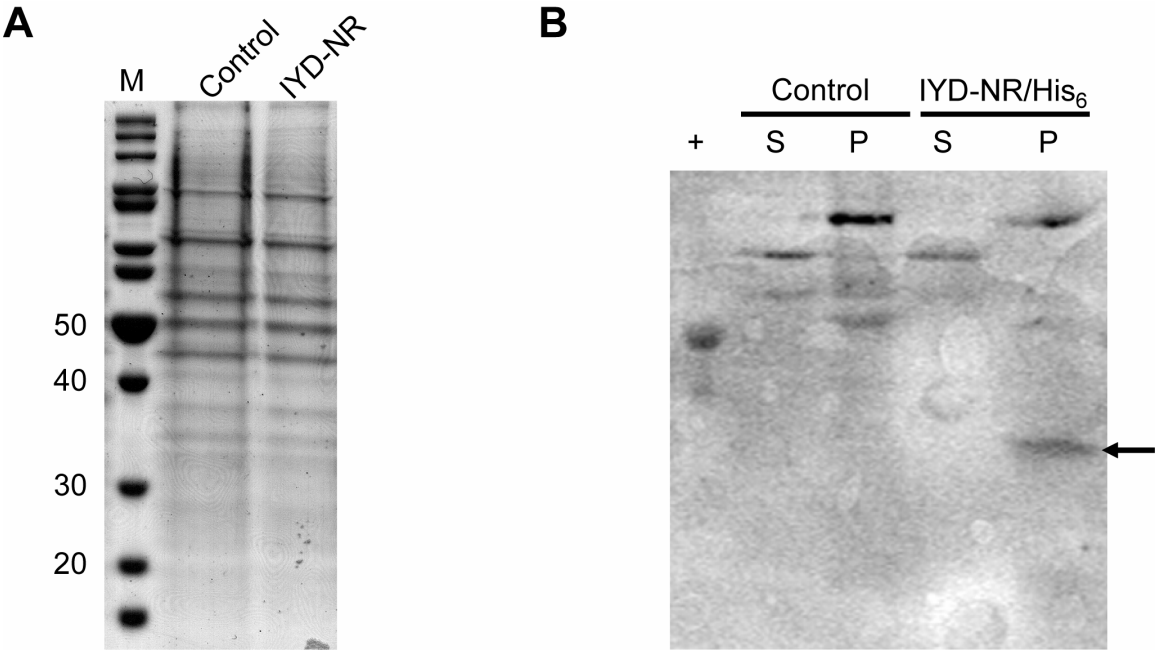

Figure 4-2. Expression of the nitroreductase domain from IYD in human embryonic kidney (HEK293) cells as monitored by polyacrylamide gel electrophoresis . A) Induced protein is not visible by Coomassie staining using lysate from untransfected cells (Control) and from cells expressing the nitroreductase domain from IYD (IYD-NR). B) Subcellular fractionation of IYD by ultracentrifugation as monitored by Western blot analysis with anti-His_6 antibody. IYD-NR/His_6 (arrow) is observed in the insoluble fraction (P) after ultracentrifugation. S is the supernatant after ultracentrifugation and + is hexahistadine labeled urate oxidase (35 kDa), a positive control. Cell lines are as described in A.

pcDNA3.1/Zeo with and without a hexahistadine tag at the *C*-terminus, (IYD-ΔTM)/His_6 and IYD-ΔTM, respectively. The plasmids were expressed in HEK293 cells and analyzed by PAGE analysis (Figure 4-3). Wild type IYD and (IYD-ΔTM)/His_6 were visible upon Coomassie staining as bands estimated to be 1% of total cellular protein (measured by densitometry) while IYD-ΔTM was estimated to be 5% of the total protein.

To examine whether IYD-ΔTM was soluble, the lysate of HEK293 cells expressing the protein was subjected to ultracentrifugation. The increased expression level of IYD-ΔTM, relative to IYD-NR, permitted analysis of the ultracentrifugation results by Coomassie-stained PAGE gel instead of by Western blot (Figure 4-4). A

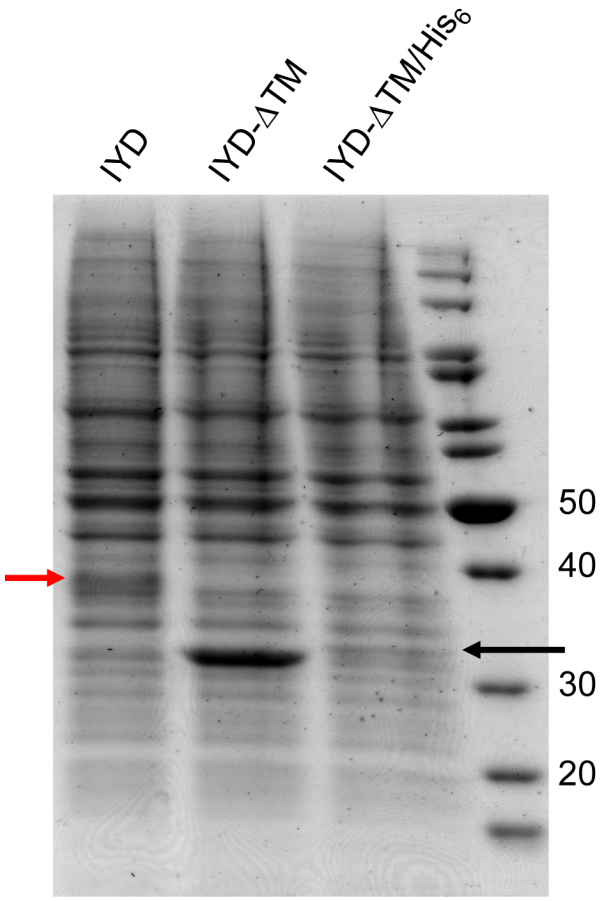

Figure 4-3. Expression of IYD and truncation mutants with deleted transmembrane domain. Red arrow indicates IYD expressed in HEK293 cells. The black arrow indicates the transmembrane domain deleted (IYD-ΔTM) and hexahistadine-labeled (IYD-ΔTM/His_6) truncation mutants of IYD expressed in HEK293 cells. IYD IYD and IYD-ΔTM/His_6 are expressed to approximately 1% of the total cellular protein, while IYD/ΔTM is expressed at approximately 5% of total protein.

protein band corresponding to IYD-ΔTM was found in the supernatant after each centrifugation step.

The presence of IYD-ΔTM in the supernatant confirms our prediction that the N-terminus anchors IYD to the microsomal membrane. Furthermore, this finding definitively refutes the assertion that residues 209-225 are involved in membrane attachment, as has been suggested for the equivalent residues in the human protein.[101]

More importantly, the truncation mutants were active in the iodide release assay with dithionite. Table 4-1 summarizes the apparent kinetic parameters with DIT as

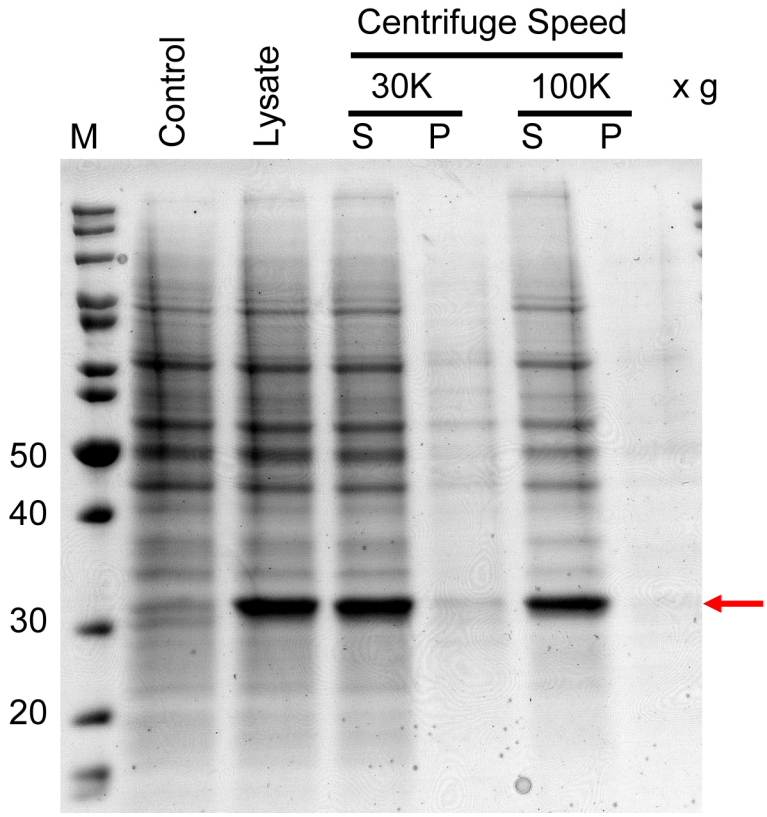

Figure 4-4. Polyacrylamide analysis of lysate from HEK293 cells expressing IYD-ΔTM (red arrow). Control lane is untransfected cells. Lysate lane is whole cell lysate from HEK293 expressing IYD-ΔTM. Remaining lanes are the supernatant (S) and insoluble (P) fractions after centrifugation at the indicated speed (30,000 or 100,000 x g).

substrate. Deletion of the transmembrane domain and the subsequent solubilization of IYD-ΔTM has little effect on the Michaelis constants (K_M = 4.6 ± 0.8 μM) compared to wild type IYD (K_M = 4.4 ± 1.7 μM). Moreover, the V_{max} values of IYD-ΔTM (7.3 ± 1.3 nmol hr^{-1} μg^{-1}) and wild type IYD (12 ± 1 nmol hr^{-1} μg^{-1}) are in reasonable agreement. The k_{cat} values measured for wild type (6.4 ± 0.7 min^{-1}) and IYD-ΔTM (5.9 ± 0.9 min^{-1}) agree within error. Addition of the His_6 sequence causes a slight decrease in the K_M (2.9 ± 0.9 μM), however no change in k_{cat} is noted (5.9 ± 0.4 min^{-1}).

Although transmembrane domain deletion results in little change when dithionite is used for catalysis, a striking difference is noted between wild type IYD and IYD-ΔTM for NADPH responsive activity. NADPH supports catalysis in wild type IYD, albeit with

Table 4-1. Apparent kinetic parameters measured for IYD and truncation mutants.

Enzyme	Electron Donor	$K_{M,DIT}$ (μM)	V_{max} (nmol hr^{-1} μg^{-1})	k_{cat} (min^{-1})
IYD	Dithionite	4.4 ± 0.7	12 ± 1	6.4 ± 0.7
IYD(Δ2-33)	Dithionite	4.6 ± 1.3	7.0 ± 0.5	5.9 ± 0.9
IYD(Δ2-33)/His_6	Dithionite	2.9 ± 0.9	5.5 ± 0.4	5.9 ± 0.4
IYD	NADPH	5.3 ± 3.2	3.3 ± 0.6	1.9 ± 0.2
IYD(Δ2-33)	NADPH	—	0.0 ± 0.4	—

an approximate three-fold decrease in k_{cat} relative to dithionite. However, deiodinase activity is at least 24-fold less responsive to NADPH (Appendix C) in lysate containing IYD-ΔTM after ultracentrifugation at 100K x g. This likely reflects the physical separation of IYD-ΔTM from the reductase described earlier.

The observations in this chapter confirm that a soluble variant of IYD can be expressed and that residues 1-33 are the transmembrane domain that anchors IYD to microsomal membranes. Furthermore, the loss of NADPH-responsive activity supports the existence of the putative reductase and implies that membrane attachment is necessary for electron transfer from NADPH to IYD because it brings IYD and the unidentified reductase into proximity.

Chapter 5

Summary and Final Discussion

The work presented in this dissertation sought to increase understanding of the molecular basis for iodotyrosine deiodinase catalysis. Toward that end, my research has provided the following insights:

Using the sequence data from the porcine enzyme, the gene responsible for production of iodotyrosine deiodinase (IYD) was tentatively identified and has been analyzed using a variety of bioinformatics tools. The results of the analysis are in agreement with the sparse literature data regarding the enzyme: a) the identified gene is highly conserved across all mammals and encodes three cysteine residues, at least one of which is expected to play a role in IYD catalysis; b) comparison of the IYD gene to the genes encoding the only other mammalian reductive dehalogenase, iodothyronine deiodinase, suggests that IYD and ID are distinct enzymes that have evolved from different protein superfamilies, NADH oxidase/flavin reductase and thioredoxin, respectively, to catalyze similar reductive deiodination reactions; and c) further studies have supported the identification of IYD as the first, and only, mammalian member of the NADH oxidase/flavin reductase superfamily. Furthermore, the identity of the gene has been confirmed by expression in a heterologous host, human embryonic kidney (HEK293) cells.

A three dimensional model of IYD nitroreductase domain has been developed based on its homology to the NADH oxidase/flavin reductase superfamily. The model agrees with the crystal structure of NfnB-NfsB (RMSD < 0.5 Å over key regions including dimer interface and putative active site) and supports the assignment of IYD as the first mammalian member of the superfamily. Furthermore, the model predicts key cysteine-flavin interactions that are implicit in the mechanism proposed for catalysis. If

confirmed, these interactions identify IYD as the first member of a new class of flavoproteins containing redox-active cysteine residues. Additionally, the model suggests that expression of the nitroreductase domain, without the remaining IYD residues, may result in a soluble, catalytically active protein. Moreover, prokaryotic expression may be possible based on the frequency with which the bacterial proteins are found.

The mechanism of electron transfer in IYD has been investigated by expression of a pair of truncation mutants in human embryonic kidney (HEK293) cells. The deletion mutant encoding solely the nitroreductase domain (IYD-NR) does not catalyze deiodination of DIT when expressed in HEK293 cells. More specifically, IYD-NR is insoluble, likely because it does not fold properly *in vivo*. Heterologous expression of the transmembrane domain deletion mutant (IYD-ΔTM) yields a soluble, cytosolic protein. Furthermore, the soluble protein deiodinates DIT and has catalytic parameters consistent with the wild-type, membrane-bound enzyme when stimulated with dithionite. Expression of the soluble IYD-ΔTM mutant completely eliminates NADPH-responsive catalysis and supports literature reports of a membrane-bound reductase that mediates electron transfer from NADPH to IYD.

Appendix

A. Representative determination of IYD concentration by densitometry

After staining with Coomassie Blue, the denaturing PAGE gel was digitized using a Kodak DC120 camera and Kodak Digital Science 1D 2.0.2 software. The image was saved in tag image file format (tiff) and analyzed using SepraScan Gel Viewer 1.1. For example, the IYD-ΔTM lane from Figure 4-3 was analyzed to yield the trace below:

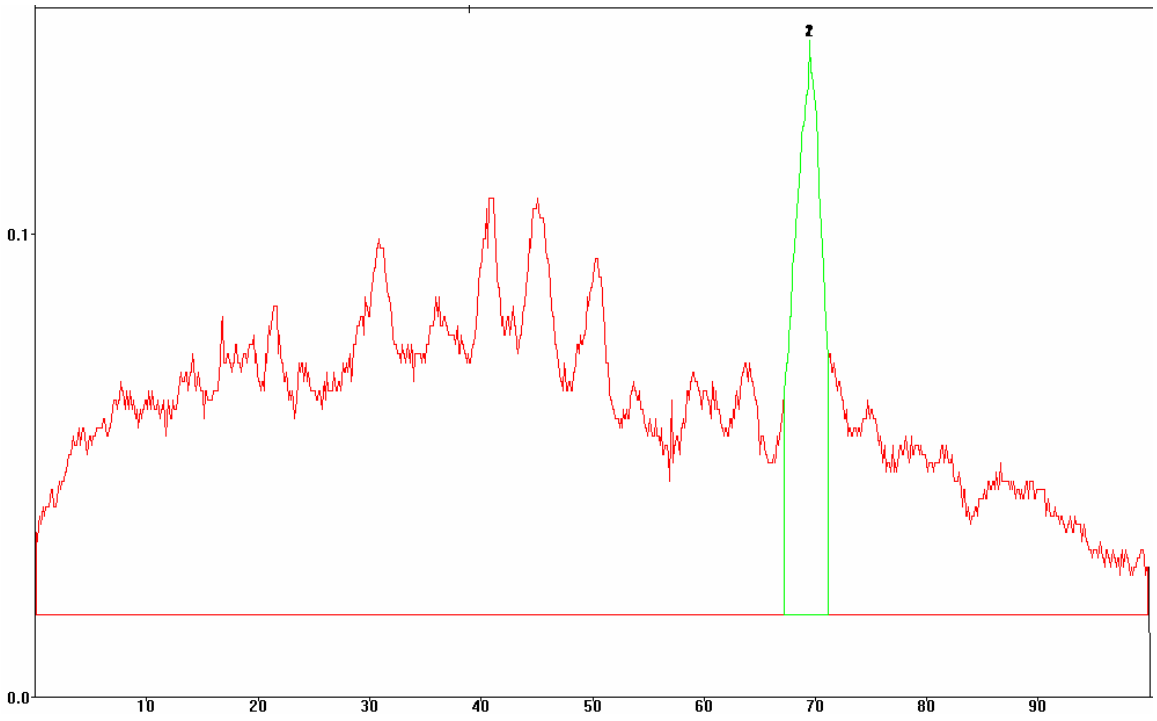

SepraScan Gel Viewer was used to integrate the peak (green) corresponding to IYD as a fraction of the total protein present (red).

B. Representative Determination of Kinetic Parameters

The data collected during a series of assays were plotted and fit to the Michaelis-Menten equation using Origin 7.0 (Microcal) as shown below for IYD assayed using dithionite:

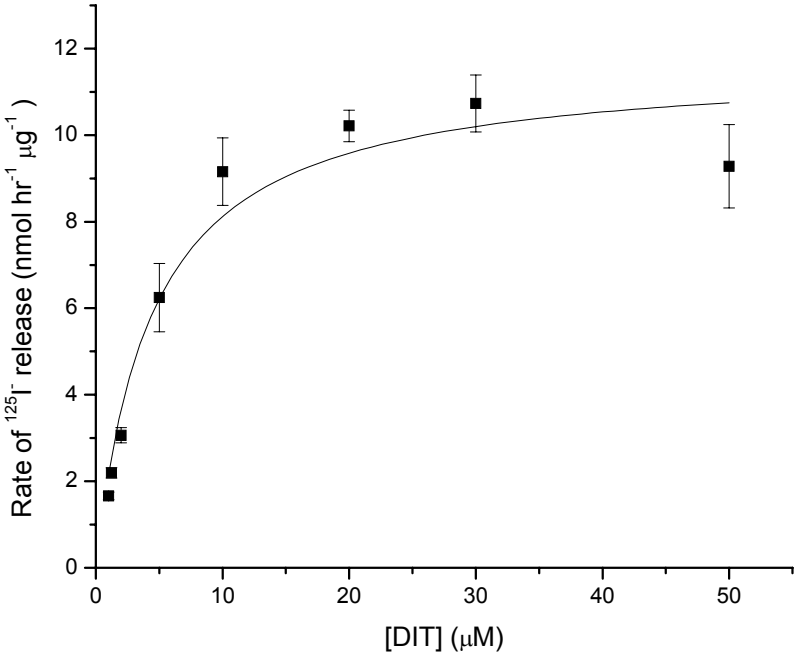

The error bars indicate the standard deviation of three independent determinations as calculated by Origin 7.0. The black line was plotted by fitting the data to the Michaelis-Menten equation using Origin 7.0.

C. Dithionite vs. NADPH-responsive activity for IYD-ΔTM

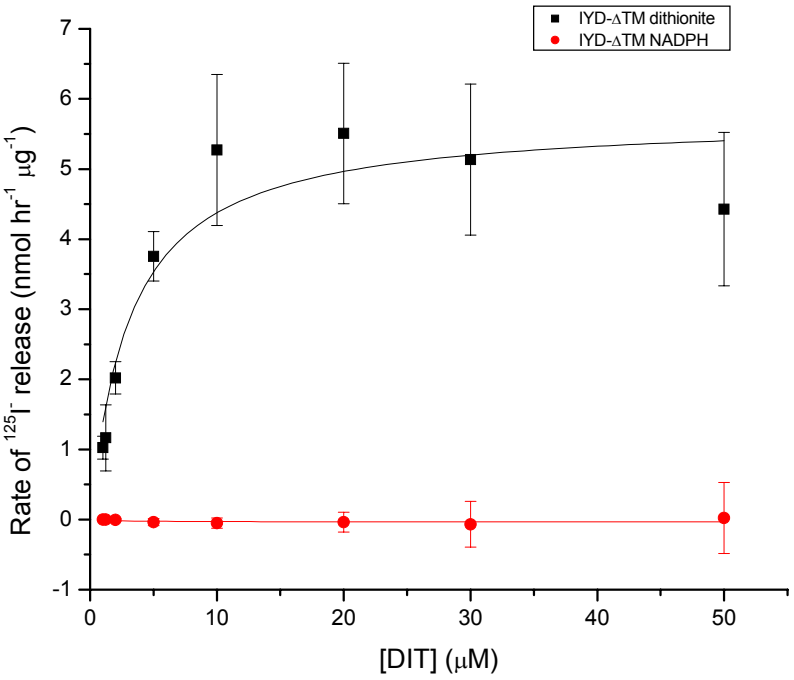

Figure C-1. Rate of $^{125}I^-$ release determined for IYD-ΔTM using standard assay conditions for dithionite and NADPH as described in the experimental section. V_{max} for dithionite is 5.5 ± 0.4 nmol hr^{-1} μg^{-1} and for NADPH is 0.0 ± 0.4 nmol hr^{-1} μg^{-1}. The error bars indicate the standard deviation of three independent determinations. The black and red lines were plotted by fitting the data to the Michaelis-Menten equation using Origin 7.0.

V_{max} determined for the NADPH-responsive activity using Origin 7.0 had standard deviation of 0.4 nmol hr^{-1} μg^{-1} (Figure C-1) indicating an approximate ten-fold loss of NADPH-responsive activity relative to dithionite.

To further examine the protein-dependence of NADPH-responsive activity, the rate of deiodination was measured at varying IYD-ΔTM concentrations (Figure C-2) using 30 μM DIT (~3 x K_M) in the standard 1 mL assay. At 2.0 μg IYD-ΔTM, the dithionite-responsive activity was 24-fold greater (2.4/0.1) than the comparable NADPH-responsive activity.

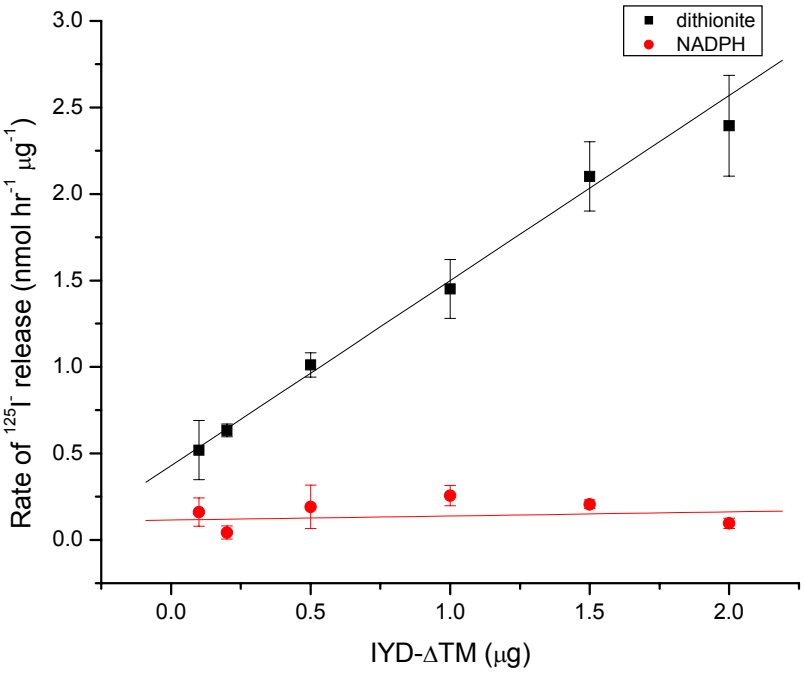

Figure C-2. Standard dithionite and NADPH assays (1 mL) were used to monitor protein-dependent deiodination in the presence of 30 μM DIT. The error bars indicate the standard deviation of three independent determinations. The black and red lines were plotted as linear fits of the data using Origin 7.0.

References

(1) Hadley, M. E. "Endocrinology." 4th ed., Prentice-Hall: Englewood Cliffs, NJ, 1995, 518.

(2) Sawin, C. T. The Heritage of the Thyroid. *In* "Werner & Ingbar's the Thyroid: a Fundamental and Clinical Text," 8th ed. (L. E. Braverman, and R. D. Utiger, Eds.); Lippincott Williams & Wilkins: Philadelphia, PA, 2000; pp. 1-6.

(3) Coindet, J.-F. Decouverte d'un Nouveau Remede Contre le Goitre. *Ann. Chim. Phys.* **1820,** *15***,** 49-59.

(4) Baumann, E. Über das normale Vorkommen von Jod im Thierkorper. *Hoppe-Seyler's Z. Physiol. Chem.* **1895,** *21***,** 319-330.

(5) Kendall, E. C. The Isolation in Crystalline Form of the Compound Which Occurs in the Thyroid: Its Chemical Nature and Physiologic Activity. *JAMA, J. Am. Med. Assoc.* **1915,** *64***,** 2042-2043.

(6) Stanbury, J. B., Meijer, J. W. A., and Kassenaar, A. A. H. Metabolism of Iodotyrosines.2. Metabolism of Mono-Iodotyrosine and Di-Iodotyrosine in Certain Patients with Familial Goiter. *J. Clin. Endocrinol. Metab.* **1956,** *16*(7)**,** 848-868.

(7) Stanbury, J. B., Kassenaar, A. A. H., and Meijer, J. W. A. Metabolism of Iodotyrosines.1. Fate of Mono-Iodotyrosine and Di-Iodotyrosine in Normal Subjects and in Patients with Various Diseases. *J. Clin. Endocrinol. Metab.* **1956,** *16*(6)**,** 735-746.

(8) Hartmann, N. Uber den Abbau von Dijotyrosin im Gewebe. *Z. Physiol. Chem.* **1950,** *285***,** 1-17.

(9) McNabb, F. M. A. Mechanism of Action of Thyroid Hormones. *In* "Thyroid Hormones," Prentice-Hall: Englewood Cliffs, NJ, 1992; pp. 135-164.

(10) McNabb, F. M. A. Physiological Actions of Thyroid Hormones. *In* "Thyroid Hormones," Prentice-Hall: Englewood Cliffs, NJ, 1992; pp. 165-196.

(11) McNabb, F. M. A. Control of Thyroid Gland Function. *In* "Thyroid Hormones," Prentice-Hall, Inc.: Englewood Cliffs, NJ, 1992; pp. 49-73.

(12) Kohrle, J. The Deiodinase Family: Selenoenzymes Regulating Thyroid Hormone Availability and Action. *Cell. Mol. Life Sci.* **2000,** *57*(13-14)**,** 1853-1863.

(13) Cavalieri, R. R. Iodine mMetabolism and Thyroid Physiology: Current Concepts. *Thyroid* **1997,** *7*(2)**,** 177-181.

(14) Bianco, A. C., Salvatore, D., Gereben, B., Berry, M. J., and Larsen, P. R. Biochemistry, Cellular and Molecular Biology, and Physiological Roles of the Iodothyronine Selenodeiodinases. *Endocr. Rev.* **2002,** *23*(1)**,** 38-89.

(15) Leonard, J. L., and Rosenberg, I. N. Thyroxine 5`-Deiodinase Activity of Rat Kidney: Observations on Activation by Thiols and Inhibition by Propylthiouracil. *Endocrinology* **1978,** *103***,** 2137-2144.

(16) Visser, T. J., Fekkes, D., Docter, R., and Hennemann, G. Sequential Deiodination of Thyroxine in Rat Liver Homogenate. *Biochem. J.* **1978,** *174***,** 221–229.

(17) Braverman, L. E., Ingbar, S. H., and Sterling, K. Conversion of Thyroxine (T4) to Triiodothyronine (T3) in Athyreotic Human Subjects. *J. Clin. Invest.* **1970,** *49*(5)**,** 855-864.

(18) Kohrle, J. Iodothyronine Deiodinases. *Methods Enzymol.* **2002,** *347***,** 125-167.

(19) Visser, T. J. Mechanism of Action of Iodothyronine-5'-Deiodinase. *Biochim. Biophys. Acta* **1979,** *569*(2)**,** 302-308.

(20) Solis-S, J. C., Villalobos, P., Orozco, A., and Valverde-R, C. Comparative Kinetic Characterization of Rat Thyroid Iodotyrosine Dehalogenase and Iodothyronine Deiodinase Type 1. *J. Endocrinol.* **2004,** *181*(3)**,** 385-392.

(21) St. Germain, D. L. The Effects and Interactions of Substrates, Inhibitors, and the Cellular Thiol-disulfide Balance on the Regulation of Type II Iodothyronine 5'-Deiodinase. *Endocrinology* **1988,** *122***,** 1860-1868.

(22) Silva, J. E., Mellen, S., and Larsen, P. R. Comparison of Kidney and Brown Adipose Tissue Iodothyronine 5'- Deiodinases. *Endocrinology* **1987,** *121***,** 650-656.

(23) Goswami, A., and Rosenberg, I. N. Iodothyronine 5'-Deiodinase in Brown Adipose Tissue: Thiol Activation and Propylthiouracil Inhibition. *Endocrinology* **1986,** *119*(2)**,** 916-23.

(24) Salvatore, D., Tu, H., Harney, J. W., and Larsen, P. R. Type 2 Iodothyronine Deiodinase is Highly Expressed in Human Thyroid. *J. Clin. Invest.* **1996,** *98***,** 962-968.

(25) Salvatore, D., Bartha, T., Harney, J. W., and Larsen, P. R. Molecular Biological and Biochemical Characterization of the Human Type 2 Selenodeiodinase. *Endocrinology* **1996,** *137***,** 3308-3315.

(26) Murakami, M., Araki, O., Hosoi, Y., Kamiya, Y., Morimura, T., Ogiwara, T., Mizuma, H., and Mori, M. Expression and Regulation of Type II Iodothyronine Deiodinase in Human Thyroid Gland. *Endocrinology* **2001,** *142***,** 2961-2967.

(27) Croteau, W., Davey, J. C., Galton, V. A., and St. Germain, D. L. Cloning of the Mammalian Type II Iodothyronine Deiodinase - A Selenoprotein Differentially Expressed and Regulated in Human and Rat Brain and other tissues. *J. Clin. Invest.* **1996,** *98*(2)**,** 405-417.

(28) McNabb, F. M. A. Circulating Thyroid Hormones and Hormone Kinetics. *In* "Thyroid Hormones," Prentice-Hall, Inc.: Englewood Cliffs, NJ, 1992; pp. 95-112.

(29) Kaminski, T., Kohrle, J., Kodding, R., and Hesch, R. D. Autoregulation of 3,3`5`-Triiodothyronine Production by Rat Liver Microsomes. *Acta Endocrinol.* **1981,** *98***,** 240-245.

(30) Goumaz, M. O., Kaiser, C. A., and Burger, A. G. Brain Cortex Reverse Triiodothyronine (rT3) and Triiodothyronine (T3) Concentrations Under Steady State Infusions of Thyroxine and rT3. *Endocrinology* **1987,** *120***,** 1590-1596.

(31) Leonard, J. L. Identification and Structure Analysis of Iodothyronine Deiodinases. *In* "The Thyroid Gland." (M. A. Greer, Ed.); Raven Press, Ltd.: New York, 1990; pp. 285-305.

(32) Larsen, P. R., and Berry, M. J. Nutritional and Hormonal-Regulation of Thyroid-Hormone Deiodinases. *Annu. Rev. Nutr.* **1995,** *15***,** 323-352.

(33) Kohrle, J. Local Activation and Inactivation of Thyroid Hormones: the Deiodinase Family. *Mol. Cell. Endocrinol.* **1999,** *151***,** 103-119.

(34) Visser, T. J. Role of Sulfation in Thyroid-Hormone Metabolism. *Chem.-Biol. Interact.* **1994,** *92*(1-3)**,** 293-303.

(35) Kaplan, M. M., Visser, T. J., Yaskoski, K. A., and Leonard, J. L. Characteristics of Iodothyronine Tyrosyl Ring Deiodination by Rat Cerebral Cortical Microsomes. *Endocrinology* **1983,** *112***,** 35-42.

(36) Berry, M. J., Kieffer, J. D., Harney, J. W., and Larsen, P. R. Selenocysteine Confers the Biochemical Properities Characteristic of the Type 1 Iodothyronine Deiodinase. *J. Biol. Chem.* **1991,** *266***,** 14155-14158.

(37) Berry, M. J., Banu, L., and Larsen, P. R. Type-I Iodothyronine Deiodinase Is a Selenocysteine-Containing Enzyme. *Nature* **1991,** *349*(6308)**,** 438-440.

(38) Montanari, S., Paradisi, C., and Scorrano, G. Thiol Anions in Nucleophilic Aromatic-Substitution Reactions with Activated Aryl Halides - Attack on Carbon Vs Attack on Halogen. *J. Org. Chem.* **1993,** *58*(21)**,** 5628-5631.

(39) Montanari, S., Paradisi, C., and Scorrano, G. Influence of Ion-Pairing, Steric Effects, and Other Specific Interactions on the Reactivity of Thioanions with Chloronitrobenzenes - Nucleophilic Aromatic-Substitution Vs Reduction. *J. Org. Chem.* **1991,** *56*(13)**,** 4274-4279.

(40) Seshadri, R., Pegg, W. J., and Israel, M. Reaction of Halomethyl Ketones with Thiols and Selenols - Substitution Vs Reduction. *J. Org. Chem.* **1981,** *46*(12)**,** 2596-2598.

(41) Dai, G., Levy, O., and Carrasco, N. Cloning and Characterization of the Thyroid Iodide Transporter. *Nature* **1996,** *379***,** 458-460.

(42) Riedel, C., Orsolya, D., De La Vieja, A., Ginter, C. S., and Carrasco, N. Journey of the Iodide Transporter NIS: from its Molecular Identification to its Clinical Role in Cancer. *Trends Biochem. Sci.* **2001,** *26*(8)**,** 490-496.

(43) Carrasco, N. Thyroid Iodide Transport: The Na^+/I^- Symporter (NIS). *In* "Werner & Ingbar's the Thyroid: a Fundamental and Clinical Text." (L. E. Braverman, and R. D. Utiger, Eds.); Lippincott Williams & Wilkins: Philadelphia, PA, 2000; pp. 52-61.

(44) Magnussun, R. P., Taurog, A., and Dorris, M. Mechanism of Iodide-Dependent Catalytic Activity of Thyroid Peroxidase and Lactoperoxidase. *J. Biol. Chem.* **1984,** *259***,** 197-205.

(45) Taurog, A., Dorris, M. L., and Doerge, D. R. Mechanism of Simultaneous Iodination and Coupling Catalyzed by Thyroid Peroxidase. *Arch. Biochem. Biophys.* **1996,** *330*(1)**,** 24-32.

(46) Taurog, A. Hormone Synthesis: Thyroid Iodine Metabolism. *In* "Werner & Ingbar's the Thyroid: a Fundamental and Clinical Text." (L. E. Braverman, and R. D. Utiger, Eds.); Lippincott Williams & Wilkins: Philadelphia, PA, 2000; pp. 61-84.

(47) Dunn, J. T., and Dunn, A. D. Update on Intrathyroidal Iodine Metabolism. *Thyroid* **2001,** *11*(5)**,** 407-14.

(48) Pommier, J., Deme, D., and Nunez, J. Effect of Iodide Concentration on Thyroxine Synthesis Catalyzed by Thyroid Peroxidase. *Eur. J. Biochem.* **1973,** *37***,** 406-414.

(49) Nunez, J., and Pommier, J. Formation of Thyroid Hormones. *Vitamin Horm.* **1982,** *39***,** 175-229.

(50) Morris, D. R., and Hager, L. P. Mechanism of the Inhibition of Enzymatic Halogenation by Antithyroid Agents. *J. Biol. Chem.* **1966,** *241***,** 3852-3859.

(51) Maloof, F., and Soodak, M. The Oxidation of Thiourea, a New Parameter of Thyroid Function. *In* "Current Topics in Thyroid Research." (C. Cassano, and M. Andreoli, Eds.); Academic: New York, 1965; pp. 277.

(52) Taurog, A., and Dorris, M. L. Myeloperoxidase-Catalyzed Iodination and Coupling. *Arch. Biochem. Biophys.* **1992,** *296*(1)**,** 239-46.

(53) Taurog, A., Dorris, M., and Doerge, D. R. Evidence for a Radical Mechanism in Peroxidase-Catalyzed Coupling. I. Steady-State Experiments with Various Peroxidases. *Arch. Biochem. Biophys.* **1994,** *315*(1)**,** 82-89.

(54) Querido, A., Stanbury, J. B., Kassenaar, A. A. H., and Meijer, J. W. A. Metabolism of Iodotyrosines.3. Di-Iodotyrosine Deshalogenating Activity of Human Thyroid Tissue. *J. Clin. Endocrinol. Metab.* **1956,** *16*(8)**,** 1096-1101.

(55) Rosenberg, I. N., and Goswami, A. Purification and Characterization of a Flavoprotein from Bovine Thyroid with Iodotyrosine Deiodinase Activity. *J. Biol. Chem.* **1979,** *254*(24)**,** 12318-12325.

(56) Stanbury, J. B. The Requirement of Monoiodotyrosine Deiodinase for Triphosphopyridine Nucleotide. *J. Biol. Chem.* **1957,** *232***,** 801-811.

(57) Goswami, A., and Rosenberg, I. N. Characterization of a Flavoprotein Iodotyrosine Deiodinase from Bovine Thyroid. Flavin Nucleotide Binding and Oxidation-Reduction Properties. *J. Biol. Chem.* **1979,** *254*(24)**,** 12326-30.

(58) Rodkey, F. L., and Donovan Jr., J. A. Oxidation-Reduction Potentials of the Triphosphopyridine Nucleotide System. *J. Biol. Chem.* **1959,** *234*(3)**,** 677-80.

(59) Rosenberg, I. N., and Goswami, A. Iodotyrosine Deiodinase from Bovine Thyroid. *Methods Enzymol.* **1984,** *107***,** 488-500.

(60) Goswami, A., and Rosenberg, I. N. Studies on a Soluble Thyroid Iodotyrosine Deiodinase: Activation by NADPH and Electron Carriers. *Endocrinology* **1977,** *101*(2)**,** 331-41.

(61) Friedman, J. E. Purification and Characterization of Iodotyrosine Deiodinase. Ph.D. Dissertation, University of Maryland, College Park, College Park, MD, 2001.

(62) Fetzner, S. Bacterial Dehalogenation. *Appl. Microbiol. Biotechnol.* **1998,** *50***,** 633-657.

(63) Copley, S. D. Microbial Dehalogenases. *Compr. Nat. Prod. Chem.* **1999,** *5***,** 401-422.

(64) Wackett, L. P., and Schanke, C. A. Mechanisms of Reductive Dehalogenation by Transition-Metal Cofactors Found in Anaerobic-Bacteria. *Met. Ions Biol. Syst.* **1992,** *28***,** 329-356.

(65) Mohn, W. W., and Tiedje, J. M. Microbial Reductive Dehalogenation. *Microbiol. Rev.* **1992,** *56*(3)**,** 482-507.

(66) Saveant, J. M. Mechanisms and Reactivity in Electron-Transfer-Induced Aromatic Nucleophilic-Substitution - Recent Advances. *Tetrahedron* **1994,** *50*(34)**,** 10117-10165.

(67) Bunnett, J. F. Some Novel Concepts in Aromatic Reactivity. *Tetrahedron* **1993,** *49*(21)**,** 4477-4484.

(68) Bunnett, J. F. Radical-Chain, Electron-Transfer Dehalogenation Reactions. *Acc. Chem. Res.* **1992,** *25*(1)**,** 2-9.

(69) Stradins, J., and Hansanli, B. Influence of pH on Electrooxidation Potentials of Substituted Phenols and Evaluation of pKa from Anodic Voltammetry Data. *J. Electroanal. Chem.* **1993,** *353***,** 57-69.

(70) Dawson, R. M. C., Elliott, D. C., Elliott, W. H., and Jones, K. M., Eds. (1989). Data for Biochemical Research. 3 ed: Oxford University Press.

(71) Rossi, R. A., De Rossi, R. H., and Lopez, A. F. Photostimulated Arylation of Cyanomethyl Anion by $S_{RN}1$ Mechanism of Aromatic Substituion. *J. Org. Chem.* **1976,** *41***,** 3371-3373.

(72) Bunnett, J. F., and Sundberg, J. E. SynthesisOf Arylacetones By $S_{RN}1$ Arylation Of Acetone Enolate Ion. *Chem. Pharm. Bull.* **1975,** *23***,** 2620-2628.

(73) Vuilleumier, S., and Pagni, M. The Elusive Roles of Bacterial Glutathione *S*-Transferases: New Lessons from Genomes. *Appl. Microbiol. Biotechnol.* **2002,** *58***,** 138-146.

(74) Van Der Aar, E. M., Tan, K. T., Commandeur, J. N. M., and Vermeulen, N. P. E. Strategies to Characterize the Mechanisms of Action and the Active Sites of Glutathione *S*-Transferases: A Review. *Drug Metab. Rev.* **1998,** *30*(3)**,** 569-643.

(75) Salinas, A. E., and Wong, M. G. Glutathione *S*-Transferases- A Review. *Curr. Med. Chem.* **1999,** *6*(4)**,** 279-309.

(76) Liou, J. Y., Huang, T. M., and Chang, G. G. Inhibition of Octopus Glutathione *S*-Transferase by Meisenheimer Complex Analog, *S*-(2,4,6-Trinitrophenyl) glutathione. *J. Protein Chem.* **2000,** *19*(7)**,** 615-620.

(77) Graminski, G. F., Zhang, P., Sesay, M. A., Ammon, H. L., and Armstrong, R. N. Formation of the 1-(*S*-Glutathionyl)-2,4,6-trinitrocyclohexadienate Anion at the Active Site of Glutathione *S*-Transferase: Evidence for Enzymic Stabilization of σ-Complex Intermediates in Nucleophilic Aromatic Substitution Reactions. *Biochemistry* **1989,** *28***,** 6252-6258.

(78) Armstrong, R. N. Glutathione *S*-Transferases: Reaction Mechanism, Structure, and Function. *Chem. Res. Toxicol.* **1991,** *4*(2)**,** 131-40.

(79) Ji, X., Armstrong, R. N., and Gilliland, G. L. Snapshots Along the Reaction Coordinate of an S(N)Ar Reaction Catalyzed by Glutathione Transferase. *Biochemistry* **1993,** *32*(48)**,** 12949-12954.

(80) Shames, S. L., Fairlamb, A. H., Cerami, A., and Walsh, C. T. Purification and Characterization of Trypanothione Reductase from *Crithidia fasciculata*, a Newly Discovered Member of the Family of Disulfide-Containing Flavoprotein Reductases. *Biochemistry* **1986,** *25***,** 3519-3526.

(81) Matthews, R. G., and Williams, J., C. H. Measurement of the Oxidation-Reduction Potentials for Two-Electron and Four-Electron Reduction of Lipoamide Dehydrogenase from Pig Heart. *J. Biol. Chem.* **1976,** *251***,** 3956-3964.

(82) Massey, V., and Williams, C. H. On the Reaction Mechanism of Yeast Glutathione Reductase. *J. Biol. Chem.* **1965,** *240***,** 4470-4480.

(83) Yamada, H., and Kumagi, H. Synthesis of L-Tyrosine-Related Amino Acids by β-Tyrosinase. *Adv. Appl. Microbiol.* **1975,** *19***,** 249-288.

(84) Talekar, R. S., Chen, G. S., Lai, S.-Y., and Chern, J.-W. Nonreductive Deiodination of *ortho*-Iodo-hydroxylated Arenes Using Tertiary Amines. *J. Org. Chem.* **2005,** *70***,** 8590-8593.

(85) Kunishima, M., Friedman, J. E., and Rokita, S. E. Transition-State Stabilization by a Mammalian Reductive Dehalogenase. *J. Am. Chem. Soc.* **1999,** *121*(19)**,** 4722-4723.

(86) Yeh, J. I., Claiborne, A., and Hol, W. G. J. Structure of the Native Cysteine-Sulfenic Acid Redox Center of Enterococcal NADH Peroxidase Refined at 2.8 Angstrom Resolution. *Biochemistry* **1996,** *35*(31)**,** 9951-9957.

(87) Stehle, T., Ahmed, S. A., Claiborne, A., and Schulz, G. E. Structure of NADH Peroxidase from *Streptococcus faecalis 10C1* Refined at 2.16 Å Resolution. *J. Mol. Biol.* **1991,** *221***,** 1325-1344.

(88) Claiborne, A., Yeh, J. I., Mallett, T. C., Luba, J., Crane, E. J., Charrier, V., and Parsonage, D. Protein-Sulfenic Acids: Diverse roles for an Unlikely Player in Enzyme Catalysis and Redox Regulation. *Biochemistry* **1999,** *38*(47)**,** 15407-15416.

(89) Claiborne, A., Miller, H., Parsonage, D., and Ross, R. P. Protein-Sulfenic Acid Stabilization and Function in Enzyme Catalysis and Gene Regulation. *FASEB J.* **1993,** *7***,** 1483-1490.

(90) Friedman, J. E., Watson Jr., J. A., Lam, D. W.-H., and Rokita, S. E. Iodotyrosine Deiodinase Is the First Mammalian Member of the NADH Oxidase / Flavin Reductase Superfamily. *J. Biol. Chem.* **2006,** *281*(5)**,** 2812-2819.

(91) Callebaut, I., Curcio-Morelli, C., Mornon, J.-P., Gereben, B., Buettner, C., Huang, S., Castro, B., Fonseca, T. L., Harney, J. W., Larsen, P. R., and Bianco, A. C. The Iodothyronine Selenodeiodinases are Thioredoxin-fold Family Proteins Containing a Glycoside Hydrolase Clan GH-A-like Structure. *J. Biol. Chem.* **2003,** *278*(38)**,** 36887-36896.

(92) Williams, J., C. H. Lipoamide Dehydrogenase, Glutathione Reductase, Thioredoxin Reductase, and Mercuric Ion Reductase - A Family of Flavoenzyme Transhydrogenases. *In* "Chemistry and Biochemistry of Flavoenzymes." (F. Muller, Ed.); CRC Press: Boca Raton, FL, 1992; Vol. 3 pp. 121-207.

(93) Altschul, S. F., Gish, W., Miller, W., Myers, E. W., and Lipman, D. J. Basic Local Alignment Search Tool. *J. Mol. Biol.* **1990,** *215***,** 403-410.

(94) Laemmli, U. K. Cleavage of Structural Proteins during the Assembly of the Head of Bacteriophage T4. *Nature* **1970,** *227***,** 680-685.

(95) Altschul, S. F., Madden, T. L., Schaffer, A. A., Zhang, J., Zhang, Z., Miller, W., and Lipman, D. J. Gapped BLAST and PSIBLAST: a New Generation of Protein Database Search Programs. *Nucl. Acids Res.* **1997,** *25***,** 3389-3402.

(96) Thompson, J. D., Higgins, D. G., and Gibson, T. J. CLUSTAL W: Improving the Sensitivity of Progressive Multiple Sequence Alignment Through Sequence Weighting, Position-Specific Gap Penalties and Weight Matrix Choice. *Nucl. Acids Res.* **1994,** *22***,** 4673-4680.

(97) Kryukov, G. V., Castellano, S., Novoselov, S. V., Lobanov, A. V., Zehtab, O., R, G., and Gladyshev, V. N. Characterization of Mammalian Selenoproteomes. *Science* **2003,** *300***,** 1439-1443.

(98) Fischer, D., Barret, C., Bryson, K., Elofsson, A., Godzik, A., Jones, D., Karplus, K. J., Kelley, L. A., Maccallum, R. M., Pawowski, K., Rost, B., Rychlewski, L., and Sternberg, M. J. CAFASP-1: Critical Assessment of Fully Automated Structure Prediction Methods. *Proteins: Structure, Function and Genetics.* **1999,** *37*(Supp. 3)**,** 209-217.

(99) Krogh, A., Larsson, B., Von Heijne, G., and Sonnhammer, E. L. L. Predicting Transmembrane Protein Topology with a Hidden Markov Model: Application to Complete Genomes. *J. Mol. Biol.* **2001,** *305*(3)**,** 567-580.

(100) Bendtsen, J. D., Nielsen, H., Heijne, G. V., and Brunak, S. Improved Prediction of Signal Peptides: SignalP 3.0. *J. Mol. Biol.* **2004,** *340***,** 783-795.

(101) Gnidehou, S., Caillou, B., Talbot, M., Ohayon, R., Kaniewski, J., Noel-Hudson, M.-S., Morand, S., Agnangji, D., Sezan, A., Courtin, F., Virion, A., and Dupuy, C. Iodotyrosine Dehalogenase 1 (DEHAL1) Is a Transmembrane Protein Involved in the Recycling of Iodide Close to the Thyroglobulin Iodination Site. *FASEB J.* **2004,** *18*(13)**,** 1574-1576.

(102) Hecht, H. J., Erdmann, H., Park, H. J., Sprinzl, M., and Schmid, R. D. Crystal-Structure of NADH Oxidase from *Thermus thermophilus*. *Nat. Struct. Biol.* **1995,** *2*(12)**,** 1109-1114.

(103) Campbell, G. R. O., Taga, M. E., Mistry, K., Lloret, J., Anderson, P. J., Roth, J. R., and Walker, G. C. *Sinorhizobium meliloti bluB* is Necessary for Production of 5,6-Dimethylbenzimidazole, the Lower Ligand of B_{12}. *Proc. Natl. Acad. Sci. U. S. A.* **2006,** *103*(12)**,** 4634-4639.

(104) Zenno, S., Saigo, K., Kanoh, H., and Inouye, S. Identification of the Gene Encoding the Major NAD(P)H-Flavin Oxidoreductase of the Bioluminescent Bacterium *Vibrio fischeri ATCC 7744*. *J. Bacteriol.* **1994,** *176***,** 3536-3543.

(105) Parkinson, G. N., Skelly, J. V., and Neidle, S. Crystal Structure of FMN-Dependent Nitroreductase from *Escherichia coli B*: a Prodrug-Activating Enzyme. *J. Med. Chem.* **2000,** *43*(20)**,** 3624-3631.

(106) Koder, R. L., Haynes, C. A., Rodgers, M. E., Rodgers, D. W., and Miller, A.-F. Flavin Thermodynamics Explain the Oxygen Insensitivity of Enteric Nitroreductases. *Biochemistry* **2002,** *41***,** 14197-14205.

(107) Tanner, J. J., Tu, S. C., Barbour, L. J., Barnes, C. L., and Krause, K. L. Unusual Folded Conformation of Nicotinamide Adenine Dinucleotide Bound to Flavin Reductase P. *Protein Sci.* **1999,** *8*(9)**,** 1725-1732.

(108) Tanner, J. J., Lei, B. F., Tu, S. C., and Krause, K. L. Flavin Reductase P: Structure of a Dimeric Enzyme that Reduces Flavin. *Biochemistry* **1996,** *35***,** 13531-13539.

(109) Jeffers, C. E., and Tu, S. C. Differential Transfers of Reduced Flavin Cofactor and Product by Bacterial Flavin Reductase to Luciferase. *Biochemistry* **2001,** *40***,** 1749-1754.

(110) Mccarthy, D. L., Navarrete, S., Willett, W. S., Babbitt, P. C., and Copley, S. D. Exploration of the Relationship Between Tetrachlorohydroquinone Dehalogenase and the Glutathione *S*-Transferase Superfamily. *Biochemistry* **1996,** *35*(46)**,** 14634-14642.

(111) Murzin, A. G., Brenner, S. E., Hubbard, T., and Chothia, C. SCOP: a Structural Classification of Proteins Database for the Investigation of Sequences and Structures. *J. Mol. Biol.* **1995,** *247***,** 536-540.

(112) Koike, H., Sasaki, H., Kobori, T., Zenno, S., Saigo, K., Murphy, M. E. P., Adman, E. T., and Tanokura, M. 1.8 angstrom Crystal Structure of the Major NAD(P)H: FMN Oxidoreductase of a Bioluminescent Bacterium, *Vibrio fischeri*: Overall Structure, Cofactor and Substrate-Analog Binding, and Comparison with Related Flavoproteins. *J. Mol. Biol.* **1998,** *280*(2)**,** 259-273.

(113) Haynes, C. A., Koder, R. L., Miller, A.-F., and Rodgers, D. W. Structures of Nitroreductase in Three States, Effects of Inhibitor Binding and Reduction. *J. Biol. Chem.* **2002,** *277*(13)**,** 11513-11520.

(114) Kobori, T., Sasaki, H., Lee, W. C., Zenno, S., Saigo, K., Murphy, M. E., and Tanokura, M. Structure and Site-Directed Mutagenesis of a Flavoprotein from *Escherichia coli* that Reduces Nitrocompounds: Alteration of Pyridine Nucleotide Binding by a Single Amino Acid Substitution. *J. Biol. Chem.* **2001,** *276***,** 2816-2823.

(115) Lovering, A. L., Hyde, E. I., Searle, P. F., and White, S. A. The Structure of *Escherichia coli* Nitroreductase Complexed with Nicotinic Acid: Three Crystal Forms at 1.7 Å, 1.8 Å and 2.4 Å resolution. *J. Mol. Biol.* **2001,** *309***,** 203-213.

(116) Sali, A., and Blundell, T. L. Comparative Protein Modeling by Satisfaction of Spatial Restraints. *In* "Protein Structure by Distance Analysis." (H. Bohr, and S. Brunak, Eds.); IOS Press: Amsterdam, 1994; pp. 64-86.

(117) Sali, A., and Blundell, T. L. Comparative Protein Modeling by Satisfaction of Spatial Restraints. *J. Mol. Biol.* **1993,** *234*(3)**,** 779-815.

(118) Pontius, J., Richelle, J., and Wodak, S. J. Deviations from Standard Atomic Volumes as a Quality Measure for Protein Crystal Structures. *J. Mol. Biol.* **1996).** *264***,** 121-136.

(119) Luthy, R., Bowie, J. U., and Eisenberg, D. Assessment of Protein Models with Three-Dimensional Profiles. *Nature* **1992,** *356***,** 83-85.

(120) Colovos, C., and Yeates, T. O. Verification of Protein Structures: Patterns of Nonbonded Atomic Interactions. *Protein Sci.* **1993,** *2***,** 1511-1519.

(121) Hooft, R. W. W., G., V., C., S., and Abola, E. E. Errors in Protein Structures. *Nature* **1996,** *381***,** 272-272.

(122) Laskoswki, R. A., Macarthur, M. W., Moss, D. S., and Thorton, J. M. PROCHECK: a Program to Check the Stereochemical Quality of Protein Structures. *J. Appl. Cryst.* **1993,** *26***,** 283-291.

(123) Studier, F. W. personal communication via e-mail.

(124) Sali, A., and Blundell, T. L. Definition of General Topological Equivalence in Protein Structures: A Procedure Involving Comparison of Properties and Relationships through Simulated Annealing adn Dynamic Programming. *J. Mol. Biol.* **1990,** *212***,** 403-428.

(125) Pettersen, E. F., Goddard, T.D., Huang, C.C., Couch, G.S., Greenblatt, D.M., Meng, E.C., and Ferrin, T.E. UCSF Chimera - A Visualization System for Exploratory Research and Analysis. *J. Comput. Chem.* **2004,** *25*(13)**,** 1605-1612.

(126) Lei, B., Wang, H., Yu, Y., and Tu, S. C. Redox Potential and Equilibria in the Reductive Half-Reaction of *Vibrio harveyi* NADPH-FMN Oxidoreductase. *Biochemistry* **2005,** *44*(1)**,** 261-267.

(127) Wang, H., Lei, B. F., and Tu, S. C. *Vibrio harveyi* NADPH-FMN Oxidoreductase Arg203 as a Critical Residue for NADPH Recognition and Binding. *Biochemistry* **2000,** *39*(26)**,** 7813-7819.

(128) Massey, V. The Chemical and Biological Versatility of Riboflavin. *Biochem. Soc. Trans.* **2000,** *28***,** 283-296.

(129) Massey, V. Flavoprotein Structure and Mechanism-Introduction. *FASEB J.* **1995,** *9***,** 473-475.

(130) Miller, H., Mande, S. S., Parsonage, D., Sarfaty, S. H., Hol, W. G., and A., C. An L40C Mutation Converts the Cysteine-Sulfenic Acid Redox Center in Enterococcal NADH Peroxidase to a Disulfide. *Biochemistry* **1995,** *34*(15)**,** 5180-5190.

(131) Hoober, K. L., and Thorpe, C. Egg White Sulfhydryl Oxidase: Kinetic Mechanism of the Catalysis of Disulfide Bond Formation. *Biochemistry* **1999,** *38*(10)**,** 3211-3217.

(132) Gross, E., Sevier, C. S., Vala, A., Kaiser, C. A., and Fass, D. A New FAD-Binding Fold and Intersubunit Disulfide Shuttle in the Thiol Oxidase Erv2p. *Nat. Struct. Biol.* **2001,** *9***,** 61-67.

(133) Coppock, D. L., Cina-Poppe, D. A., and Gilleran, S. N. The Quiescin Q6 Gene is the Fusion of Two Ancient Gene Families: Thioredoxin and ERV1. *Genomics* **1998,** *54***,** 460-468.

(134) Lavallie, E. R., Diblasio, E. A., Kovacic, S., Grant, K. L., Schendel, P. F., and Mccoy, J. M. A Thioredoxin Gene Fusion Expression System That Circumvents Inclusion Body Formation in the *E. coli* Cytoplasm. *Bio/Technology* **1993,** *11***,** 187-193.

(135) Mura, C. Rare Codon Calculator (RaCC) at http://nihserver.mbi.ucla.edu/RACC/. **2003**.

(136) Escher, A., O'kane, D. J., Lee, J., and Szalay, A. A. Bacterial Luciferase Ab Fusion Protein is Fully Active as a Monomer and Highly Sensitive in vivo to Elevated Temperatures. *Proc. Natl. Acad. Sci. U. S. A.* **1989,** *86***,** 6528–6532.

(137) Schein, C. H., and Noteborn, M. H. M. Formation of Soluble Recombinant Proteins in *Escherichia coli* Is Favored by Lower Growth Temperatures. *Bio/Technology* **1988,** *6***,** 291–294.

(138) Schein, C. H. Production of Soluble Recombinant Proteins in Bacteria. *Bio/Technology* **1989,** *7***,** 1141–1148.

(139) Studier, F. W. Protein Production by Auto-Induction in High-Density Shaking Cultures. *Protein Expression and Purification* **2005,** *41***,** 207-234.

(140) Leonard, J. L., and Visser, T. J. Biochemistry of Deiodination. *In* "Thyroid Hormone Metabolism." (G. Henneman, Ed.); Dekker: New York, NY, 1986; pp. 189-229.

(141) Berry, M. J., Maia, A. L., Kieffer, J. D., Harney, J. W., and Larsen, P. R. Substitution of Cysteine for Selenocysteine in Type-I Iodothyronine Deiodinase

Reduces the Catalytic Efficiency of the Protein but Enhances Its Translation. *Endocrinology* **1992,** *131*(4)**,** 1848-1852.

(142) Hatfield, D. L., and Gladyshev, V. N. Selenium Has Altered Our Understanding of the Genetic Code. *Mol. Cell. Biol.* **2002,** *22***,** 3565-3576.

(143) Sun, B. C., Harney, J. W., Berry, M. J., and Larsen, P. R. The Role of the Active Site Cysteine in Catalysis by Type 1 Iodothyronine Deiodinase. *Endocrinology* **1997,** *138*(12)**,** 5452-5458.

(144) Croteau, W., Bodwell, J. E., Richardson, J. M., and St. Germain, D. L. Conserved Cysteines in the Type 1 Deiodinase Selenoprotein Are Not Essential for Catalytic Activity. **1998**.

(145) Lian, G., Ding, L., M., C., Z., L., D., Z., and J., N. Preparation and Properties of Selenium-Containing Catalytic Antibody as Type I Deiodinase Mimic. *J. Biol. Chem.* **2001,** *276***,** 28037-28041.

(146) Hartmann, K., and Hartmann, N. Nichtenzymatische Halogenabspaltugen-ein Modell der enzymatischen Dejodierung? *Acta Biol. Med. Ger.* **1968,** *21*(4)**,** 585-586.

(147) Hartmann, K., Hartmann, N., and Bulka, E. Untersuchungen zum Reaktionsablauf der Dejodierung von 3,5-Dijod-tyrosin durch Cystein. *Z. Chem.* **1971,** *11***,** 344-345.

(148) Lith, M. V., Hartigan, N., Hatch, J., and Benham, A. M. PDILT, a Divergent Testis-Specific Protein Disulfide Isomerase with a Non-Classical SXXC Motif That Engages in Disulfide-dependent Interactions in the Endoplasmic Reticulum. *J. Biol. Chem.* **2005,** *280***,** 1376-1383.

(149) Fomenko, D. E., and Gladyshev, V. N. Identity and Functions of CxxC-Derived Motifs. *Biochemistry* **2003,** *42*(38)**,** 11214-11225.

(150) Chopra, I. J. A Study of Extrathyroidal Conversion of Thyroxine (T4) to 3,3,5-Trioodothyronine (T3) In Vitro. *Endocrinology* **1977,** *101***,** 453-463.

(151) Chopra, I. J. Sulfhydryl Groups and the Monodeiodination of Thyroxine to Triiodothyronine. *Science* **1978,** *199***,** 904-905.

(152) Goswami, A., and Rosenberg, I. N. Stimulation of Iodothyronine Outer Ring Monodeiodinase by Dihydrolipoamide. *Endocrinology* **1983,** *112*(4)**,** 1180-7.

(153) Goswami, A., and Rosenberg, I. N. Thioredoxin Stimulates Enzymatic Outer Ring Monodeiodination of Reverse Triiodothronine. *Endocrinology* **1987,** *121*(6)**,** 1937-45.

(154) Goswami, A., and Rosenberg, I. N. NADPH-Responsive Thyroidal Deiodination. *In* "Thyroid Research." (J. Robbins, L. E. Braverman, F. J. G. Ebling, and I. W. Henderson, Eds.); American Elsevier: New York, 1976; pp. 162-165.

(155) Pistorius, E. K., and Axelrod, B. Iron, an Essential Component of Lipoxygenase. *J. Biol. Chem.* **1974,** *249***,** 3183-3186.

(156) Jeffers, C. E., Nichols, J. C., and Tu, S.-C. Complex Formation between *Vibrio harveyi* Luciferase and Monomeric NADPH:FMN Oxidoreductase. *Biochemistry* **2003,** *42***,** 529-534.

(157) Liu, M., Lei, B., Ding, Q., Lee, J. C., and Tu, S.-C. *Vibrio harveyi* NADPH:FMN Oxidoreductase: Preparation and Characterization of the Apoenzyme and Monomer-Dimer Equilibrium. *Arch. Biochem. Biophys.* **1997,** *337***,** 89-95.

(158) Tang, C.-K., Jeffers, C. E., Nichols, J. C., and Tu, S.-C. Flavin Specificity and Subunit Interaction of *Vibrio fischeri* General NAD(P)H-Flavin Oxidoreductase FRG/FRase I. *Arch. Biochem. Biophys.* **2001,** *392***,** 110-116.

(159) Tu, S. C., Becvar, J. E., and Hastings, J. W. Kinetic Studies on the Mechanism of bacterial NAD(P)H:flavin oxidoreductase. *Arch. Biochem. Biophys.* **1979,** *193***,** 110-116.

(160) Hastings, J. W., Potrikus, C. J., Gupta, S. C., Kurfurst, M., and Makemson, J. C. Biochemistry and Physiology of Bioluminescent Bacteria. *Adv. Microb. Physiol.* **1985,** *26***,** 235-291.